STARS

2012

Structural Identification Through Monitoring, Modeling And Predictive Analysis Under Uncertainty

Hasan Burak GÖKÇE
University of Central Florida

STARS Citation

STRUCTURAL IDENTIFICATION
THROUGH MONITORING, MODELING, AND PREDICTIVE ANALYSIS
UNDER UNCERTAINTY

by

HASAN BURAK GÖKÇE
B.Sc. Istanbul Technical University, 2007
M.Sc. University of Central Florida, 2010

A dissertation submitted in partial fulfillment of the requirements
for the degree of Doctor of Philosophy
in the Department of Civil, Environmental and Construction Engineering
in the College of Engineering and Computer Science
at the University of Central Florida
Orlando, Florida

Spring Term
2012

Major Professor: F. Necati Çatbaş

ABSTRACT

Bridges are critical components of highway networks, which provide mobility and economical vitality to a nation. Ensuring the safety and regular operation as well as accurate structural assessment of bridges is essential. Structural Identification (St-Id) can be utilized for better assessment of structures by integrating experimental and analytical technologies in support of decision-making. St-Id is defined as creating parametric or nonparametric models to characterize structural behavior based on structural health monitoring (SHM) data. In a recent study by the ASCE St-Id Committee, St-Id framework is given in six steps, including modeling, experimentation and ultimately decision making for estimating the performance and vulnerability of structural systems reliably through the improved simulations using monitoring data. In some St-Id applications, there can be challenges and considerations related to this six-step framework. For instance not all of the steps can be employed; thereby a subset of the six steps can be adapted for some cases based on the various limitations. In addition, each step has its own characteristics, challenges, and uncertainties due to the considerations such as time varying nature of civil structures, modeling and measurements. It is often discussed that even a calibrated model has limitations in fully representing an existing structure; therefore, a family of models may be well suited to represent the structure's response and performance in a probabilistic manner.

The principle objective of this dissertation is to investigate nonparametric and parametric St-Id approaches by considering uncertainties coming from different sources to better assess the structural condition for decision making. In the first part of the dissertation, a nonparametric St-Id approach is employed without the use of an analytical model. The new methodology, which is

successfully demonstrated on both lab and real-life structures, can identify and locate the damage by tracking correlation coefficients between strain time histories and can locate the damage from the generated correlation matrices of different strain time histories. This methodology is found to be load independent, computationally efficient, easy to use, especially for handling large amounts of monitoring data, and capable of identifying the effectiveness of the maintenance. In the second part, a parametric St-Id approach is introduced by developing a family of models using Monte Carlo simulations and finite element analyses to explore the uncertainty effects on performance predictions in terms of load rating and structural reliability. The family of models is developed from a parent model, which is calibrated using monitoring data. In this dissertation, the calibration is carried out using artificial neural networks (ANNs) and the approach and results are demonstrated on a laboratory structure and a real-life movable bridge, where predictive analyses are carried out for performance decrease due to deterioration, damage, and traffic increase over time. In addition, a long-span bridge is investigated using the same approach when the bridge is retrofitted. The family of models for these structures is employed to determine the component and system reliability, as well as the load rating, with a distribution that incorporates various uncertainties that were defined and characterized. It is observed that the uncertainties play a considerable role even when compared to calibrated model-based predictions for reliability and load rating, especially when the structure is complex, deteriorated and aged, and subjected to variable environmental and operational conditions. It is recommended that a family-of-models approach is suitable for structures that have less redundancy, high operational importance, are deteriorated, and are performing under close capacity and demand levels.

To my mother, grandmother, aunt and uncles
who brought me to these days…

To my brother
for his understanding during the moments when we were apart…

To my soul mate
for her endless support, encouragement, patience, and most importantly love…

ACKNOWLEDGMENTS

First and foremost, I would like to express my thanks and my deepest gratitude to Dr. F. Necati Çatbaş for his guidance as well as his friendship throughout this study. He gave me the opportunity to balance both the fun and the hard times, to publish articles, and to collaborate with internationally recognized researchers. None of these experiences would have been possible or enjoyable without his mentorship and help.

I am thankful to the members of my dissertation committee, Dr. Manoj Chopra, Dr. Kevin Mackie, Dr. Hae-Bum Yun, and Dr. Ronald DeMara, for their time and feedback. I would like to gratefully acknowledge the help and feedback of our collaborators Dr. Mustafa Gul, Dr. Ricardo Zaurin, and Dr. Dan M. Frangopol during various parts of this study.

I sincerely thank my friends Cagdas Ozturk, Egemen Tavsanci, Bayram Aygun, Coskun Kuzu, Turhan Tokatli, and Emrecan Ergin for their friendship and continuous support. Many thanks to the current and former members of our research team, Taha Dumlupinar, Ozerk Sazak, Tom Terrell, Danny Maier, Masoud Malekzadeh, Tung Khuc, Serhat Erdogan, and Alex Hanhold.

Finally, I would like to thank Buket, who has been one of my strongest supporters during the most difficult times of this study. And last, but most certainly not least, I would like to express my deepest love and gratitude to my family; I cannot thank them enough for their love and support.

Thanks to you all…

TABLE OF CONTENTS

LIST OF FIGURES

xiii

LIST OF TABLES

CHAPTER 1.
INTRODUCTION

1.1. Structural Identification (St-Id)

Structural identification (St-Id), which is adopted from system identification (Ljung 1999), is the area of developing mathematical and/or geometric models from observations to characterize the input-output relationship based on experimental data for performance assessment of structures and decision making. Pioneering efforts on this important paradigm, which was presented to the engineering mechanics community by Hart and Yao (1977) and to the structural engineering community by Liu and Yao (1978), hitherto, inspired many researchers to explore different aspects of St-Id. Detailed overviews related to different aspects of St-Id research have been documented in various studies (Doebling et al. 1998; Sohn et al. 2004; Moon and Aktan 2006b; Catbas and Kijewski-Correa 2012).

In a recent study by the ASCE SEI Committee on Structural Identification of Constructed Systems (Catbas et al. 2012d), St-Id framework is presented in six steps, which are described in detail with case studies in the next chapter of the dissertation. These steps are:

- *Drivers for Identification*

- *A-Priori Modeling*

- *Experimentation*

- *Data Analysis*

- *Model Calibration*

- *Utilization*

The aim of the St-Id framework is to link the gap between the model and the real structure for estimating the performance and vulnerability of structural systems reliably through improved simulations using experimental observations/data. To achieve this objective, parametric (physics-based or model-based) and nonparametric (non–physics-based or data-driven) models can be employed.

While parametric methods can be useful for better physical conceptualization, as well as for predicting future behavior, the level of expertise and time required to develop such models sometimes makes this approach difficult for researchers (Worden 1997; Laory et al. 2011). In the literature, the use of parametric-based St-Id approaches were investigated by several researchers to identify the civil infrastructure by addressing the boundary conditions, continuity conditions, equilibrium, and kinematics (Natke and Yao 1987; Aktan et al. 1997; Aktan et al. 1998b; Doebling et al. 1998; Farrar and Jaureguiz 1998; Brownjohn 2003; Brownjohn et al. 2003; Maeck and De Roeck 2003). The main advantage of using identified parametric models for the structures is to simulate the behavior under critical loading or damage conditions. Due to this advantage for simulating the behavior, parametric models can be utilized for diagnosing the causes of behavior changes and the impacts of these changes on the performance of the components and the overall system. Although several studies can be found on the use of nonlinear models, linear models are commonly employed for St-Id.

On the other hand, the idea of nonparametric methods is that only training data from the normal operating condition of the structure or system is used to establish the diagnostics (Worden and Dulieu-Barton 2004). Different methods were utilized as nonparametric models for St-Id, including artificial neural networks (Masri et al. 1996; Nakamura et al. 1998; Masri et al.

2000; Chang et al. 2001; Zapico et al. 2003; Yun et al. 2009), wavelet decomposition (Gurley and Kareem 1999; Hou et al. 2000; Kijewski and Kareem 2003), and auto-regressive moving average vector models (Ghanem and Shinozuka 1995; Bodeux and Golinval 2001; Gul and Catbas 2011; Gul and Catbas 2012). Benefits of nonparametric approaches are automation, more efficient real-time St-Id, ease of continuous monitoring, and minimization of errors due to user interaction, practicality of use, and computational efficiency in handling large amounts of data due to its data-driven nature. However, it should be noted that data-driven methods can only identify whether a change in behavior has occurred and cannot identify the cause of the change or its effect on overall performance without physics-based models.

Today, there are powerful parametric and nonparametric approaches that have the ability to identify local and global behavior of constructed systems, but the challenge in the performance evaluation of constructed systems is more than the adoption of more refined models. Although such refined models have the ability to identify behavior with more resolution, there is a need to mitigate the influences of uncertainties. While there has been a growing awareness of the importance of incorporating uncertainty within the St-Id process for constructed systems over the past decade, characterization of the uncertainties is not an easy task. As a result, the interest in this challenge has resulted in a growing recognition for the need to improve the monitoring design and model predictions with the consideration of uncertainties.

1.2. *Structural Health Monitoring (SHM)*

With the need to better evaluate new and existing structures and with the advances in information and sensing technologies, the interest for structural health monitoring (SHM) is

growing exponentially worldwide. As there is not a standard approach for SHM, there is not a unique, accepted definition. In this dissertation, the following definition is adopted: SHM is, *the measurement of the operating and loading environment and the critical responses of a structure to track and evaluate the symptoms of operational incidents, anomalies, and/or deterioration or damage indicators that may affect operation, serviceability, or safety reliability* (Aktan et al. 2000a). With a properly designed and executed SHM, it may be possible to capture long-term structural behavior with continuous or discrete intervals of monitoring, also capturing seasonal and environmental changes that may not be easily extracted from intermittent or onetime structural tests, such as load tests or ambient vibration studies.

Several research studies have been conducted in the SHM area. In addition, some of these studies were extended to existing structures to demonstrate the implementation with the issues and challenges for real-life structures. However, it is still an open question whether SHM is fully developed and standardized for routine use in real life, even with the major advances in supporting technologies. One major hurdle is that there are not many research studies that recognize "all aspects" or "challenges" in SHM applications. For example, while sensor technologies evolve, become less expensive, and provide us with large amounts of data, proper use of the data is still a major research subject. Some researchers focus on developing new technologies even though such work may not correspond to the immediate needs of infrastructure owners. As a result, organizational issues, fundamental studies, and advances in technology need to be interrelated, as presented in Figure 1, for successful and useful health monitoring applications (Catbas et al. 2004b). For real-life applications, infrastructure owners (end-users) would like to take advantage of health monitoring for efficient operation, timely

4

maintenance, reduced costs, and improved safety. In that respect, the areas of interest and expertise of the stakeholders, infrastructure owners, researchers, and industry need to intersect for SHM to be a routinely implemented technology for civil structures, just like the successful applications in automobile and aerospace industries.
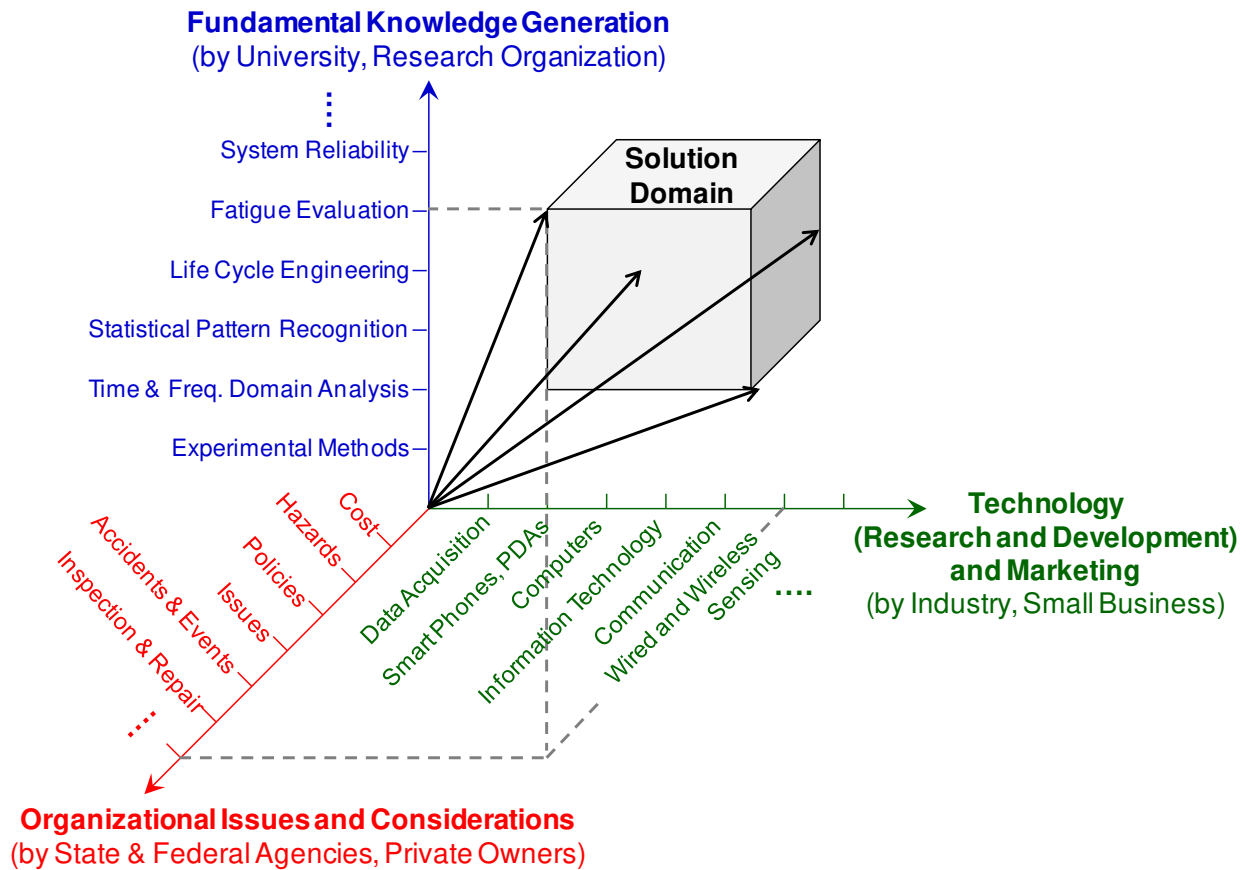
Figure 1: Main components of a health monitoring design (adapted from Catbas et al. (2004b))

Over the years, inspection, maintenance, and effective management of bridges have long been a concern to engineers, government officials, and researchers due to the fact that approximately 25% of a total 601,411 bridges in the United States are deemed structurally deficient or functionally obsolete (FHWA 2008). To develop and explore solutions for this

problem, new technologies have been used on several bridges, and several case studies can be found in the literature (Toksoy and Aktan 1994; Brownjohn et al. 1995; Aktan et al. 1996; Enright and Frangopol 1999; Lus et al. 1999; Farhey et al. 2000; Chang et al. 2001; Fujino 2002; Casas and Cruz 2003; Dyke et al. 2003; Maeck and De Roeck 2003; Masri et al. 2004; Ko and Ni 2005; Catbas et al. 2007; Catbas et al. 2011), but the wide-range and integrated implementation of these technologies still needs more attention. The concept of asset management is defined by the American Association of State Highway and Transportation Officials (AASHTO 2002) as "a systematic process of maintaining, upgrading, and operating physical assets cost effectively. It includes preservation, upgrading, and timely replacement of assets through cost-effective management, programming, and resource allocation decisions." Infrastructure asset management includes decision making, long-term planning, optimum maintenance scheduling, and minimizing operating costs through a holistic approach with advanced management functions. As such, SHM can be expected to be an invaluable technology for successful asset management.

Efficient asset management is possible with effective integration of technologies such as SHM to the current practice of inspecting and assessing bridges. An SHM system has the potential to provide comprehensive and objective data by means of sensors, data acquisition systems, assessment and evaluation algorithms, and data-based decision-making strategies. An integrated SHM system could be developed to link the structural monitoring data, environmental measurements, traffic, and operational inputs. With an integrated approach implemented to a network of structures, bridges can be operated with optimum performance, providing the best

6

utilization of their capacity. In addition, recording and analyzing the information from health monitoring data will lead to improvements in maintenance and structural design methods.

For a complete structural health monitoring system, sensors, data acquisition systems, condition/damage assessment algorithms, and data-management procedures (storage, retrieval, presentation, sharing, data fusion, visualization, and correlation) have to be designed properly. With an SHM approach, global and local structural conditional parameters can be determined based on the analysis of data measured by a network of sensors deployed on a structure. For infrastructure owners, SHM technologies provide invaluable tools that can support maintenance and operation decisions and can diagnose pre- and post-hazard conditions for emergency management.

A review of civil infrastructure SHM applications was presented by Brownjohn et al. (2004). A number of publications with emphasis on monitoring to bridges can be found in the literature, including *structural identification* (Aktan et al. 1998a; Huang et al. 1999; Brownjohn 2003; Kijewski and Kareem 2003; Yang et al. 2004; Robert-Nicoud et al. 2005b; Catbas et al. 2007; Soyoz and Feng 2009), *damage identification* (Hogue et al. 1991; Toksoy and Aktan 1994; Doebling et al. 1996; Worden et al. 2000; Sohn and Farrar 2001; Bernal 2002; Catbas and Aktan 2002; Chang et al. 2003; Kao and Hung 2003; Giraldo and Dyke 2004; Lynch et al. 2004; Sanayei et al. 2006; Carden and Brownjohn 2008; Gul and Catbas 2009), *structural reliability* (Catbas et al. 2008b; Frangopol et al. 2008; Liu et al. 2009; Kwon and Frangopol 2010; Liu et al. 2010), *life cycle cost* (Biondini and Frangopol 2009; Kim and Frangopol 2011a; Kim and Frangopol 2011b), and *load rating* (Boothby and Craig 1997; Chajes et al. 1997; Bhattacharya et

al. 2005; Garrett 2007; LeBeau and Wadia-Fascetti 2007; Gokce et al. 2011; Catbas et al. 2012c; Catbas et al. 2012e).

1.3. *Objective and Scope*

SHM is a multidisciplinary and broad research area and becomes more feasible with the recent technological advances and reduced cost of sensing technologies. In addition, SHM data, which is a crucial component of St-Id framework, can be utilized by means of parametric (model-based) or nonparametric (data-driven) approaches for effective management of civil infrastructure systems. The principle objective of this dissertation is to investigate parametric and nonparametric St-Id approaches by taking uncertainties into account to improve the robustness of decision making (see Figure 2). In an effort to illustrate the implementation of the St-Id frame, each step of the general framework is discussed and illustrated with real-life examples. Then, a novel nonparametric methodology is investigated for issues related to movable bridges that are of concern to maintenance engineers. This effective method can be implemented easily and employed effectively. For exploring and discussing the parametric approach, a family-of-models technique is presented to demonstrate the importance of continuous monitoring and model updating for performance predictions. Performance changes due to deterioration, damage, traffic increase, and retrofit are investigated for real-life structures within the St-Id framework by means of family-of-models approach.
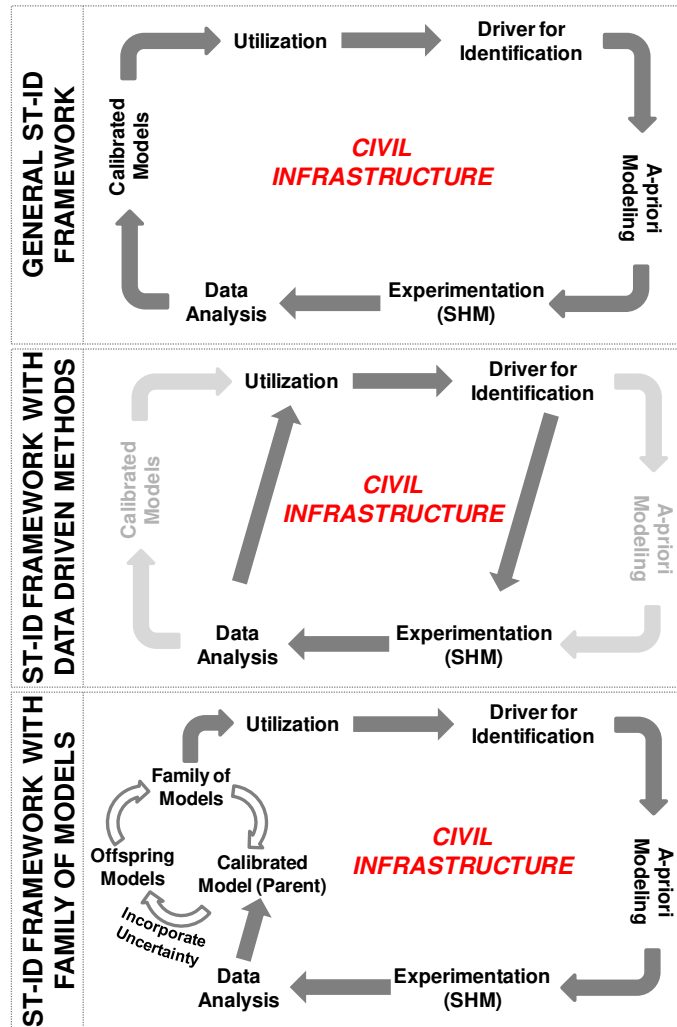
Figure 2: Different approaches for St-Id

1.4. *Organization of the Dissertation*

The organization of the dissertation is as follows:

In Chapter 2, steps of the general St-Id framework are described and exemplified with case studies. These steps include needs and drivers for identification, a-priori modeling, experimentation, data analysis, calibrated models, and utilization. To illustrate the drivers for identification, issues related to movable bridges are covered. Then, the nominal model and its

development are discussed for a particular movable bridge. Next, the implementation of the monitoring system and the execution of experimental studies are presented. Afterward, a strategy for calibration of the nominal model is presented along with the need for a family-of-models approach for the inclusion of possible uncertainties in the analyses. Finally, some representative performance metrics are introduced and obtained for decision-making purposes within the framework presented.

Chapter 3 presents a new nonparametric (data-driven) approach for the identification and localization of structural changes due to damage as well as repair of structures to bring them to previous performance levels. In this approach, cross-correlation analyses between strain data sets are utilized for damage detection, whereas correlation matrices are employed for damage localization. This new methodology, which is first applied on a laboratory structure for verification and then on a real-life bridge for validation, is found to be simple, effective, and load independent.

In Chapter 4, a family-of-models approach is introduced and demonstrated on a laboratory structure to explore the impact of uncertainty in predicting the system reliability obtained by a single calibrated finite element model (FEM) and a family of models that are continuously calibrated with SHM data. After discussing the laboratory structure, instrumentation plan, and experimentation plan, an artificial neural network (ANN) based FEM updating is illustrated for obtaining the parent (calibrated) model. The family of models, which includes parent and offspring models, is employed for system reliability calculations. Finally, a discussion for system reliability predictions obtained using a single model and a family of models is presented along with the results and interpretations.

Chapter 5 is dedicated mainly to the development and demonstration of the family of models for performance evaluation of a movable bridge as a real-life demonstration. After the calibration is completed for the movable bridge model, the performance due to deterioration of the sections, traffic load increase over years, and sudden damage are investigated, and the performance is predicted in terms of probabilistic load rating and system reliability.

Chapter 6 contains the exploration of a family-of-models approach for a different case where performance increase is expected for a long-span cantilever truss bridge due to retrofit application. Although such retrofit applications are very common for these types of structures, load rating, component reliability, and system reliability changes due to the applications have not been explored in detail. In this chapter, load rating using a single model and load rating distributions from a family of models are compared for the fracture critical hanger element. In addition, the system reliability of the hanger assembly is compared before and after the retrofit application.

Lastly, Chapter 7 provides the summary and presents the conclusions for the different St-Id framework stages that are described in different chapters of the dissertation. General comments about the different St-Id framework procedures described in this dissertation are reviewed along with recommendations and possible directions for future research. The methods and approaches along with the significant results are discussed and evaluated. Based on the understanding from real-life needs and drivers, experimental and analytical technologies, and decision making, a general direction for future research is presented with specific recommendations for immediate follow-up studies.

CHAPTER 2.
GENERAL FRAMEWORK FOR STRUCTURAL IDENTIFICATION

The implementation of Structural Identification (St-Id) will be based on the six-step procedure which mainly includes establishing the needs and drivers, using experimental and analytical technologies, and finally utilization of the findings for decision making. This chapter will provide a more detailed discussion of the six-step procedure along with examples and case studies.

2.1. *Drivers for Identification*

2.1.1. *General Remarks*

The initial requirement for successful St-Id implementation is to define the problem, address the issues, and identify the needs for St-Id. A major issue is to avoid any disconnections between these drivers and the technologies to be employed. As a result, the first step of the St-Id framework is getting familiar with the issues related to construction, operation, maintenance, or life-cycle asset management. These issues are to be well-defined and established before the execution of the St-Id program. These drivers can change from structure to structure (long-span bridges, movable bridges, etc.) and application to application (i.e., damage after an accident, deterioration due to aging, retrofit to increase reliability).

Some examples that initiate the need for St-Id are the need to more objectively determine the load carrying capacity of buildings under wind and earthquake loadings or the load carrying capacity of bridges for load rating purposes to make decisions such as retrofit, strengthening, or

load restrictions. Moreover, design verification and construction quality control especially in new designs may also create a need to identify the current condition of the structure. On the other hand, there can be other drivers that necessitate an St-Id process for more accurate predictive analysis for future performance. As an illustration, it is possible to consider documenting the current structural characteristics and monitoring the structure over the long term in order to define a baseline for assessing any future changes due to deterioration, damage, or retrofit.

While each of the specific issues above may appear distinct, the underlying driver in each case is the need to understand and address some fundamental engineering questions for decision making: (1) how constructed systems are actually loaded, (2) how they perform/behave, and (3) how they transfer forces through their members to their boundaries. These questions can be answered with an St-Id framework that utilizes monitoring data. In the following section, a case study is presented to illustrate such drivers for St-Id of movable bridges.

2.1.2. *Case Study: Description, Condition, and Issues of Movable Bridges*

In this section, movable bridges are covered to explain the drivers for identification. First, a general description of a movable bridge is presented along with movable bridge types. Secondly, the movable bridge population in Florida is analyzed for structural characteristics (i.e., age and span length) and condition ratings of different components. Thirdly, inspection reports of a smaller set of movable bridges are explored to find out the most problematic components, and the critical issues related to these components are presented.

The fusion of mechanical and electrical components with structural elements creates a very unique type of structure called a movable bridge. These types of bridges are often referred

to as "kinematic architecture" and provide the flexibility to increase the usage of these structures with different configurations. The main advantage of this type of structure is that, because of its moving condition, the bridge can be constructed with little vertical clearance, avoiding the expense of high piers and long approaches. Moving components of these bridges are operated by various types of machinery to open the passageway for waterborne traffic.

Movable bridges are a viable alternative to high fixed bridges over a waterway; however, they also present significant drawbacks and problems associated with operation and performance. Rapid deterioration is an issue since movable bridges are subject to harsh conditions as they are located over waterways and often close to the coast, which constitute conditions suitable for corrosion, causing section losses. Mechanical component failures due to friction and wear caused by the movement during opening and closings are deemed very critical by bridge owners. Even with regular maintenance, continuous downgrading of all parts of such complex bridges is inevitable, leading to breakdowns that cause problems for both land and maritime traffic. These problems result in high maintenance costs associated with the complex operation system and mechanical parts. In Florida, which has the second-highest number of movable bridges in the United States, it is estimated that the unit maintenance cost of a movable bridge can be up to 100 times that of a fixed bridge per square foot.

Movable bridges have been used and their designs have been studied with the first handbook published as early as 1882 by Fränkel (1882). More documentation about the design of some early movable bridges can be found in Waddell (1895), Greene and McKeen (1938), Quade (1954), Hardesty et al. (1975a; 1975b), and Wengenroth (1975). In addition, replacement of movable spans (Fisher and Robitaille 2011) and kinematics of movable bridges (Wallner and

Pircher 2007) are retrieved for movable bridges. For bascule bridges, a brief review of the Chicago-type bascule bridge design (Ecale and Lu 1983) and full-scale testing of procedures for assembling trunnion-hub-girder interactions by Besterfield (2003) are found. Other than these, there are also three publications on lift bridges, mainly related to construction (Ramey 1983; Griggs 2006; Zhao et al. 2012). However, movable bridges, or more specifically bascule bridges, are not extensively documented in the literature as compared to steel or concrete bridges.

Movable bridges can be seen in many parts of the world, especially close to the waterways and coastal topographical regions. In the United States, Florida has a large population number of movable bridges, most of which are owned by the Florida Department of Transportation (FDOT). As a result, the bridge population and specific cases presented from Florida are obtained from the inventory of 146 movable bridges, including three lift type, 133 bascule type (the highest in the nation), and 10 swing type bridges (National Bridge Inventory 2009) (shown in Figure 3). The majority of these movable bridges have main spans between 65 and 365 ft (20 and 111 m) with a mean span length of about 131 ft (40 m). Almost half of this bridge population is 40 to 50 years old, with a mean of 43 years. Figure 4 presents the distribution of the movable bridges in terms of their type, span length, and year built.

Figure 3: Main types of movable bridges
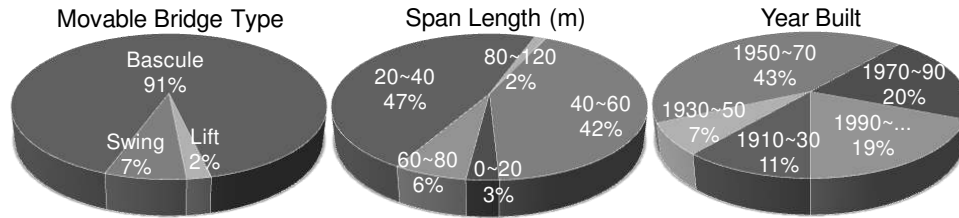
Figure 4: Distribution of movable bridges in Florida

On the other hand, the condition rating of the movable bridges has a mean of 6.54, 6.33, and 6.53 for the deck, superstructure, and substructure, respectively. Condition rating histograms of movable bridges with respect to the deck, superstructure, and substructure are shown in Figure 5. As per the condition rating definition given in the National Bridge Inventory (NBI) Condition Guide (FHWA 1995), a rating of 6 corresponds to satisfactory conditions, or in other words, structural elements show some minor deterioration. Based on our interviews with bridge engineers, it is also expressed that the mechanical components interacting with structural components are more critical for day-to-day operation and maintenance of these bridges.
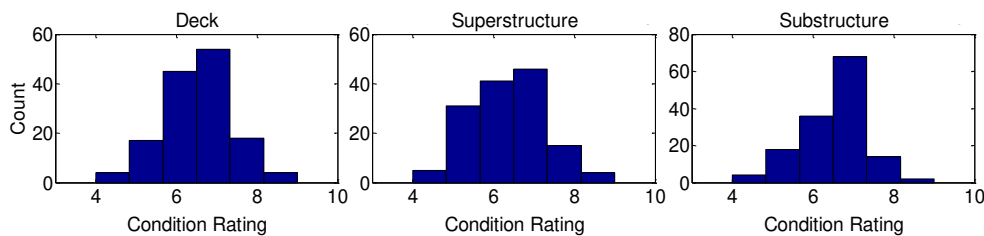
Figure 5: Condition rating histograms of deck, superstructure, and substructure

Inspection reports, which are generated with biennial inspections, include information ranging from the general characteristics of the bridge, such as, location, age, dimensions, type, and date of inspection, to element condition ratings. These notes are documented along with related pictures. Recommended actions are specified for each deficient element. Although it is

acknowledged that condition ratings given in bridge inspection reports are subjective and limited (Turner-Fairbank Highway Research Center 2005), analysis of current and past inspection reports can provide valuable representative information for the general condition and critical components of movable bridges.

Consequently, a sample population of 51 movable bridges was analyzed by processing the data from the inspection reports to investigate the most common problems, the components that experience these problems, and the number of occurrences. Figure 6 illustrates the condition rating distribution of critical components obtained from the analysis of 51 bridges using the data that were made available for research studies. In this figure, the identified element types are shown as well as the percentage of bridges within each category with a condition rating less than or equal to 2, as per the FDOT condition rating. Best and worst conditions are given as "1" and "5", respectively, as obtained from the inspection reports as per the rating system that is used by the state engineers and is different from NBI scales.
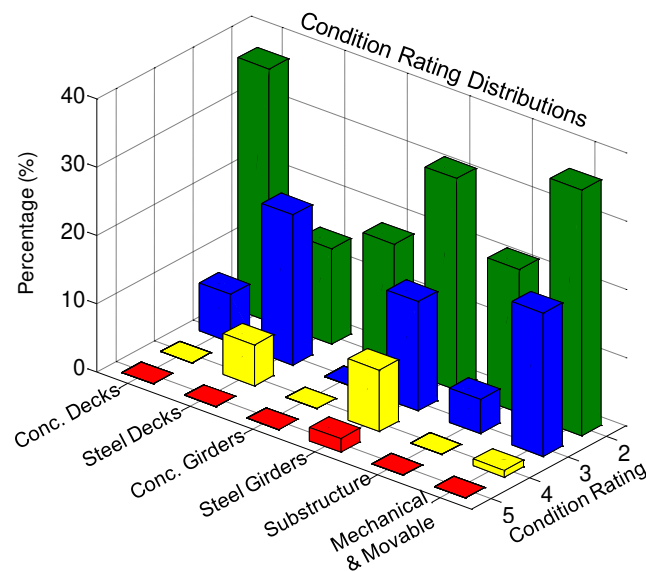
Figure 6: Analysis results of the condition ratings for different components

17

Although the most common problems observed are related to steel girders, the highest maintenance costs are associated with the movable components. Movable components shown in Figure 6 include all mechanical parts and machinery that operate for opening and closing of the bridge, and their proper function is critical for the bridge operation, such as shafts, trunnions, gear boxes, and open gears. For these elements, 58% present a condition rating of 2 or worse and 22% with condition rating of 3 or worse. As a result, a large portion of the bridge malfunctions is due to failure of these mechanical systems.

Further analysis is conducted on the most commonly observed problems, which are then analyzed to identify the number of occurrences of these critical problems related to movable components. Based on this analysis, six common types of movable component problems are identified: missing fasteners, cracking, leakage, misalignment, section loss, and inadequate lubrication. For each mechanical component, the total number of occurrences of a particular type of problem is indicated, and leakage is found to be the most frequent issue for these components (Figure 7).

This investigation of the inspection reports identifies the criticality of span locks for movable bridges from the condition ratings and the observed number of issues related to them from the number of occurrences figure. In Chapter 3, a new methodology is presented for identification of issues related to span lock shims, and this new methodology will help the movable bridge owners to reduce the maintenance costs by changing their preventive maintenance strategy into a predictive one. In addition, possible span lock failure effects on the performance of the structure are discussed later in Chapter 5.
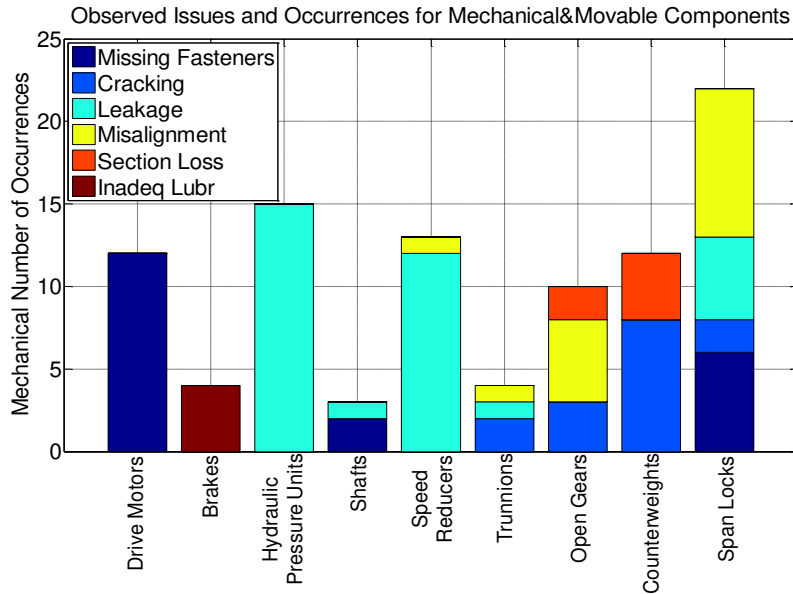
Figure 7: Most commonly observed movable component issues and number of occurrences identified from the inspections reports of the studied sample set

2.2. *A-Priori Modeling*

2.2.1. *General Remarks*

The development of an a-priori model within the St-Id framework serves to provide estimates of structural responses for the subsequent experimental steps. This model is then calibrated using monitoring data. Virtual reconstruction of the structure through computer-aided drafting (CAD) software can be considered as the early stage for the development of an a-priori model.

The development and use of an a-priori model, relies on the attention and experience of the engineer or researcher. The actual modeling approach adopted is dependent on the objectives of the St-Id as well as the complexity of the structure being identified. As an illustration, simple models are sufficient for some cases for global assessment and characterization, whereas detailed

structural models or high-resolution finite element models may be necessary in other cases where global and local responses are needed in high spatial resolution. In all cases, the effect of modeling considerations should be examined through the comparison of several models or modeling approaches, and the sensitivity of parameters with significant uncertainty should be established to have a good command of model fidelity. These preliminary studies also serve to identify key structural responses and their bounds. In the following section, a-priori modeling of a movable bridge is presented as a case study.

2.2.2. *Case Study: A-priori Model of Sunrise Boulevard Bridge*

Sunrise Boulevard Bridge in Ft. Lauderdale, Florida is a bascule type movable bridge over Florida SR-838 constructed in 1989 (Figure 8). The bridge has double bascule leaves with a total span length of 117 ft (36 m) and a width of 53.5 ft (16.4 m) and carries three traffic lanes. The bridge can be opened every 30 minutes when requested. Depending on the boat traffic, the bridge usually opens about 10 to 15 times a day. Considerations for structural, mechanical, and electrical component monitoring and the SHM system are discussed in the following sections.
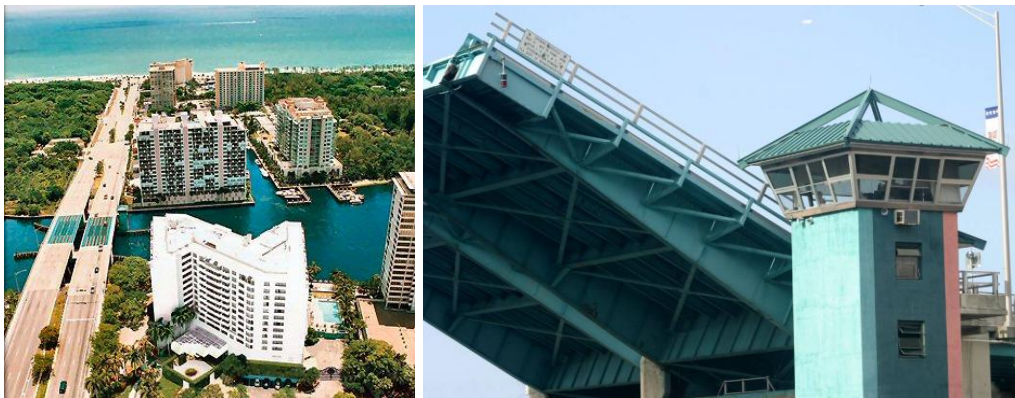
Figure 8: Sunrise Boulevard Bridge in Ft. Lauderdale, FL

When modeling a structure, a thorough inspection and verification of the structural components and behavior is often crucial to ensure that the model represents the actual structure. As a result, construction plans and details of the Sunrise Boulevard Bridge are closely studied to ensure a proper modeling of the superstructure. Then, a 3-D CAD model of the bridge reflecting the structure according to geometric information provided in the design drawings is constructed (Figure 9). These 3-D CAD models can be imported into finite element analysis software and can be used as a basis for developing the finite element models (FEMs).

A nominal FEM of the Sunrise Boulevard Bridge is constructed using commercial finite element software to characterize its behavior and conduct different simulations. Discretization, connections, and constraints of the structural elements are created considering the geometric requirements. Before the creation of the a-priori model, equivalent deck analysis for the orthotropic deck is conducted. More discussion about these studies can be found in Catbas et al. (2010).
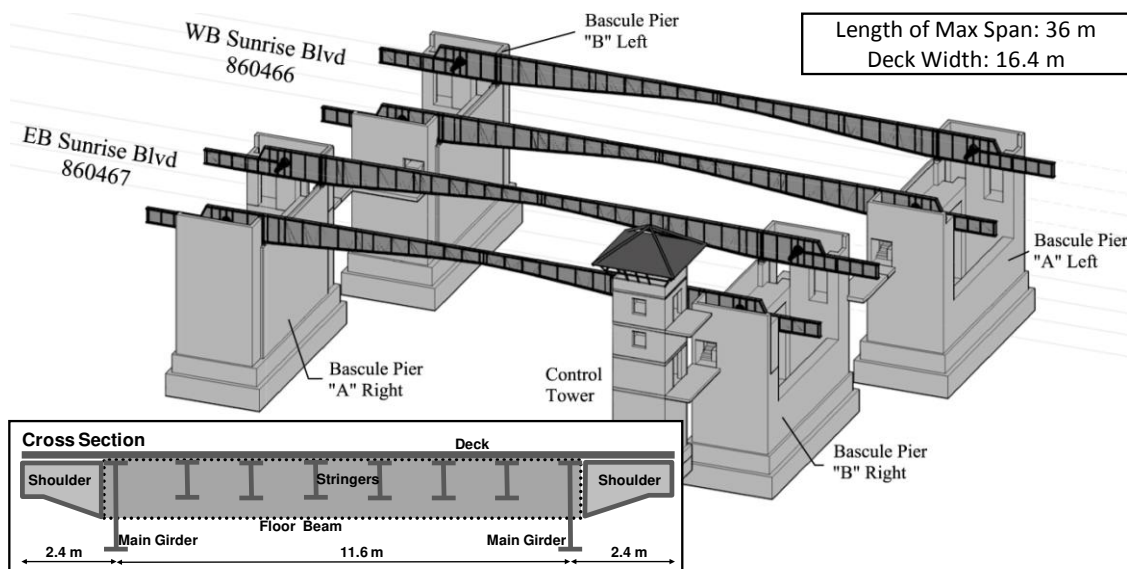
Figure 9: 3-D CAD model of the movable bridge

21

There are a number of bridge superstructure components that are critical for accurately modeling the global and local behavior of the bridge. The critical structural components of the movable bridge are the main girders, where boundary conditions are imposed at the trunnion, live load shoe, and span lock locations. The trunnion is modeled as a circular element connected to the main girders with rigid links. This rigid region representing the trunnion-hub-girder assembly is assumed to include the effects of the stiffeners at the trunnion. The connection between the two spans is also modeled using rigid links, transferring only shear forces between the two leaves, which is the desired function of the span lock (SL). The rigid links in this area are modeled with the assumption of no restraint in the axial direction considering the design specifications and investigations in the field. The live load shoe (LLS) is defined as pin supports, since the leaves rest on these elements only at the closed position.

Floor beams, sidewalk brackets, and diagonal bracings are constructed using frame elements. These elements are connected to the main girders and with each other using rigid links at the centroids. Once all secondary beams are created, the deck of the bridge is constructed. The deck is modeled using four-node quadrilateral shell elements, and it is connected to the main girders and secondary beams using rigid links based on the preliminary equivalent deck analysis. Finally, solid elements are used to model the concrete counterweight. The FEM consists of 1,084 frame elements, 720 shell elements, 32 solid elements, 963 links, and a total of 11,112 degrees of freedom (DOFs). In Figure 10, different views from the a-priori FEM are presented.

It should be noted that users of these FEMs should be aware of the uncertainties in these models, because constructing these models requires considerable time, effort, and expertise even for an a-priori model. In addition, idealized assumptions (i.e., pin, roller boundary conditions)

may have profound impacts on the structural behavior. In Chapter 6, use of these a-priori models versus calibrated models with the consideration of uncertainties in the form of a family of models is presented in a comparative fashion.

3-D VIEW (TOP)

3-D VIEW (BOTTOM)

TOP VIEW

SIDE VIEW
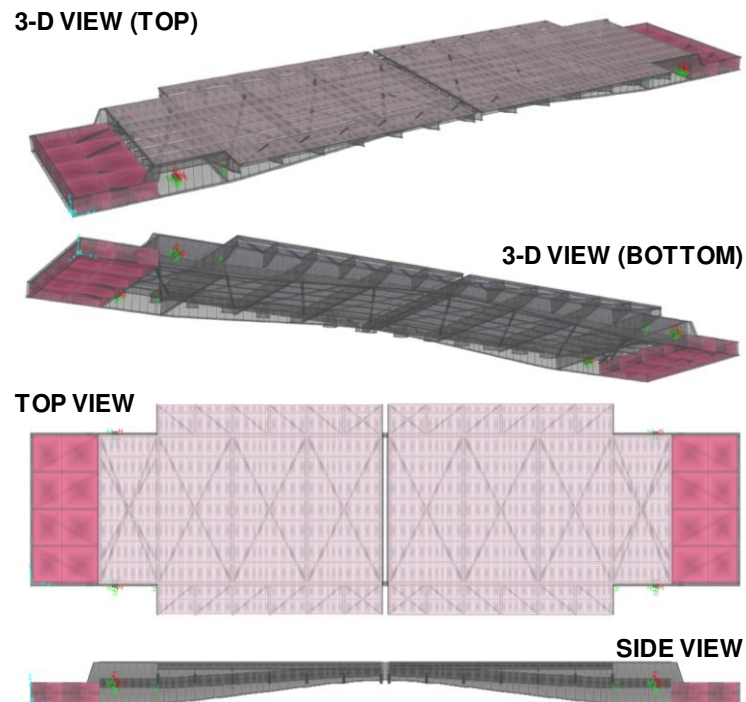
Figure 10: Different views of the Sunrise Boulevard Bridge a-priori FEM

2.3. *Experimentation*

2.3.1. *General Remarks*

Experimentation of a structure, which is the indispensable step of the St-Id process, includes loading/excitation, instrumentation, data acquisition, data quality assurance (including pre-processing), data communication/archival, and, most importantly, documentation of the overall experiment. In the past, visual inspection, testing concrete cores, and steel coupons retrieved from a structure were the only linkage to capture the condition of the constructed

systems. Now, civil engineers have many different technologies at their disposal for measuring strain, displacement, acceleration, velocity, tilt, etc. along with various non-destructive evaluation (NDE) methodologies for material- and element-level characterization.

The fundamental challenge in structural testing and monitoring is to acquire the most meaningful data and minimize the uncertainties inherent in the data due to reasons such as sensor calibration, sensor mounting, and environmental effects. As a result, it is important to recognize and define the sources of uncertainties and minimize these with more detailed and better models calibrated with experimental data.

The major constraints of an experimental program for characterizing and evaluating full-scale performance of civil infrastructure can be summarized as follows: (1) defining expected data to be used for data analysis and/or modeling, (2) duration of the experiment, (3) structural attributes that will affect the quantity and types of instrumentation used, (4) environmental and operational constraints, and (5) logistics, budget, and accessibility of the structure.

Moreover, the key components of experimental studies can be summarized as: (1) selection of inputs, their locations, and their measurement types, (2) selections of outputs, their locations, and their measurement types, (3) collecting and transferring the signals to data acquisition, (4) data storage on a local or remote computer, (5) data inspection/quality control by real time, and, if possible, (6) user interface and real-time alerting/reporting.

Experimentation can be broadly categorized as static and dynamic measurements, and it is also a critical step toward developing more reliable analytical or numerical (finite element) models in the St-Id process. These models are used to evaluate and predict in-service structural performance and to support operational and maintenance decisions. It should be noted that the

24

ultimate success of any experiment will be heavily influenced by the experience, appropriate use of technologies, and effective analysis of the data by the experimental specialists.

2.3.2. *Case Study: Monitoring of Sunrise Boulevard Bridge*

The demonstration of the experimental studies on a real structure will be carried out with a particular movable bridge in Florida. The statistical data and analysis of inspection results discussed above serve as the basis for the selection of the representative movable bridge for monitoring design and demonstration. Although movable bridges vary widely in type, dimensions, condition, and geometry, a detailed investigation of a representative movable bridge for its monitoring design considerations will serve as a benchmark. According to the distributions presented above, bascule bridges constitute by far the majority of movable bridge types. Based on this analysis and interaction with FDOT structures and maintenance engineers, the bascule bridge over Florida SR-838, known as Sunrise Boulevard Bridge (see Figure 8), was selected as the representative bridge for monitoring applications, considering its type, span length, age, opening frequency, type of traffic, and accessibility. The selected representative movable span is the west-bound span of two parallel spans on Sunrise Boulevard in Ft. Lauderdale, Florida.

Sunrise Boulevard Bridge is a common bascule type, with a rack-and-pinion mechanism. The bascule leaves are rotated at the point of the trunnions, which are the pivot points on the main girders. The counterweight of the main girder stays below the approach span deck in the closed position. The weight of the span is balanced with a cast-in-place concrete counterweight that minimizes the required torque to lift the leaf. When the bridge is opening, the leaves rotate

upward, and the counterweight goes down. The electrical motor generates the driving torque, which is then distributed to the drive shafts via the gear box. The gear box involves an assembly of gears operating similar to automobile differentials and provides equal lifting of both sides. The drive shafts transmit the torque to the final gear, called the pinion, which engages the rack assembly and is directly attached to the main girder. In the closed position, the girder rests on a support called "live load shoe" on the pier, and traffic loads are not transferred to the mechanical system. In addition, two-leaf bascule bridges have a locking device at the tips (span locks) and are arranged to act as cantilevers when closed. The span locks keep the ends of the leaves from bouncing as traffic passes over the bridge (Koglin 2003). The movable bridge also involves fixed components, such as reinforced concrete piers and approach spans. Issues with all of these structural, mechanical, and electrical components will be discussed in detail with measurement strategies in the following section.

Operation of the movable bridges, the most common problems, the condition ratings of components, and the number of occurrences based on inspection reports were presented in previous sections. In this section, the inspection information is combined with the expert opinions of bridge engineers, FDOT officials, and consultants for specific issues and possible monitoring needs of a movable bridge. The kinematic behavior of a movable bridge is the main reason for significant drawbacks and problems associated with its operation and performance. These bridges have high maintenance costs associated with the complex operation system, mechanical parts requiring special expertise, and deterioration causing more extensive repair. In addition, the maintenance of the movable bridge is conducted by contractors, and the bridge owners would like to have a means to check if the maintenance is done properly and in a timely

fashion. Consequently, monitoring of components that require frequent inspection and maintenance becomes very critical. For static structures, monitoring of structural components is usually the only concern for maintenance, safety, and operations; however, for movable bridges, monitoring of the mechanical and electrical components is equally important. As a result, measurement needs can be identified based on the issues observed and discussed with experts. Figure 11, Figure 12, and Figure 13 provide an overview of some of the issues with corresponding instrumentation as identified from the inspection reports and expert opinions from several meetings and site visits. Data analysis methods and expected outcomes for structural, mechanical, and electrical components, as well as operational and environmental effects, are developed based on the issues and related measurement needs. With the expected outcomes outlined in these figures, it is anticipated that maintenance can be condition-based in a proactive manner, saving time as well as labor costs. It should be mentioned here that cost evaluation is beyond the scope of this dissertation. Finally, the root causes of the structural and mechanical problems can be determined, and future designs can be improved using the information generated by the monitoring system.

Structural Components		Issues	Installed Sensors	Data Analysis Methods	Expected Outcome
Live Load Shoes		•Loss of contact, pounding, impact loading on the shoes •Corrective action in case of high impact loads •Fully/Particularly seated girders	•Strain Rosette •Accelerometer •Dynamic Strain Gage •Vibrating Wire Strain Gage	•Dynamic analysis in time and frequency domain	•Calculate the shear at the live load shoe for load rating •Track condition of live load shoe and shims
Girder & Beam & Stringer		•Section loss due to corrosion •Bending, deformation, misalignment •Missing fasteners, bolts	•Accelerometer •Dynamic Strain Gage •Vibrating Wire Strain Gage •Strain Rosette	•Dynamic analysis in time and frequency domain •Strain Correlation •Time series analysis	•Monitor the stress levels •Determine the structural condition at critical and vulnerable locations •Track shear and moment for load rating

Figure 11: SHM considerations for structural components of Sunrise Boulevard Bridge

Mechanical and Electrical Components	Issues	Installed Sensors	Data Analysis Methods	Expected Outcome
Electrical Motors	•Unexpected interruption, schedule maintenance, replacement ahead of time •Predictive maintenance for replacement	•Accelerometer •Infrared Temperature •Ampmeter	•Frequency Domain Analysis •Root Mean Square Analysis	•Define baseline and track changes of acceleration, temperature and electric current •Correlate various Electrical Motor monitoring parameters for predictive maintenance
Gear Boxes	•Lubrication, wearing of the gears, load transfer within the system •Maintenance of the Gearbox	•Accelerometer •Microphone	•Frequency Domain Analysis •Root Mean Square Analysis •ANN	•Track acoustic print and the vibration characteristics to determine if the gearbox lubrication is normal and the gear condition is satisfactory
Shafts	•Load transfer within the system, differential working of shafts and loading on the system •Bridge balance, changes in friction numbers	•Strain Rosette	•Friction, Torque, Balance Calculation •Correlation analysis	•Track torque and friction values for balance problems of the counterweight •Correlate wind and temperature with torque and friction characteristics
Open Gears & Racks	•Lubrication, corrosion, cracks, missing bolts •Determine if maintenance needed based on measurement history	•Accelerometer •Video Camera	•Image Processing •Artificial Neural Networks (ANN)	•Detect lubrication level and corrosion •Track bolt conditions of the racks
Trunnions	•Maintenance for lubrication measures from torque data •Stress monitoring around this critical area	•Tiltmeter •Microphone •Strain Rosette	•Balance Calculation •Shear, Rotation, Pressure Calculation	•Track friction over time for lubrication in the trunnion •Track shear force on the trunnion area •Track rotation of two main girders for balance
Span Locks	•Alignment problems, fatigue effects and dynamic loading leading to failure, excessive shear •Hydraulic pressure problems	•Pressure Gage •Strain Rosette •Tiltmeter	•Shear, Rotation, Pressure Calculation •Strain Correlation	•Check for excessive stress on the lock bar •Tilt meters on the lock bars for horizontal and vertical alignment •Track condition of span lock shims and track hydraulic pressure

Figure 12: SHM considerations for mechanical and electrical components of Sunrise Boulevard Bridge

Operational & Environmental Effects Monitoring	Issues	Installed Sensors	Data Analysis Methods	Expected Outcome
	•Evaluation of environmental inputs on mechanical and structural responses for maintenance purposes •Evaluation of operational inputs on structural components	•Weather Station •Video Camera	•Time domain and frequency domain analysis •Image processing and image-sensor correlation	•Track the environmental effects on the components •Track critical traffic inputs to the structure

Figure 13: SHM considerations for operational and environmental monitoring of Sunrise Boulevard Bridge

In this monitoring application, the data acquisition equipment is installed in permanent protective and temperature-humidity-controlled enclosures located in both machinery rooms at each side of the bridge. The sensors are connected by weatherproof cables and specially designed connectors. Since the two leaves of the movable bridge are physically separated from each other, wireless communication is established to ensure data transmission between the leaves of the bridge, and two GPS units are used for synchronization. Figure 14 shows the scheme used for the data collection and transmission. It should be noted that the SHM system is controlled by two personal computers on each leaf. Data collection comprises four groups, which are as follows: (1) scheduled data collection during rush hours, (2) data collection during opening/closing, (3) on-demand data collection, and (4) trigger-based data collection.
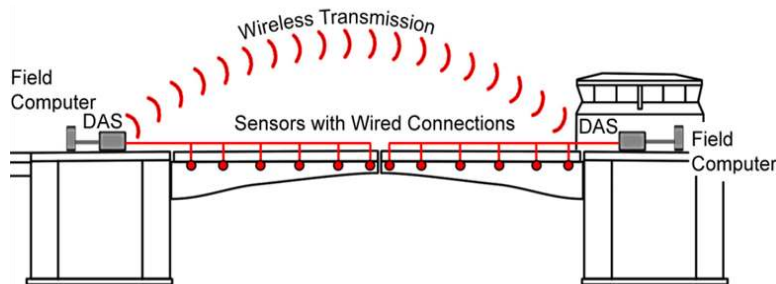
Figure 14: Sunrise Boulevard Bridge wireless communication scheme

The instrumentation plan is designed to monitor the most critical structural, mechanical, and electrical components. The current installation consists of an array of 160 sensors, which add more than 200 channels. It should be noted that the sensor count was finalized after a number of meetings and site visits with bridge engineers and researchers. The bridge engineers particularly requested extensive measurement at all critical parts. For instance, three out of six accelerometers on the gear box, two out of four accelerometers and two out of three ampmeters on the electrical motor can be considered as redundant. The detailed analysis of each sensor and sensor clusters will provide an optimum sensor count for future routine applications as all the data are processed from the monitoring system. A summary of the sensors used in the study is shown in Table 1.

Table 1: Summary of the sensor installed on Sunrise Boulevard Bridge

Sensor type	Structural Sensors	Mechanical and Electrical Sensors	Total
High-Speed Strain Gage	36	0	36
Vibrating Wire Strain Gage	36	0	36
Strain Rosette	6	16	22
Tiltmeter	4	4	8
Accelerometer	16	24	40
Pressure Gage	0	4	4
Microphone	0	6	6
Infrared Temperature	0	2	2
Video Camera	1	1	2
Ampmeter	0	3	6
Weather Station	1	0	1
Total	100	60	160

In Figure 15, the detailed geometry of the main girder and the installed sensors are shown. 3-D overviews of the mechanical room with sensor locations of different components are given in Figure 16. It should be noted that main girders are the fracture critical elements of the movable bridge. Therefore, main girders have the top priority among the structural components from the instrumentation point of view. The uses of strain gages on these components are presented in more detail in Chapters 3 and 5.
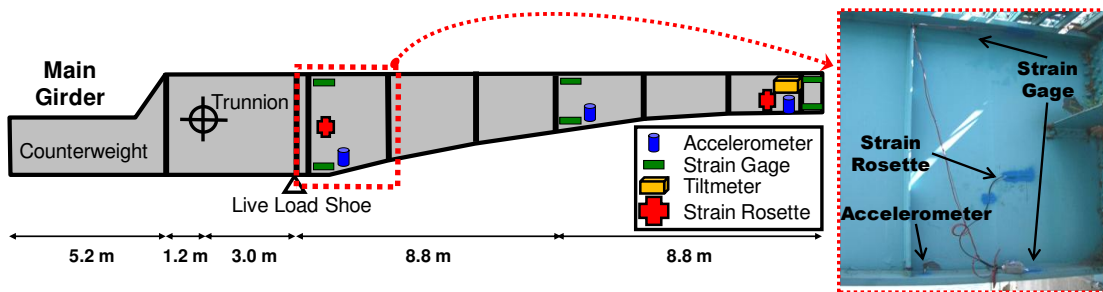
Figure 15: Sunrise Boulevard Bridge main girder and sensor locations
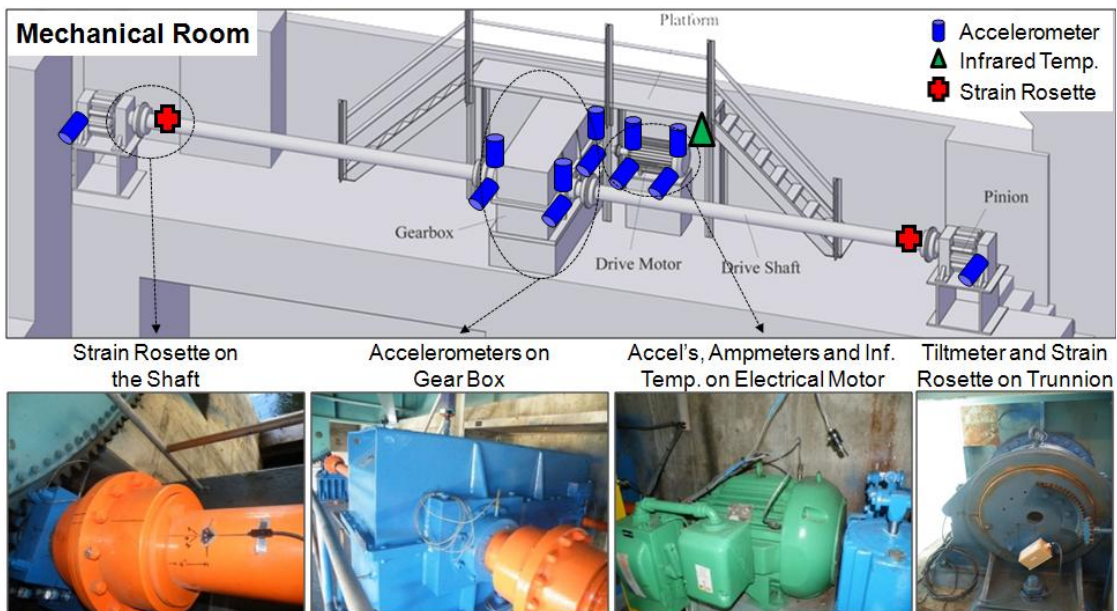
Figure 16: Mechanical room overview, mechanical and electrical components with sensors

31

Installation of the monitoring system components is illustrated in Figure 17. A specific

challenge in the implementation of an SHM system on the movable bridge is the coordination of

fieldwork with infrastructure owners and the Coast Guard in such a way that the installation of

the sensors and cables has minimal impact on land and maritime traffic. During normal

operation, the movable bridge is opened every half and full hour if requested by the boat owners.

Such interruptions increase the installation time and introduce additional delays. More details of

the Sunrise Boulevard Bridge monitoring system can be found in Catbas et al. (2010).
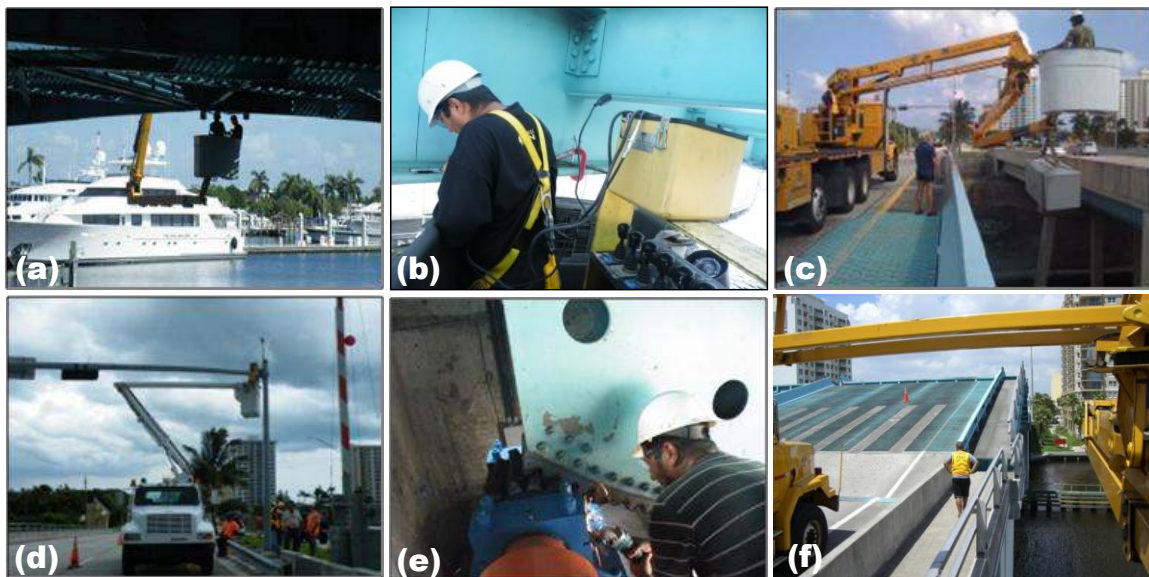
Figure 17: Field installation of the sensors, cabinets, and weather station

2.3.3. *Case Study: Field Testing of Sunrise Boulevard Bridge*

Field testing of Sunrise Boulevard Bridge can be grouped into two parts: controlled and

uncontrolled field tests. Controlled tests consist of truck load tests (Figure 18), where the input to

the structure and input location are pre-defined. The uncontrolled tests are performed when

damage is induced to the bridge and it was open to regular operation (Figure 19), that is, subject

to routine operation such as opening-closing events and under daily traffic (Figure 20). It should be noted that a detailed discussion of all these tests can be found in Catbas et al. (2010).

The load truck (see Figure 18), which has a total vehicle weight of 96.7 kips, was provided by FDOT Structures Laboratory in Tallahassee and operated by FDOT personnel. The data collection was carried out with the monitoring system that was already in place. Three separate load tests were performed (a static load test, a crawl speed load test, and a dynamic load test) in order to capture the bridge behavior in a comprehensive manner and to create a database for possible studies, such as influence line generation, dynamic allowance factors, and more reliable calibration of analytical models. The primary objectives of the static diagnostic load tests executed are to establish stress levels on various structural elements of the bridge and to validate and calibrate the FEM. In general terms, these tests are conducted by recording measurements of known loads, as well as their corresponding effects on critical bridge members, and comparing these measured load effects with values computed by an analytical model.

Figure 18: Truck load test on Sunrise Boulevard Bridge

One of the important objectives of this monitoring application of a movable bridge is to collect data that would serve two purposes: (1) to better understand the operation environment of a movable bridge, and (2) to establish criteria for system-wide monitoring of a bridge population. Long-term monitoring of the bridge is conducted to determine the operating conditions of the critical structural, as well as mechanical and electrical components. Monitoring also serves to increase the understanding of the behavior of the movable bridge and the causes of this behavior. Damage tests were conducted to establish thresholds for conditions that are critical for the maintenance and operation of the bridge. In collaboration with FDOT engineers, some of the most common structural maintenance problems are identified and subsequently implemented on the movable bridge to simulate such damage conditions (Figure 19). In Chapter 3, some of these damage tests are utilized for damage identification and localization purposes.

Figure 19: Damage tests on Sunrise Boulevard Bridge

The data from the bridge are acquired during regular data collection times, which are set to pre-established time windows for rush hour as well as triggered events. An event that triggers data collection is an opening-closing operation of the movable bridge (see Figure 20a). This operation can help to verify the dead-load-induced strains on the structure. A major data collection is carried out during regular traffic, where the input to the structures cannot be fully controlled or characterized (see Figure 20b). The vehicles on the bridge can be captured from the video frames; however, it is not possible to exactly determine the axle loadings and spacings for the validation of the FEMs. In Chapter 5, the utilization of the load tests and opening-closing operation for the calibration of the Sunrise Boulevard Bridge is presented in more detail.
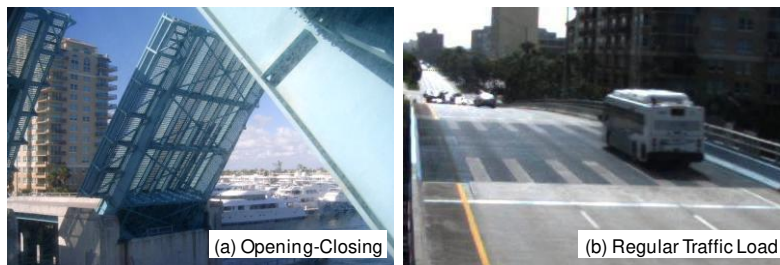
Figure 20: Uncontrolled testing of Sunrise Boulevard Bridge

2.4. *Data Processing and Direct Data Interpretation*

2.4.1. *General Remarks*

A well-designed and executed experimental program requires appropriate data processing for the interpretation and utilization of the data. In the beginning of this step, data should be prepared by cleansing the blatant and subtle errors (i.e., spikes and malfunctioning sensors), by improving the quality (i.e., averaging, filtering, and windowing), and by compressing or transforming into a more observable format (i.e., statistical and modal parameters). Then, the

optional following steps, which depend greatly on the objectives and constraints associated with the St-Id application, involves various parametric and nonparametric data analysis methods, such as artificial neural networks (Masri et al. 1996; Nakamura et al. 1998; Chang et al. 2001; Zapico et al. 2003), auto-regressive models (Shinozuka and Ghanem 1995; Sohn and Farrar 2001), and state space models (Skolnik et al. 2006).

A practical and, in most cases, effective approach is to use nonparametric models to detect anomalies in behavior. Anomalies are detected by tracking the changes in measurements with respect to measurements recorded during an initial period as a baseline or comparative analysis of moving data windows over time. In addition, these approaches, which examine changes over a certain period during the life of a structure, are completely data driven in the sense that the evolution of the data is estimated without information of physical processes. Moreover, the main advantage of these applications is the easy applicability to long-term monitoring studies due to a minimal requirement of user interaction through automated data analysis and handling large amounts of data.

It should be noted that there are critical points related to these methods. First, the researchers should always be aware that the daily, monthly, seasonally, and yearly changes in the weather and climate may greatly affect the predefined thresholds. Second, it might not be possible to directly measure every possible phenomenon of interest at every location of complex civil structures.

With the increasing need for developing better inspection and maintenance strategies for aging infrastructure, it is desirable to provide timely support from an SHM integrated condition-assessment framework (Gokce et al. 2012b). Since low-cost sensor and data acquisition systems

are now available, the attempts of such nonparametric (data-driven) methodologies are expected to increase in the following years. In the section presented below, a case study on long-term monitoring of a movable bridge is presented to illustrate direct data interpretation by tracking descriptive statistics obtained from the analysis of the data.

2.4.2. *Case Study: Identification of Unexpected Events by Long-Term Monitoring of Sunrise Boulevard Bridge*

To show the effectiveness of an SHM system on the movable bridge, two real-life events are presented for illustrating the direct data interpretation with simple yet efficient statistical approaches. The opening-closing event of the Sunrise Boulevard Bridge is shown in Figure 21, with real-life data from the trunnion tiltmeter, the span lock pressure gage, and the gear box accelerometer.

Movable bridge operation starts with the closing of the pedestrian and traffic gates, which is followed by retracting the span lock bars to open the bridge. Then, the electrical motor transfers the power to the gear box, which rotates the shaft. Next, shafts rotate open gears that are directly attached to main girders. Finally, the structural components start rotating upward. Span locks are one of the critical components of this operation (Gul et al. 2011). The issues related to the span locks and the problems that can be observed due to their malfunctioning are explored in the previous sections. To identify possible alignment problems, dynamic loading leading to failure, excessive shear, and hydraulic pressure problems, the installation of tiltmeters, accelerometers, strain rosettes, and pressure gages, respectively, is required. In this section, the behavior of each different component is identified with the help of long-term SHM data. The

general behavior of the span lock pressure data is presented in Figure 21, where the sudden increase of pressure is seen and kept almost constant for a short period of time. It is interesting to note that the flat (constant) region during span lock opening has one small peak that is barely visible when a single data set is visually inspected. However, after a large set of data is collected over a period of time, this behavior, along with the small peak, is seen with this flat region.
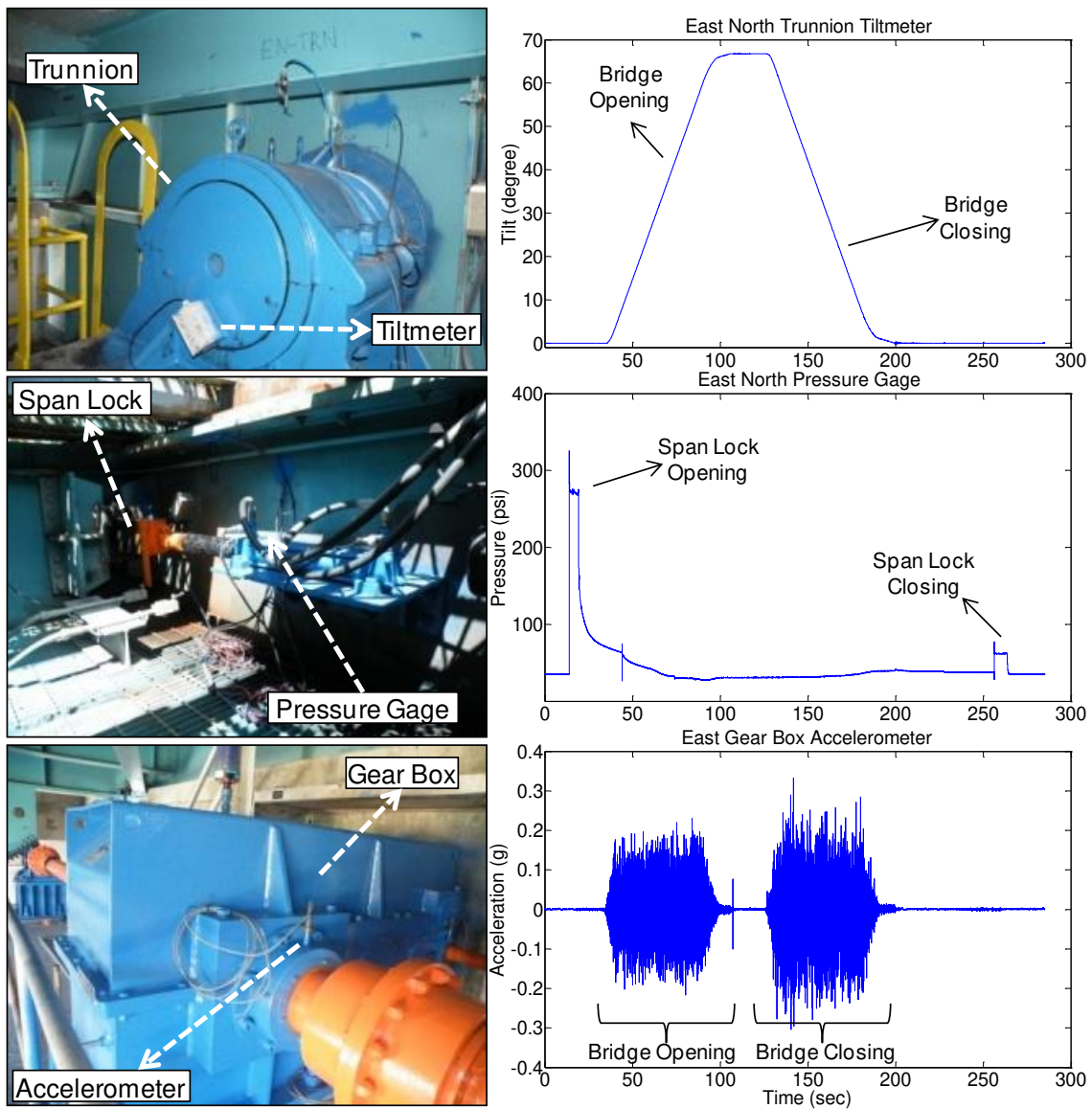
Figure 21: Representative tiltmeter, span lock pressure gage, and gear box acceleration data

After observation of this behavior, a simple data analysis can be conducted to extract features based on the statistical information for the opening part of the pressure data. When the long-term data was analyzed, an increase in the coefficient of variation (c.o.v) of the opening pressure was detected between 6/13/2011 and 6/19/2011. Based on the statistical analysis conducted over the flat region, the c.o.v. of the pressure data is found as 1% for the day of 6/12/2011. For the following days between 6/13/2011 and 6/19/2011, the variance in the pressure gage data distribution of the flat region is increased to 4%. On 6/20/2011 the c.o.v. decreased to its normal level (1%). The increase of the c.o.v. from 1% to 4% can be seen as a small change, but it should be remembered that the increase is detected only for a one-week period (6/13-6/19) of the long-term data. For the rest of the data sets consistency of 1% in the coefficient of variations are observed.

Afterward, a more detailed analysis was conducted for these dates as discussed below. Sample snapshots from these dates and corresponding behavior along with the extracted statistical information are illustrated in Figure 22. It is observed that on 6/12/2011 (7:03 PM), the span lock operates similar to previous established behavior based on the opening and closing pressure levels and flat region characteristics during span lock opening. On 6/13/2011 (11:00 AM), it is seen that the first peak is followed by another ~25 psi secondary peak, which was not observed before. On 6/16/2011 (9:58 AM), the secondary peak level increased to a ~30 psi level. On 6/20/2011 (8:59 PM), span lock seemed to be operating normally again based on the pressure data.
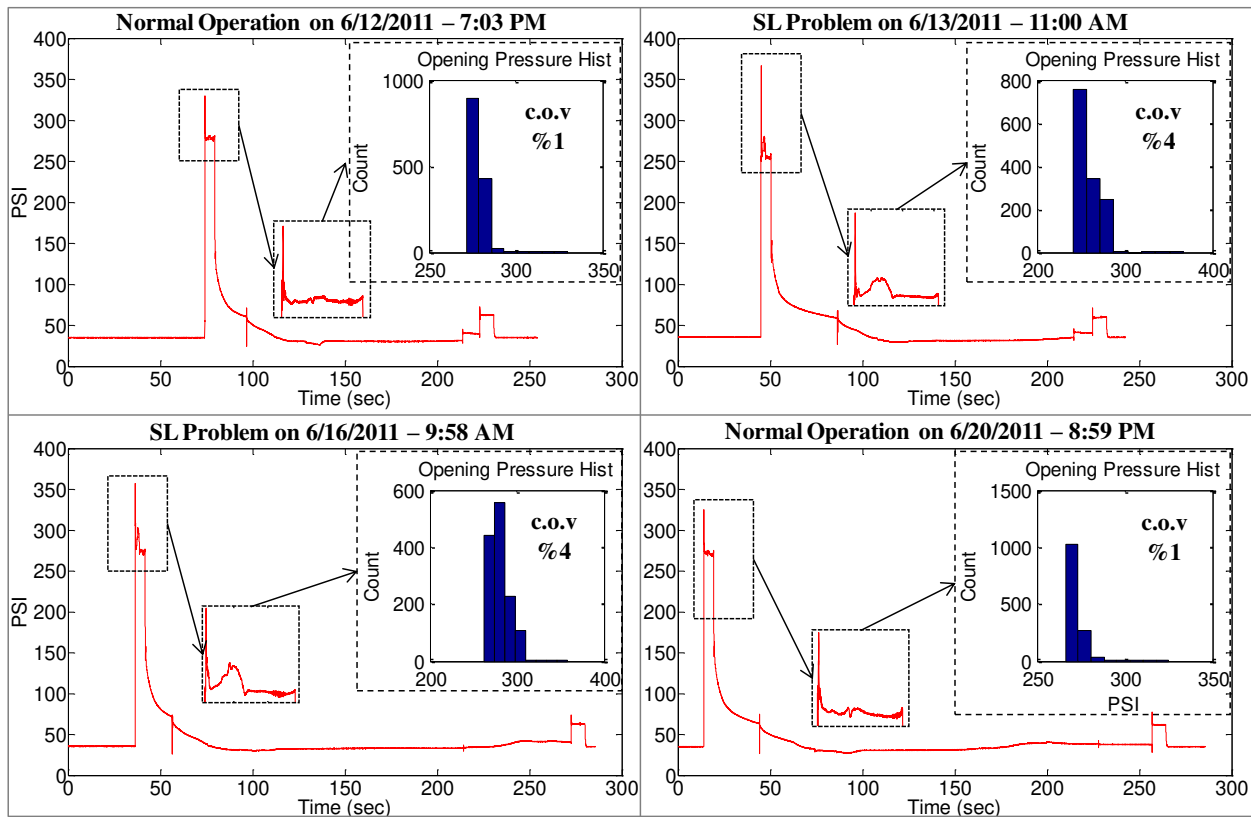
Figure 22: Behavior change of the pressure gage data

The observations of change in behavior based on statistical information are validated using the maintenance reports that are submitted to bridge owners by the contractors. A summary of this maintenance report of the corresponding month (June 2011) is given in Table 2. According to this report, maintenance crew troubleshot the span lock system and fixed the issue on 6/19/2011. In addition, it is seen in the maintenance reports that the normal preventive maintenance frequency for span lock system is one week. This crosscheck validates the observations from monitoring data and also shows the importance of an integrated SHM system, because the span lock problem occurred on 6/13/2011, and the preventive action was taken on 6/19/2011, which can cause an unexpected load distribution in the structural components during

this time. In a study by Catbas et al. (2011), it is explored that the malfunction of the span lock can cause a significant increase in the stresses that also increase the probability of failure of the main girders.

Another example for direct data analysis is presented by employing the data obtained from the gear box accelerometer during opening-closing operation. Gear boxes are critical components of the movable bridge operation, and they transfer the power to the shafts. The main issues regarding gear boxes are lubrication problems, the wearing of speed reducers, and load transfer problems due to shaft seals. Accelerometers are installed on the gear box for tracking the vibration characteristics to determine the gear box condition. The typical gear box acceleration data is also shown in Figure 21.

Table 2: Sunrise Boulevard Bridge maintenance log for June 2011

Bridge Maintenance Log					
Bridge#	860466	Month	June	Year	2011
Date	*Type of Crew*	*Time In*	*Time Out*	*Tender Initials*	*Crew Initials*
6/16	Transfield	9:00	12:30	…	…
Notes: Welding on the deck					
6/19	GSI	23:45	3:00	…	…
Notes: Troubleshoot span-lock system, replaced time delay relay					
6/19	GSI	1:30	3:00	…	…
Notes: Assist with span-lock trouble					
6/28	GSI	6:15	10:15	…	…
Notes: Weekly maintenance, replace output shaft seal on gear box					
6/28	GSI	9:00	12:30	…	…
Notes: Repair outlet in machinery room					

From long-term continuous monitoring of the gear box, it is seen that a significant increase in the vibration levels started on 6/28/2011 while tracking the statistical properties of the

gear box accelerations (Figure 23a). Before this date, the maximum vibration levels are slightly higher than 0.2 g, whereas the vibration levels increased to 0.3–0.5 g after 6/28/2011. The change in the standard deviation (0.05 g) characteristics is also shown in Figure 23a. In mechanical components of movable bridges, such as gear boxes and electrical motors, excessive vibrations are critical because these may yield to cracking, leakage, and misalignment (Catbas et al. 2011).
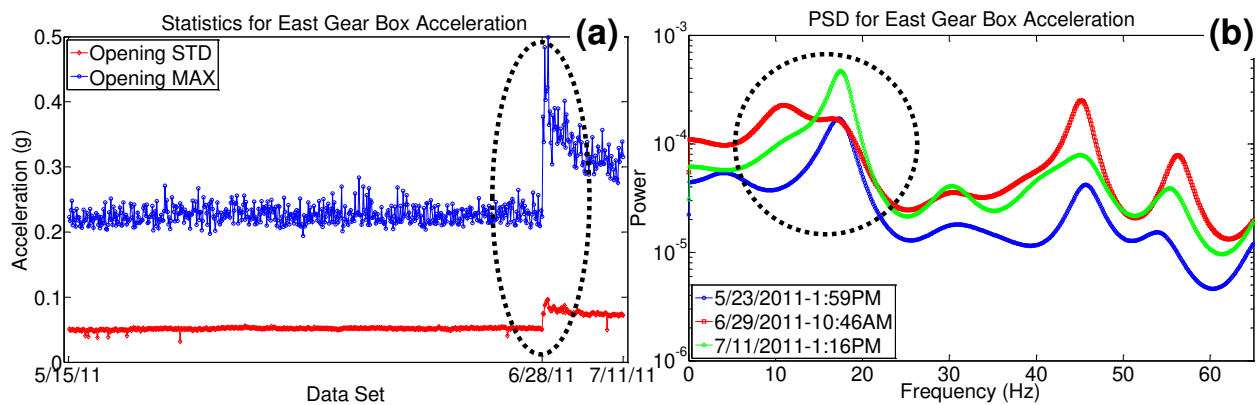
Figure 23: Gear box acceleration statistical analysis (a) and frequency domain analysis of three different data sets (b)

In addition to this observation, the frequency domain results of some data sets from 5/23/2011, 6/29/2011, and 7/11/2011 are also investigated to see the change in vibration characteristics. In Figure 23b, a change in dynamic response of the east gear box is observed, especially around 10–20 Hz bandwidth. The change began on 6/28/2011, and this effect can be observed from the power spectral density plots. By 7/11/2011, the change was returning to its "typical" condition. The peaks observed around 10 Hz of the gear box might be attributed mostly to its own dynamic characteristics (mass, stiffness, damping, connection to the concrete, etc.). In addition to SHM data analysis, maintenance reports corresponding to June 2011 are also

42

examined (Table 2), and it is seen that on 6/28/2011 during the scheduled inspection, the maintenance crew replaced the output shaft seal on the gear box, which changed the vibration characteristics at this location. It is also noteworthy to indicate that this preventive maintenance action increased the vibration levels, which may directly affect the movable bridge operation. This case also illustrated that the use of SHM for maintenance is crucial, as it is possible to obtain information about the effectiveness of the maintenance. It should be emphasized that the data from visual inspections, maintenance work, and SHM can serve in a complementary manner, even cross-checking each other.

2.5. *Calibrated Models*

2.5.1. *General Remarks*

Nonparametric models can effectively identify the change in data, however, these models are not capable of identifying the root causes of the changes and cannot be used for simulations or precise predictive analysis. As a result, parametric models such as field-calibrated finite element models (FEMs) become crucial for decision-making purposes.

The general practice of using geometric models (such as an FEM) includes different levels of complexity, discretization, and detail. In this discussion, the FEMs are considered as parametric models. Such models are employed for most of the research studies as well as most of the practical applications. In rare applications involving existing structures, the FEMs are supported by the field experiments for model validation and calibration purposes.

The model calibration is mainly optimizing a set of selected model parameters to minimize the difference between the a-priori model and the experimental results. Several

approaches for model calibration/updating process can be considered based on the selection of the parameters to identify, the formulation of the objective functions to minimize error between the model and experimental results, the optimization approach, and addressing the uncertainties both in model and measurement data.

The other common issue related to the calibration studies is the validation of the model. It should be noted that model calibration and model validations are two separate tasks. Calibration of a model that has not been validated is likely to lead to results that do not represent real structure behavior. For this purpose, different field tests should be conducted, and these different measurements should be used with multi-objective criteria for validation of the model.

In certain cases where more accurate analysis is warranted with detailed models that are also calibrated with field data, it is also important to recognize the uncertainties in the model, engineering assumptions, and idealizations, as well as the uncertainties in the data. For example, to predict the remaining life of a bridge under increasing load and deterioration due to aging, a calibrated model can provide better results, yet it is clear that the results cannot be deterministic due to the uncertainties as well as the nature of the predictive analysis. As a result, such structural models are defined in a probabilistic sense.

2.5.2. *Uncertainties*

The uncertainties in the analytical and experimental steps need to be considered for improved decision making based on the results obtained from nonparametric or parametric models used for St-Id. There are two broad types of uncertainty. The first type is the aleatory uncertainty, which is associated with natural randomness and cannot be reduced or eliminated.

An example of aleatory uncertainty is the uncertainty in natural events, such as wind speed and direction and earthquake loads. The second type is the epistemic uncertainty, which is associated with imperfect knowledge due to a lack of data or crude models (Ang and De Leon 2005). This type of uncertainty can be reduced by improving the accuracy of models, having more data, and better utilizing the data. Possible sources of uncertainties related to modeling and monitoring structures are shown in Table 3.

Table 3: Possible sources of uncertainty

Structural Sources	Data Acquisition
* Interactions and correlation between different components * Non-stationarity * Structural nonlinearity * Intrinsic stresses, redundancy, local deterioration * Boundary and continuity conditions	* Dynamic range of the system * Interferences and spurious energy input * Spatial aliasing * Asynchronous filters * Noise & Bias * Bandwidth
Loading and Input	Sensor Uncertainty
* Load-structure interaction * Amplitude and frequency content of the loading function * Spatial location * Directionality * Duration * Non-stationarity	* Range & Resolution * Sensitivity * Hysteresis * Repeatability * Linearity * Noise * Precision & Accuracy

As indicated previously, St-Id steps such as a-priori modeling, experimentation, and model calibration are often governed by different sources of uncertainties. Soil-foundation interaction, sub- and superstructure interface, randomness in external loading, and non-stationary behavior due to aging are some of the challenging issues related to the structural modeling, monitoring data analysis, and model calibration using monitoring data. In order to ensure a

successful St-Id application, proper consideration of uncertainties into St-Id framework is essential. Consideration and incorporating uncertainty is becoming crucial, especially for aged civil structures as the safety margins diminish over time and the need to better quantify the load carrying capacity or reliability becomes more critical. Another important aspect is the availability of experimental and computational technologies. For example, it is becoming more feasible to employ methods such as Monte Carlo techniques, where large numbers of models can be utilized.

2.5.3. *Family of Models*

For St-Id of real-life structures using field-calibrated models, it is assumed that a single calibrated model reflects the global (i.e., mode shapes, frequencies) and local (i.e., stresses, displacements) behavior of the structure within the specified threshold error (Brownjohn et al. 2000; Zhang et al. 2001; Teughels et al. 2002; Jaishi and Ren 2005; Sanayei et al. 2006; Bell et al. 2007b). However, the uncertainties especially related to civil structures are unique and need to be considered depending on the level of accuracy needed for the particular St-Id application. In the most general sense, a civil structure changes its behavior over time not only due to deterioration but also due to environmental effects, which makes civil structures time variant. As a result, it is quite difficult to expect that a model, which is calibrated with monitoring data collected from a certain time window, can represent the structure under all conditions and effects. It is well-established that the structural dynamic characteristics (i.e., structural frequencies, mode shapes) used for calibration vary over time. As such, even a well-calibrated single model may not be a full representation of the current condition due to the uncertainties as

well as the time-variant nature of the structure. On the other hand, a population of models can be more appropriate and promising if such variations in the structure (i.e., change in boundary conditions) and uncertainties in various parameters are considered.

Use of a population of models has been also proposed in the literature in order to consider uncertainties in model development and calibration. Some researchers focus on Bayesian approaches for model updating studies on numerical examples (Beck and Katafygiotis 1998; Katafygiotis and Beck 1998; Papadimitriou et al. 2001). In these studies, researchers mainly discuss identifiability of multiple calibrated models, and they illustrated a Bayesian probabilistic framework on the identification of parameter sets for different candidate models. In a following study, Beck and Au (2002) proposed an adaptive Markov chain Monte Carlo simulation approach to evaluate the probability of failure on a two-dimensional FEM of a two-story one-bay moment resisting frame for identifiable and unidentifiable cases. Here, the identifiable cases refer to cases where the number of model parameters is less than the number of effective constraints, and the unidentifiable cases refer to where the number of model parameters is larger than the number of effective constraints. Beck and Au (2002) indicate that the complexity and computational effort will grow since the difference between the number of parameters and the number of constraints increases. Therefore, it is desired to have a calibration methodology that can effectively update the models for the unidentifiable cases.

Moreover, other researchers took different approaches for identifying multiple models for structures. For instance, clustering, which is a powerful data mining technique, was employed to obtain the topology of the candidate model space (Saitta et al. 2008). In that study, cluster centers provide the candidate models that can represent the structural behavior. In another study

by Robert-Nicoud et al. (2005b), stochastic global search algorithms were utilized to generate a set of candidate models that satisfied the threshold error level between the model predictions and measured values. In this study, it was shown that the increase of sensor information can reduce the number of candidate models and this reduction directly affects the system identification process. For this reason, more measurement information can directly reduce the number of candidates, but the difference between prediction and measurement still remains for the best candidate model. Therefore, SHM data collected from various sensors during controlled and uncontrolled tests is crucial for reducing the number of candidate models for especially complex civil structures such as bridges with tapered sections or long span cantilever truss bridges. Additional multiple- and candidate-model studies can be found in the literature (Robert-Nicoud et al. 2005a; Smith and Saitta 2008; Kripakaran and Smith 2009; Goulet et al. 2010).

In this dissertation, uncertainties will be incorporated in a representative set of models, and the results from these models will be employed. With the developments in the software and computational technologies enabling us to perform large numbers of FEM simulations more practically, it is possible to generate a large set of models (it will be refereed to as *family of models* from now on) to represent variations, as well as uncertainties, in the modeling and measurements. Some of the reasons for using a family-of-models approach can be summarized as follows:

- Complex civil structures do exhibit non-stationarity due to environmental effects, which also leads to nonlinear behavior as the structural response changes over time. In addition, many structures may have a nonlinear response that can be represented with a piece-wise linear approximation. For example, the boundary conditions at the supports and piers have been

observed to vary in different seasons in a nonlinear manner due to material properties and soil-structure interaction, as well as friction at the continuity conditions (Catbas and Aktan 2002; Catbas et al. 2007). In other words, the nonlinear response can be represented using the linear response coupled with some uncertainty. Therefore, a family-of-models approach can be expected to characterize a structure over its operating conditions by providing a non-deterministic prediction with the incorporation of possible uncertainties in different steps. However, it should be noted that a nonlinear structural analysis or a nonlinear parameter identification is beyond the scope of this dissertation.

- While monitoring of structural systems can provide data that can be used to predict future performance, it may not be always feasible to conduct certain controlled tests (i.e., static and crawl-speed load tests on bridges) multiple times over time to generate a distribution for response. Repeatability of such tests may not be feasible or practical for St-Id on real-life structures. A family-of-models approach may be a more practical option for such applications.

- While multiple-model St-Id studies provide concepts of candidate models, the use of numerous models for determining some of the practical engineering concepts, such as the load rating of bridges, or more advanced concepts, such as system-level reliability with the consideration of correlation of different components with each other, were not explored for real-life structures.

- In the worst-case scenario for performance prediction of real-life structures, real-life data may be very scarce, limited, or even not existent. With the use of a family of models, it might

be possible to consider uncertainties, correlations, distributions with a realistic assumption, and as a result, system reliability bounds can be obtained for performance predictions.

- In bridge engineering, load ratings are calculated using idealized FEMs by defining HL-93 loads based on AASHTO specifications. The HL-93 loads, which include truck and lane loads, are considered imaginary loads, and they do not exist in real life. In addition, weakest-link failure is considered in load-rating applications instead of redundancy. This bridge performance metric is also utilized for decision-making purposes, such as retrofit, repair, and load postings. In this dissertation, load rating is also presented in a probabilistic manner based on a family of models, and this can provide the upper and lower bounds by incorporating the uncertainties to benefit the bridge engineers for utilization decisions.

- Uncertainty incorporation through a family-of-models approach is more suitable especially for bridges that have less redundancy due to fracture-critical members (i.e., span locks of movable bridges, hanger elements of long-span bridges), bear high operational importance (i.e., movable bridges that are critical members of highways and waterways), are deteriorated, and seem to perform for demands approaching capacity.

2.6. *Utilization for Decision Making*

2.6.1. *General Remarks*

The last step of the St-Id framework is the utilization of the data and/or models for decision making (i.e., maintenance, repair, or replacement for the civil infrastructure) based on

some type of decision metric. These decisions can be made by utilizing calibrated (parametric) or trained (nonparametric) models.

It is possible to establish different metrics in terms of structural behavior, damage features, or other metrics related to loading and resistance of a structure. In this dissertation, two main performance metrics are employed for decision-making purposes. The first is load rating, which is commonly used for bridge engineers, and the second is structural reliability, which is a measure of probability of failure/survival of a structure. Both of these metrics incorporate load and resistance and are commonly used in various engineering applications as detailed in the following.

2.6.2. *Load Rating*

The load rating of a bridge can be expressed as the ratio of the critical live load effect to the available capacity for a certain limit state. Load ratings represent a quantitative measure of identifying the need for load posting and/or bridge strengthening, as well as for making overweight vehicle permit decisions. The final load rating represents the rating of the weakest point within the bridge members. The load rating is commonly used for bridge engineering practice and is also described in AASHTO LRFD Bridge Design Specifications (2004). Depending on the load rating needed, it may not be necessary to perform each of the load rating procedures. Three main load rating procedures are:

- Design load rating: The design load rating assesses the performance of existing bridges utilizing the LRFD design HL-93 loading. It can serve as a screening process to identify bridges that should be load rated for legal loads. The design load rating can be performed at

two levels: inventory and/or operating level. The inventory load rating, which is the higher rating, is performed at the same design level reliability adopted for new bridges. A bridge that passes the design load check at the inventory level will have a satisfactory load rating for all legal loads. The operating load rating is performed at a lower reliability, which is comparable to the operating-level reliability inherent in past load rating practices.

- Legal load rating: The legal load rating is a second level rating and is for bridges that do not have sufficient capacity under the design load rating. Legal load rating establishes whether there is a need for load posting or strengthening. It determines the safe load capacity of a bridge for the AASHTO family of legal loads and state legal loads, using safety and serviceability criteria considered appropriate for evaluation.

- Permit load rating: The permit load rating checks the safety and serviceability of bridges in the review of permit applications for the passage of vehicles above the legally established weight limits. Since this is a third level rating it should only be applied to bridges having sufficient capacity for AASHTO legal loads.

One of the most common methods for determining a load rating for a bridge is through an analytical method (such as beam-line analysis) by utilizing a simple model. However, as discussed in the literature, these simplified methods commonly result in conservative load ratings (Catbas et al. 2012c). If these simplified rating calculations result in load posting of a bridge or restriction to permit vehicles, more accurate 3-D models may be developed, or load tests can be conducted, to better assess the load-carrying capability of the bridge. For certain types of bridges, such as arch bridges and bridges with tapered sections (as seen in Sunrise Boulevard Bridge), load rating calculation using a model and field measurements may not be a trivial task

due to the fact that critical load placement may vary for different sections (Garrett 2007; LeBeau and Wadia-Fascetti 2007).

In this dissertation, the load ratings that are presented in the upcoming chapters are calculated based on the HL-93 loading, which includes HL-93 truck (72 kip) and HL-93 lane load (0.64 kip/ft) according to the AASHTO Guide (2004). The load factors change according to the type of load rating (i.e., inventory or operating load rating); only the inventory load ratings are presented in this dissertation. The general formulation for the rating factor is:

$$LR = \frac{C - \gamma_{DC} \times DC - \gamma_{DW} \times DW \pm \gamma_P \times P}{\gamma_{LL} \times LL \times (1 + IM)} \tag{2.1}$$

where C is the factored load-carrying capacity, DC is the dead load of structural components, DW is the dead load of the wearing surface, P is a dead load concentrated at a single point, LL is the live-load effect, IM is the impact factor (33% is used), and γ's are the safety factors.

2.6.3. *Component and System Reliability*

The second metric that is employed for decision-making demonstration in this dissertation is the reliability index, which can be defined as the probabilistic modeling of capacities (R) and demands (S) under a given limit state. In other words, reliability is a probabilistic measure of assurance of safe performance (Ang and Tang 1984). As an illustration, if R and S are defined by probability distribution functions (PDF), such as $f_R(r)$ and $f_S(s)$, the probability that S will not exceed R, $P(R>S)$ represents the reliability of the structural component. If R and S are statistically independent, the probability of failure, $P(R<S)$ can be defined as:

$$p_F = \int_0^\infty F_R(s) f_s(s) ds \qquad (2.2)$$

where $F_R(s)$ is the cumulative distribution function (CDF) of R. Then, the reliability can be expressed as:

$$p_S = 1 - \int_0^\infty F_R(s) f_s(s) ds \qquad (2.3)$$

In another case, if R and S are not independent, the probability of failure can be formulated in terms of joint PDF of the random variables R and S, $f_{R,S}(r,s)$, as:

$$p_F = \int_0^\infty \left[\int_0^s f_{R,S}(r,s) dr \right] ds \qquad (2.4)$$

Another important concept in reliability calculations is the safety margin ($M=R\text{-}S$) which can be defined as the difference between the capacity and demand. The safety margin is also a random variable with PDF, $f_M(m)$, and the probability of failure can be expressed as:

$$p_F = \int_{-\infty}^0 f_M(m) dm \qquad (2.5)$$

From the assumptions about distributions of R, S, and M, it is observed that the reliability is a function of the ratio (μ_M / σ_M), which is the safety margin expressed in units of σ_M and called the reliability index. In other words, generalized reliability index (β) is the distance from the tangent plane of the failure surface; it can be expressed as:

$$\beta = \frac{\mu_M}{\sigma_M} \qquad (2.6)$$

where μ_M and σ_M are the mean and standard deviation of the safety margin, respectively. If R and S are statistically independent and normally distributed, Eq. (2.6) becomes

$$\beta = \frac{\mu_R - \mu_S}{\sqrt{\sigma_R^2 + \sigma_S^2}} \qquad (2.7)$$

where μ_R, μ_S and σ_R, σ_S are the means and standard deviations of the capacity and demand, respectively. Moreover, depending on the first-order approximation, the reliability index can be calculated as:

$$\beta = \Phi^{-1}(p_S) = \Phi^{-1}(1 - p_F) \qquad (2.8)$$

where Φ^{-1} is the inverse of the standard normal CDF. Furthermore, the limit state function is directly related to the safety margin ($M=R\text{-}S$), but the capacities and demands may consist of several variables. For generalization of the concept, the safety margin (M) is formulated as a state function, $g(X)$, by Ang and Tang (1984):

$$g(X) = g(X_1, X_2, ..., X_n) \qquad (2.9)$$

where $X=(X_1, X_2,..., X_n)$ is a vector of design variables. If the state function is positive, $g(X) > 0$, it is called the safe state. If the state function is negative, $g(X) < 0$, it is called the failure state. Lastly, If the state function is zero, $g(X) = 0$, it is called the limit state, which will be utilized in the following chapters.

System reliability is a major concept in reliability analysis, because individual limit-state functions are assembled together in a system model. The failure conditions are determined by the system model, since failure of one or two members may not be important due to redundancy. On the other hand, there may be critical components (fracture-critical) which have to stay intact for the structural integrity of the whole system.

System reliability can be modeled with certain considerations such as assembling the failure limit states as parallel or series links after determining the failure modes. In a series

systems (Figure 24a), failure of any of its components constitutes failure of the entire system.

The probability of failure of a series system can be expressed as the probability of the union of

component failure events:

$$P_F^{sys} = p\left(\bigcup_{i=1}^{N}\{g_i(\boldsymbol{X}) \le 0\}\right) \tag{2.10}$$

The probability of failure of any system depends on the correlation among the safety

margins of the components. The probability of failure of a series system in the perfectly

correlated case is as follows:

$$P_F^{sys} = max(p_{F_i}) \tag{2.11}$$

whereas the probability of failure of a series system in the statistically independent case is as

follows:

$$P_F^{sys} = 1 - \prod_{i=1}^{N}(1 - p_{F_i}) \tag{2.12}$$
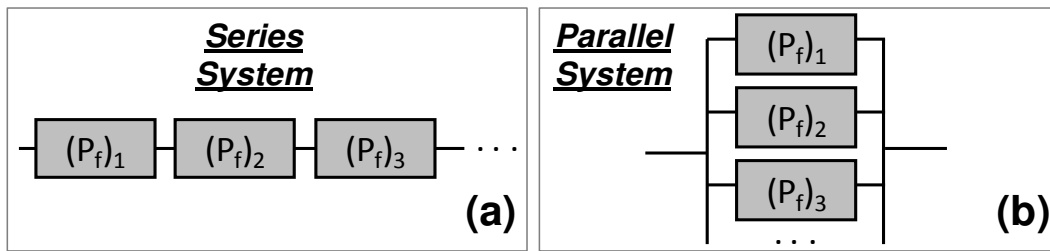
Figure 24: Series (a) and parallel system (b)

On the other hand, failure of a parallel system requires failures of all its components

(Figure 24b). The probability of failure of a parallel system can be expressed as the probability

of the intersections of component failure events:

$$P_F^{sys} = p\left(\bigcap_{i=1}^{N}\{g_i(\boldsymbol{X}) \leq 0\}\right) \tag{2.13}$$

The probability of failure of a parallel system in the perfectly correlated case is as follows:

$$P_F^{sys} = min(p_{F_i}) \tag{2.14}$$

whereas the probability of failure of a parallel system in the statistically independent case is as follows:

$$P_F^{sys} = \prod_{i=1}^{N}(p_{F_i}) \tag{2.15}$$

A combined system can be modeled as a series system of parallel subsystems. Evaluation of a system model is performed by reducing first the parallel components. Then, the reduced series system is evaluated. Calculation of the bounds for the reliability of series, parallel, and combined systems can be found in Ditlevsen (1979). Additional information on the effect of the correlation of components on system reliability and the use of different system models can be found in Liu et al. (2009) and Kim and Frangopol (2011c). Finally, there are several computer programs, such as CalREL (Der Kiureghian et al. 2006), FERUM-MSR (Song and Kang 2009), OpenSees (2009), and RELSYS (Estes and Frangopol 1998), that are developed to compute the probability of failure of combined systems.

CHAPTER 3.
NONPARAMETRIC STRUCTURAL ASSESSMENT

3.1. *Introduction*

Application of SHM to civil infrastructure systems such as buildings, roads, dams, and bridges is relatively recent compared with applications to aerospace and automotive structures. For civil infrastructures, a main focus has been on monitoring bridges for identifying condition and determining if damage exists, as well as assessing their safety and serviceability (Brownjohn et al. 1995; Aktan et al. 1996; Enright and Frangopol 1999; Dyke et al. 2003).

A structure can be monitored to obtain its global (such as vibration) and/or local (such as strain) responses. For global condition monitoring, a variety of studies utilizing vibration data can be found in the literature (Sohn et al. 2001; Catbas and Aktan 2002; Giraldo and Dyke 2004; Lynch et al. 2004; Catbas et al. 2006; Sanayei et al. 2006; Gul and Catbas 2009). On the other hand, local condition assessment, such as monitoring using strain measurements, have also been explored by many researchers such as Bakhtiari et al.(2005), Omenzetter and Brownjohn (2006), Catbas et al. (2008b), Philips et al. (2009), Li et al. (2010), Catbas et al. (2012e). In summary, the objective of local and/or global monitoring is to extract useful information for tracking the responses, identifying the deviations from the "normal" operational conditions, and/or detecting damage.

To obtain useful information about the structure and its performance, SHM data analysis approaches can be categorized as parametric (model-based or physics-based methods) and nonparametric methods (model-free or data-driven methods). While parametric methods can be useful for better physical conceptualization and also for predicting future behavior, the level of

expertise and time required to develop such models sometimes make this approach impractical (Worden 1997; Laory et al. 2011). On the other hand, nonparametric methods can be very efficient when utilized only for diagnostics (i.e., detection and localization). The idea of such methods is that only training data from the normal operating condition of the structure or system is used to establish the diagnostics(Worden and Dulieu-Barton 2004).

Consequently, nonparametric methods may not provide a physical understanding or predictive analysis; however, they are shown to be very practical to use, computationally efficient in handling large amounts of data, and efficient in detecting changes in structures in a timely manner. Among several data-driven applications, some of the studies that are closely related to the contents of this paper can be given as follows: A nonparametric approach, artificial neural networks, was employed on large-scale viscous dampers for detecting damage, and this application provided successful identification of nonlinear systems (Yun et al. 2009). Other methods, such as moving principal component analysis and robust regression analysis, were demonstrated to be useful for damage detection during continuous static monitoring of civil structures (Posenato et al. 2010). An overview of such methods was recently presented by Smith (2011) in a comparative fashion. The applicability of any parametric or nonparametric methods needs to be shown first with laboratory demonstrations and then, if possible, on real-life structures with damage scenarios to test the approaches and methodologies more reliably.

In some situations, measured data may exist, but it is not always possible to have a-priori or calibrated models in the structural identification framework. Therefore, a nonparametric study is conducted in this chapter as illustrated in Figure 25. The objective of this chapter is to employ a cross-correlation analysis method for detecting and localizing the changes in the structure due

to damage and/or a change in intrinsic stress distribution by using strain monitoring data under unknown loading conditions on the structure. This approach can be applicable to any type of structure, such as bridges, buildings, wind turbine blades, etc., where the structure is monitored over a period of time. For example, structural strain response at critical locations due to operating traffic on a bridge or response of a building structure due to ground excitation or wind-induced loading can be employed for detecting structural changes. It should also be mentioned that strain monitoring is the least expensive and the most commonly utilized measurement on bridges as well as other structures. While strain measurements can provide data that can be used in a number of ways (i.e., in relation to the yield strain levels), tracking the strain response for change/damage detection makes it essential that the loading creating that particular strain is known. A novelty of the approach in this dissertation is in employing the strain responses to detect and localize the changes and damage without the need for the input information, as this would be required for most cases with strain data.
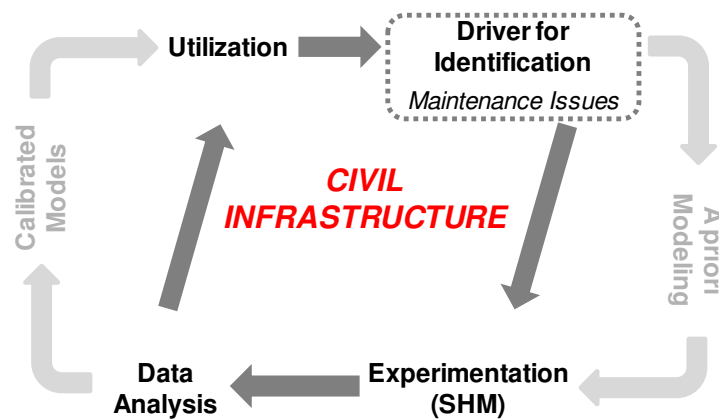
Figure 25: Use of nonparametric (data-driven) methods for St-Id of a movable bridge due to maintenance issues

Detection and localization are achieved by applying the proposed approach to track the cross-correlation matrices between the strain measurements that are spatially distributed on the critical elements of the structure. The change in the correlation coefficient between two measurement channels is related to the change in structural behavior. In addition, the correlation matrix obtained from the measurements of all channels is employed for localization. Previously, cross-correlation or moving cross-correlation has mainly been evaluated with numerical models and simple test structures. In this study, a phenomenological laboratory structure is employed for the analysis of different damage conditions, which are induced to the structure first separately and then simultaneously. A critical contribution of the study is that the method is then demonstrated on a real-life bridge in a similar fashion to the laboratory design, i.e., damage conditions are induced first separately and then simultaneously. Because it is an operating structure, the bridge is repaired shortly after damage, which allows the researchers to monitor and assess the response of the bridge after repair.

3.2. *Theory and Methodology*

Extraction of useful information from large amounts of data coming from long-term monitoring studies is always a challenging task for engineers and researchers. The data can be analyzed using a number of methods to obtain different features, including the most common statistical properties of the data, such as maximum, minimum, mean, standard deviation, and correlation.

In this chapter, correlation of the strain measurements is employed for damage identification and localization. In theory, the correlation coefficient is a measure of similarity of

two data sets and may take a value between +1 and -1. Having similar behavior in data sets gives higher magnitude correlation (values close to +1 and -1), while low-magnitude correlation (values close to 0) indicates either low or no correlated response. For continuous monitoring, the new data are appended to the raw data set, and a moving window is used to obtain the correlation coefficients between sensors for each window with the following formulation:

$$\rho_{ij}(t_n) = \frac{\sum_{k=n-N_w}^{n}(S_i(t_k) - \mu_i) \times (S_j(t_k) - \mu_j)}{\sqrt{\sum_{k=n-N_w}^{n}(S_i(t_k) - \mu_i)^2} \times \sqrt{\sum_{k=n-N_w}^{n}(S_j(t_k) - \mu_j)^2}} \tag{3.1}$$

where $\rho_{ij}(t_n)$ is the correlation between the sensors i and j at the time t_n, only for the last N_w measurements from the identified window size, n is the total number of time observations during the monitoring duration, $S_i(t_k)$ and $S_j(t_k)$ are the values of the sensors i and j at time t_k, and μ_i, μ_j are the mean values of data from the sensors i and j. The moving data can be employed in such a way that there is an overlap in the data windows selected, or the moving windows can be consecutive with zero overlap with a similar analogy that is employed in digital signal processing (i.e., averaging of ambient vibration data using Hanning windows). The window overlap can be determined based on the initial inspection of the data characteristics, duration and sampling of monitoring, and available data.

To illustrate the correlation feature, representative scatter plots of the different strain channels are shown in Figure 26. If the scatter can be bounded closely, this indicates a high correlation, whereas the opposite means a low correlation. As shown in Figure 26, the correlation between the first and second strain gage is very low, or, in other words, there is almost no dependence between these two data sets. On the other hand, the correlation is higher between the

first and third strain gage, and the highest correlation is seen between the first and fourth strain gage.
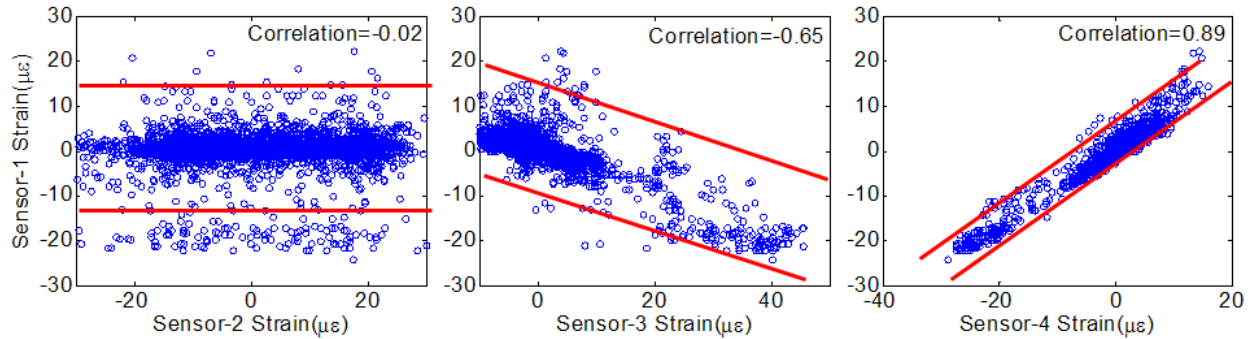
Figure 26: Scatter plots of strain channels (Sensor 2, 3, 4) versus one strain channel (Sensor 1)

The methodology is based on the premise that the correlation coefficients between two sensor signals ideally should be "constant" or "stationary" over time until a change or damage occurs in the structural configuration. The schematic representation of the methodology is shown in Figure 27. As seen in the figure, continuous monitoring data are collected from the structure. At one point, damage occurs while the monitoring data are still being collected. First, dynamic components of the sufficiently long strain data are filtered out before the correlation analysis. Then, the correlation coefficient of each channel is calculated against all the channels to form the correlation matrix for each data set.

The same procedure is repeated to obtain the correlation matrices throughout the monitoring of the structure. During undamaged and damaged periods, several sets of experimental data are collected to create a population of matrices from each data set. Finally, the set of matrices are averaged for undamaged and damaged cases, and the difference matrix is obtained by subtracting the mean matrices obtained from two cases. This difference matrix will

show whether there is a change in the correlation coefficients in each cell. After observing the changes in the cells, the whole matrix is used to detect the damage location easily by locating sensors that have the maximum change with respect to the other sensors.
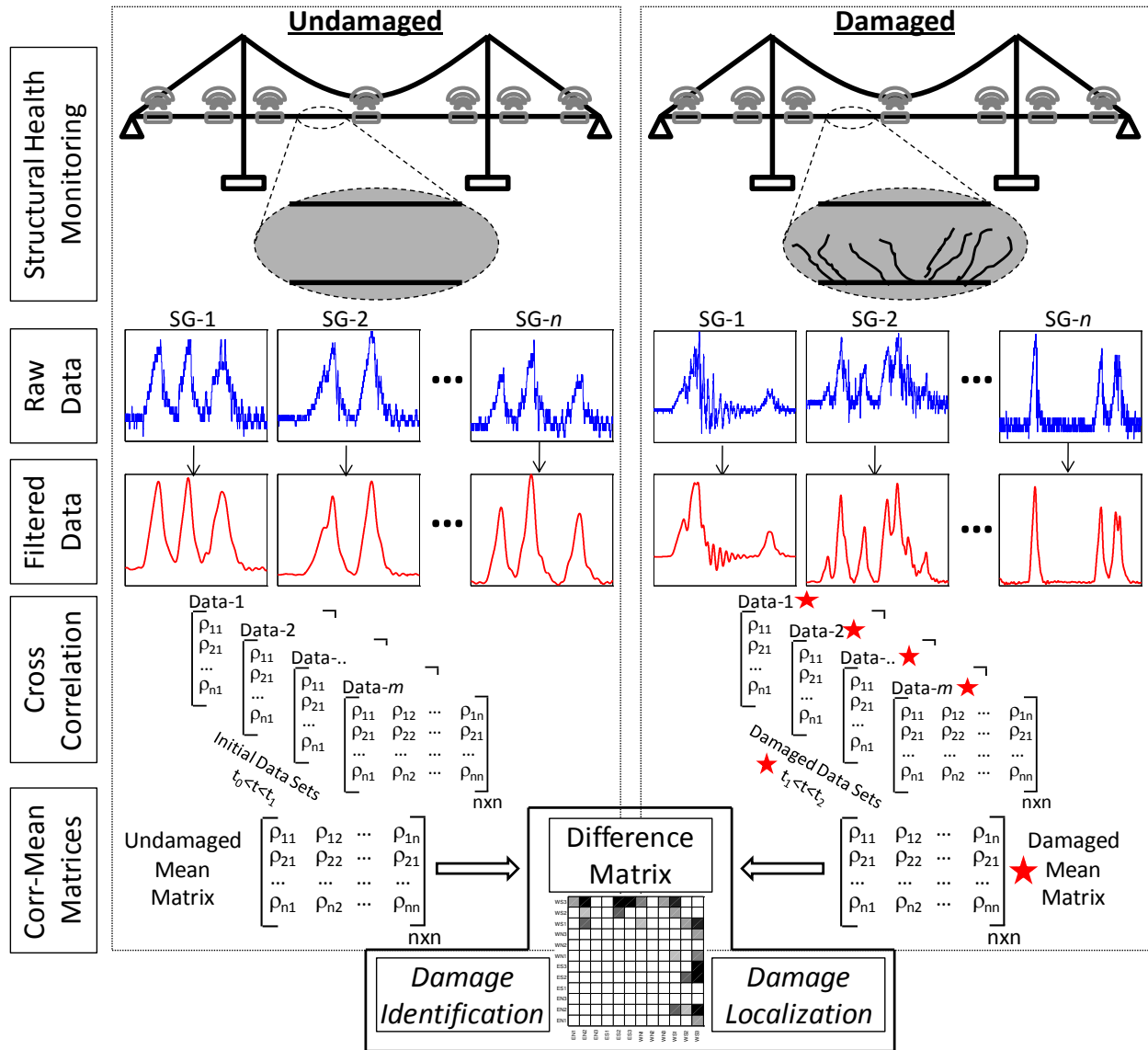
Figure 27: Overview of the correlation-based damage identification methodology

3.3. *Lab Demonstration*

3.3.1. *Test Specimen, Instrumentation, Experiments, and Data Filtering*

For the demonstration of the correlation-based damage identification and localization methodology, a four-span bridge model, which has structural response characteristics of a medium-span bridge, is employed (Figure 28). The setup consists of two approach spans (120 cm) and two main spans (305 cm) with a 3.2 mm thick, 120 cm wide steel deck supported by two 25x25x3 mm steel girders separated at 60 cm from each other. In addition, specially designed supports can be easily changed to roller, pin, or fixed boundary conditions as also shown in Figure 28.
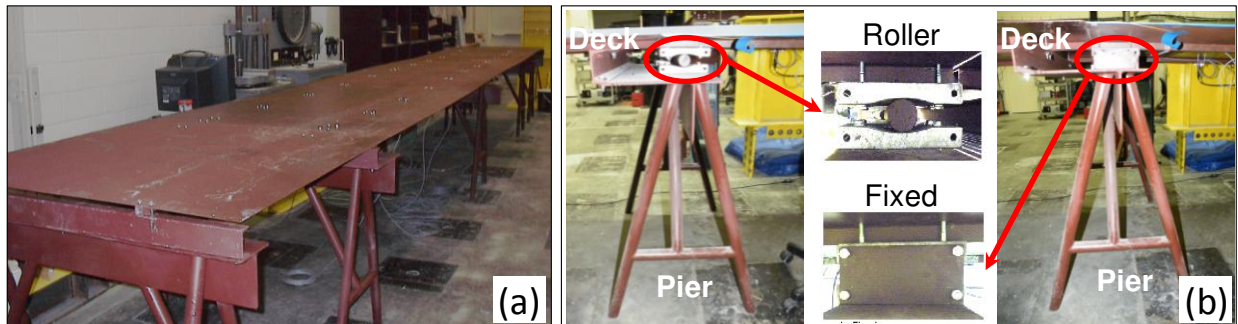
Figure 28: Four-span bridge in the laboratory (a) and different boundary conditions (b)

The four-span bridge is instrumented with various sensors, such as accelerometers (16), tiltmeters (2), a video camera (1), and strain gages (20), as shown in the instrumentation plan in Figure 29. However, only strain gage data, which is collected with a sampling rate of 250 Hz, is utilized for the demonstration of the strain correlation-based damage identification and localization. Furthermore, a two-axle radio-controlled vehicle, which has 68.7 N and 78.5 N axle loads with a spacing of 45 cm is used as a live load (Figure 30a). To obtain a population of data

sets, the vehicle crawled over the left lane of the bridge 15 times for each structural condition (baseline and damage cases).
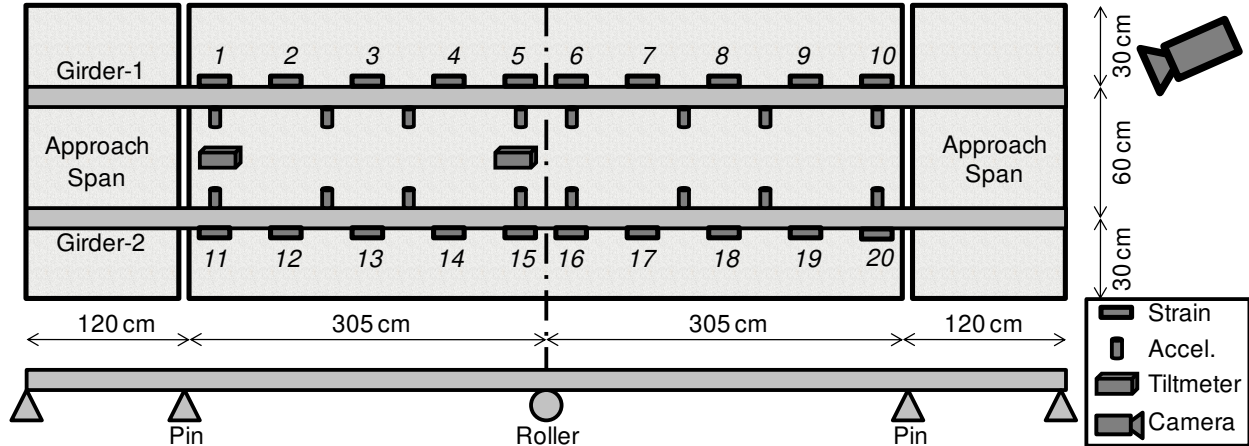
Figure 29: Instrumentation plan of the four-span bridge
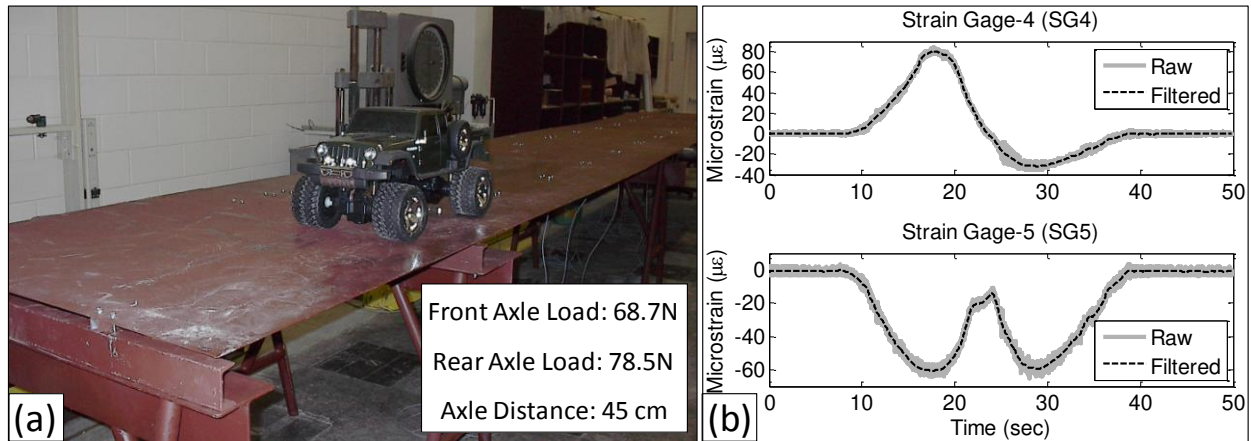
Figure 30: Four-span bridge and vehicle properties (a) and sample raw and filtered data (b)

Prior to the correlation analysis, a filter study is carried out to eliminate the dynamic effects of the traffic since this is observed to inversely affect the correlations. This may be mainly due to the dynamic strain effects being local responses as observed in strain signals, and

noise is also mostly observed in the higher-frequency bands. After a detailed filter study, it is decided to use a low pass filter with the following properties: third-order fit is selected for decreasing the computational time without losing the data behavior. In addition, the cutoff frequency is decided based on the first vertical mode of the structure to observe only the static behavior. Moreover, zero phasing and peak matching are also very important to catch the peak locations and amplitudes. In Figure 30b, typical raw strain data collected at 250 Hz and filtered strain data from the four-span bridge are presented. As observed from the figure, each test run took around 50 seconds. The average vehicle speed was 0.2 m/s during the tests. It should be noted that the duration of the signals used for correlation is many multiples of the highest period of the bridge. Although there is a decrease in the peak values of the filtered data, it is seen that the peak locations before and after filtering match, while the dynamic effects and noise in the strain data are eliminated.

3.3.2. *Damage Simulations and Results*

The damage scenarios applied on the four-span bridge model are determined based on the feedback from Department of Transportation (DOT) bridge engineers (Catbas et al. 2008a). These damage scenarios involve changes in boundary conditions corresponding to a case usually found when rollers or pinned supports of a bridge become corroded or blocked and the structural configuration of the bridge changes. These changes on the structure can cause stress redistribution, and, consequently, the structural members will be subjected to unexpected additional forces caused by this redistribution. This kind of problem is simulated on the four-span bridge model by fixing the supports as shown in Figure 28. Baseline (Case-0) and three

different damage cases (Case-1, 2, 3) for the laboratory structure are illustrated in Figure 31. More details about damage cases can be found in Catbas et al. (2012b).
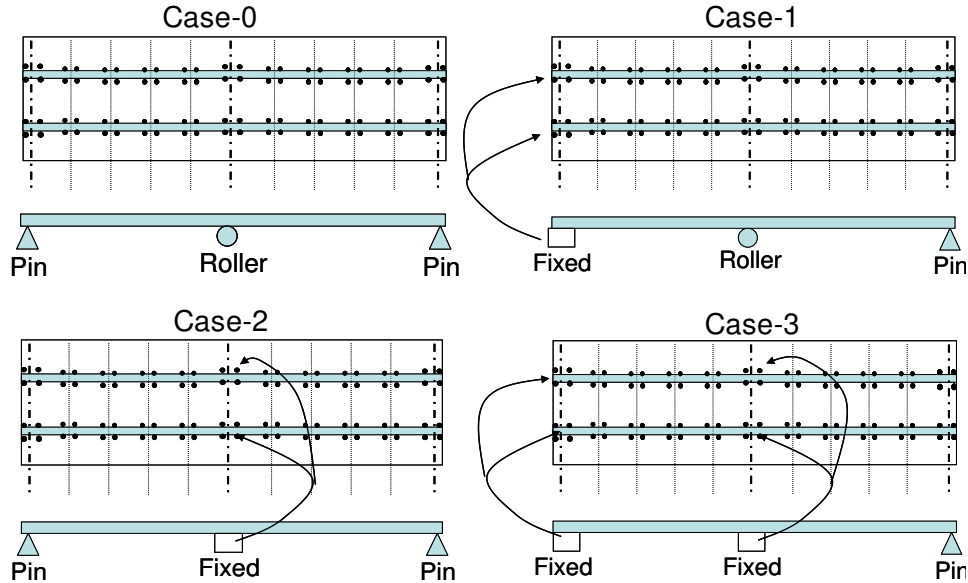
Figure 31: Baseline (case-0) and applied damage scenarios (case-1, 2, 3) on four-span bridge

Collection of 15 data sets per each case is followed by the data analysis of the proposed correlation-based methodology. First, the specially designed low-pass filter, which is described in the previous section, is applied to all the data sets to eliminate the dynamic effects on the strain channels. The cut-off frequency is decided to be less than the first vertical mode of the four-span bridge, which is around 4.9 Hz, to observe the static behavior (Zaurin and Catbas 2011). Then, the correlation matrices are generated for each data set. Due to the malfunctioning of strain gage-20, it was omitted from the study, resulting in a 19 by 19 correlation matrix for each data set. For instance, the first row of this matrix consists of the correlation coefficients between strain gage-1 and the other strain gages. The other rows are calculated in the same manner. The correlation matrix is symmetric, and the diagonal terms should be unity because the

correlation of each channel with itself is one. Fifteen matrices are generated from the 15 test runs to create a population of correlation matrices for the baseline case. The mean correlation matrix is obtained from these matrices. In the same manner, the mean matrices are also obtained for the three damage cases. Consequently, these four matrices are employed to determine the existence of structural changes and change locations in a comparative fashion. Finally, the difference matrices are investigated to better understand and interpret the changes in these matrices.

Figure 32 illustrates the damage locations for Case-1 (a), the difference matrix between Case-0 and Case-1 in an 19 by 19 matrix form (b), and the sample from the correlation data used for the cell for the correlation difference between strain gage 1 (SG1) and SG7, as well as for SG11 and SG6 (c). The correlation data clearly indicate change/damage as well as its location as the darker areas show the maximum change in the correlation coefficients for the SG1 and SG11. The change can be observed more easily in SG1 since the vehicle is moving on girder-1 (Figure 29). In addition, the damage was induced by tightening the bolts at the supports manually. The final effect of this damage cannot be expected to be identical at both supports. As a result, the change at two different supports is observed at different levels. In fact, similar results are also reported by Zaurin (2009) by using completely different data analysis methods using the same data.

To better represent the changes in the correlation coefficients, some of the cells in the difference matrix are closely investigated as seen in Figure 32c. For example, the correlation coefficient between the SG1 and SG7 was around -0.25 for the baseline tests, but this became 0.65 during Case-1 tests. The changes in the correlation coefficients are also illustrated between SG11 and SG6 (Figure 32c). The change in the correlation coefficients between different sets of

data is an indication of structural change (in this case, due to simulated damage) since the correlation coefficients are assumed to be "constant" or "stationary" under normal conditions, as seen during the baseline condition. In Figure 32c, it is seen that the difference between the mean values of the correlation coefficients is several times the standard deviation of the data, giving a confidence in change detection. This approach is demonstrated with 15 sets of data before damage and 15 sets of data after damage for the illustration of the efficacy of the method. A moving window of strain time histories can be employed to obtain the correlation coefficients for the identification and location of damage as presented in Figure 32b.

Furthermore, Case-2 and Case-3 are also clearly identified and located as presented in Figure 33 and Figure 34, respectively. In Case-2, the middle supports are fixed; therefore, the changes in the difference matrix are observed for SG5, SG6, SG15, and SG16, which are near the middle supports. When compared to Case-1, Case-2 did not introduce significant changes in the structure because the difference matrix showed relatively lower changes for Case-2. These changes can be seen in Figure 33c. Moreover, the new correlation-based methodology can identify and localize the damage for Case-3, which is a combination of Case-1 and Case-2. Sample correlation coefficient change plots between SG5 and SG15, as well as SG5 and SG18, are shown in Figure 34c. In conclusion, the methodology is validated for damage identification and localization from these laboratory studies. Validation of the new methodology with a real-life application is also carried out, and the findings are presented in the next section of this chapter.

Figure 32: Damage locations (a), difference matrix between case-0 and case-1 (b), and sample correlation data used for the corresponding cell of strain gage pairs (c)

71

Figure 33: Damage locations (a), difference matrix between case-0 and case-2 (b), and sample correlation data used for the corresponding cell of strain gage pairs (c)

Figure 34: Damage locations (a), difference matrix between case-0 and case-3 (b), and sample correlation data used for the corresponding cell of strain gage pairs (c)

3.4. *Real-Life Demonstration: Sunrise Boulevard Bridge*

Sunrise Boulevard Bridge (Figure 35a) is employed as a real-life demonstration for the validation of the correlation-based damage identification methodology. Details about the bridge description and the monitoring system were discussed in the second chapter of the dissertation. For this section of the dissertation, data from the strain gages, a total of 12 sensors, at the bottom flanges of the main girders are used to identify and locate the structural alterations with the new methodology. The data collection rate is 250 Hz, and the locations for the strain gages and corresponding nomenclatures are given in Figure 35b. For example, WN refers to West North and ES refers to East South.
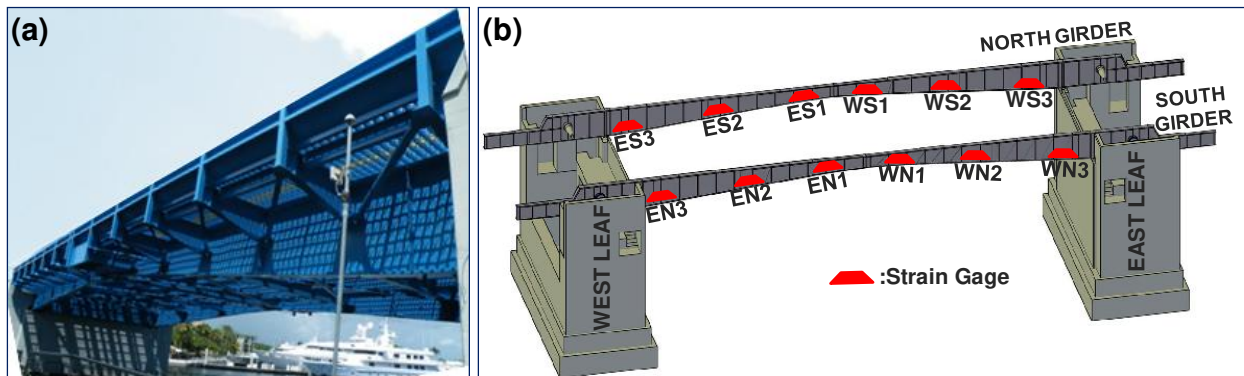
Figure 35: Sunrise Boulevard Bridge (a), strain gage locations and nomenclature (b)

The monitoring system of the movable bridge collects data during three pre-scheduled time slots (morning, early afternoon, and late afternoon), corresponding to peak hours of operation in a 24-hour period. Each data set is collected for five minutes continuously, and a representative two-minute strain-time history at the EN2 location of the Sunrise Boulevard Bridge is shown with a corresponding video frame from the monitoring camera.
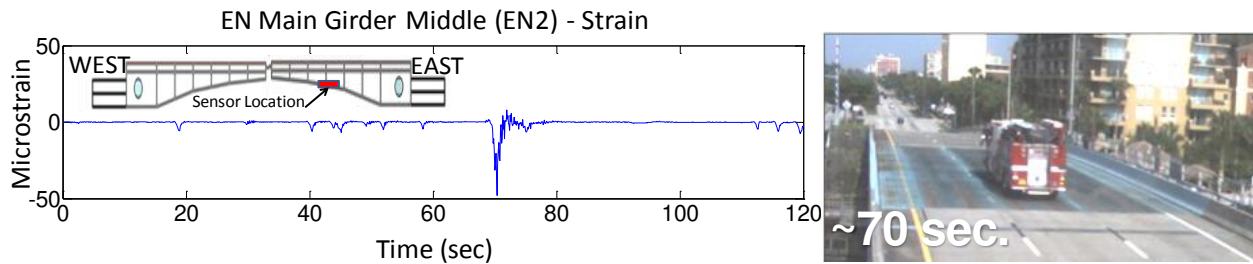
Figure 36: Sunrise Boulevard Bridge sample data and video frame

3.4.1. *Structural Changes*

Critical issues that create maintenance problems on the movable bridge, which were discussed in the previous chapters, are simulated on the Sunrise Boulevard Bridge based on the detailed investigation of the bridge inspection reports and interviews with the bridge engineers (Catbas et al. 2010). In the second chapter, some of the most common structural maintenance problems were identified as live load shoe (LLS) and span lock (SL) shim deformations. These two problems are subsequently implemented on the movable bridge separately and jointly. First, the West South LLS (WS3) shims are removed (Case-1), then the West South SL (WS1) shims are removed (Case-2), and, finally, shims from LLS and SL of West South side are removed for the combined damage scenario (Case-3).

Live Load Shoes (LLS), which are the support locations of the main girders in the closed position, are one of the critical structural components of the movable bridges. The main operational concern of LLS is the loss of contact, which makes the shims at these locations crucial. Small gaps due to deterioration of the shims lead the girders to pound on the live load shoes, which results in further misalignment, additional stresses, stress redistributions, fatigue damage, and excessive wear. The LLS and shim-removal operation can be seen in Figure 37.

Case-1 is the creation of a gap (around 0.3 cm up to 0.5 cm) between the West South LLS (WS3) and resting support pads, which corresponds to non-fully seated LLS (Figure 37).
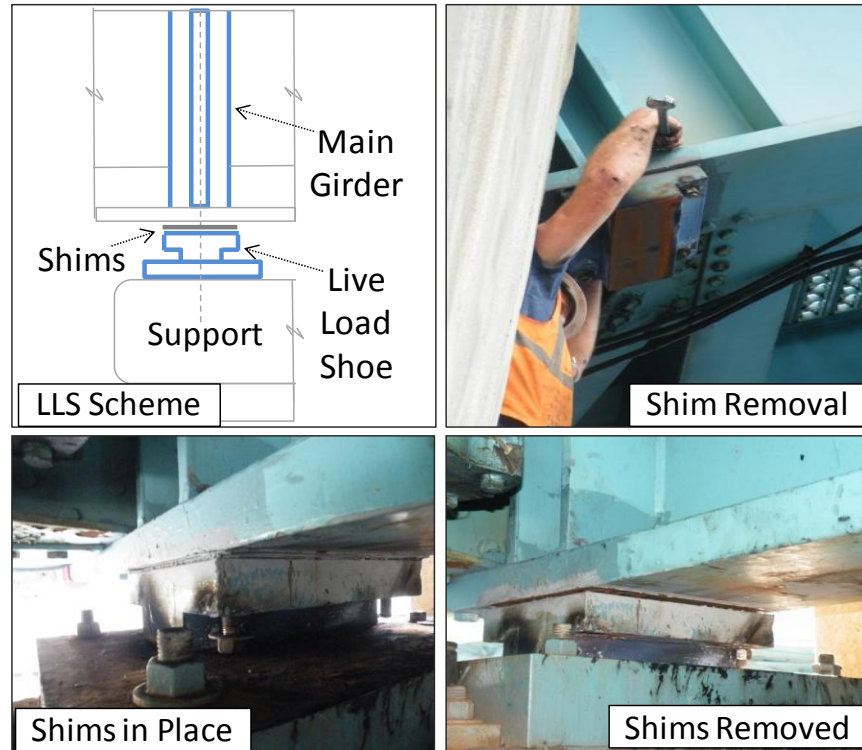
Figure 37: Live load shoe (LLS) and the shim-removal operation

Span Locks (SL), which are one of the members that fail the most due to deterioration or incorrect operation (Catbas et al. 2011), are used to connect the tip ends of the two cantilever leaves in bascule bridges. Consequently, both leaves are forced to deflect equally, preventing a discontinuity in the deck during operational traffic. Two main components of the SL are the receiver and the lock bar (Figure 38). These elements are located in different leaves. During operation, the lock bar slides with a hydraulic system across the bronze shoes, mounted in the rectangular guide and receiver housings. The main concern for the SL is that the coupling has to be loose enough to allow a proper opening operation, but at the same time, the gap between the

bar and the receiver has to be small enough to ensure the adequate connection with minimal bouncing while vehicles cross from one leaf to the other. This is achieved by placing shims to adjust the spacing. Case-2 is the creation of a gap (around 0.3 cm up to 0.5 cm) on the West South Span Lock (WS1) by removing the shims. The last structural alteration on the Sunrise Boulevard Bridge is Case-3, which is the combination of the Case-1 and Case-2.

Figure 38: Span lock (SL) and the shim removal operation

For the validation of the methodology, 10 different data sets were collected between October 11 and October 20 for the baseline case (before damage). Then, the structural changes were implemented on the structure on October 21. On this day, five data sets were collected for each damage case (Case-1, 2, and 3). Afterward, the shims were replaced on the structure, and 10 additional data sets were collected between October 22 and October 31 for the after-damage case to see whether the correlation coefficients were still returning to the same level as the before-damage data sets.

It should also be emphasized that the data collected from the monitoring system is based on operating traffic, and no special trucks or lane closures are required. From an operational point of view, this input-independent analysis is also desirable for real-life applications, since it reduces the cost of load tests, minimizes extra manpower, and eliminates traffic interruptions.

3.4.2. *Results*

After data collection and filtering high frequency components from the signals, mean correlation matrices are obtained for different data sets and these correlation matrices are compared as given in Figure 27 previously to determine structural changes and/or structural damage. The comparison is carried out by subtracting the mean correlation matrix from one state of the bridge to another state. The difference matrix serves as an indicator as exemplified in the following.

Figure 39 illustrates the damage locations for LLS shims removal (a), the difference matrix between the before-damage results and the LLS shims removal in a 12x12 matrix form (b), and sample correlation data used for the WS3 and EN2 cell. From the difference matrix, the

damage can be easily identified and also localized. In Figure 39b, it is observed that the darkest colors are seen for the WS3 location, where the structural change is applied. In addition, Figure 39c shows the change in the correlation coefficients before, during, and after the damage for the cell that corresponds to the correlation between WS3 and EN2. After replacing the shims at the LLS location (after damage), the coefficients are almost equal to the before-damage mean value of correlation, which demonstrates effective repair of the damage.

Additionally, damage is also identified and localized for SL shims removal and both shims removal from LLS and SL, which are shown in Figure 40 and Figure 41, respectively. The change in the correlation coefficient of SL shims removal is illustrated for the WS1 and WN1 strain gages (Figure 40c), and the change of LLS+SL shims removal is illustrated for the WS3 and ES2 strain gages (Figure 41c). It is observed that the variation of the correlation coefficient for SL shims removal is not as low as seen in the LLS and LLS+SL shims removal cases. Since the tip locations are exposed to lower strain levels due to a cantilever type behavior, the variation in the correlation coefficients for this location is a little bit higher. Nonetheless, the darkest colors in Figure 40b indicate the maximum change is at WS1 where the span-lock shims were removed. When both LLS and SL shims are removed, it is seen that two rows and two columns corresponding to WS1 and WS3 simultaneously indicate the maximum change (Figure 41b).
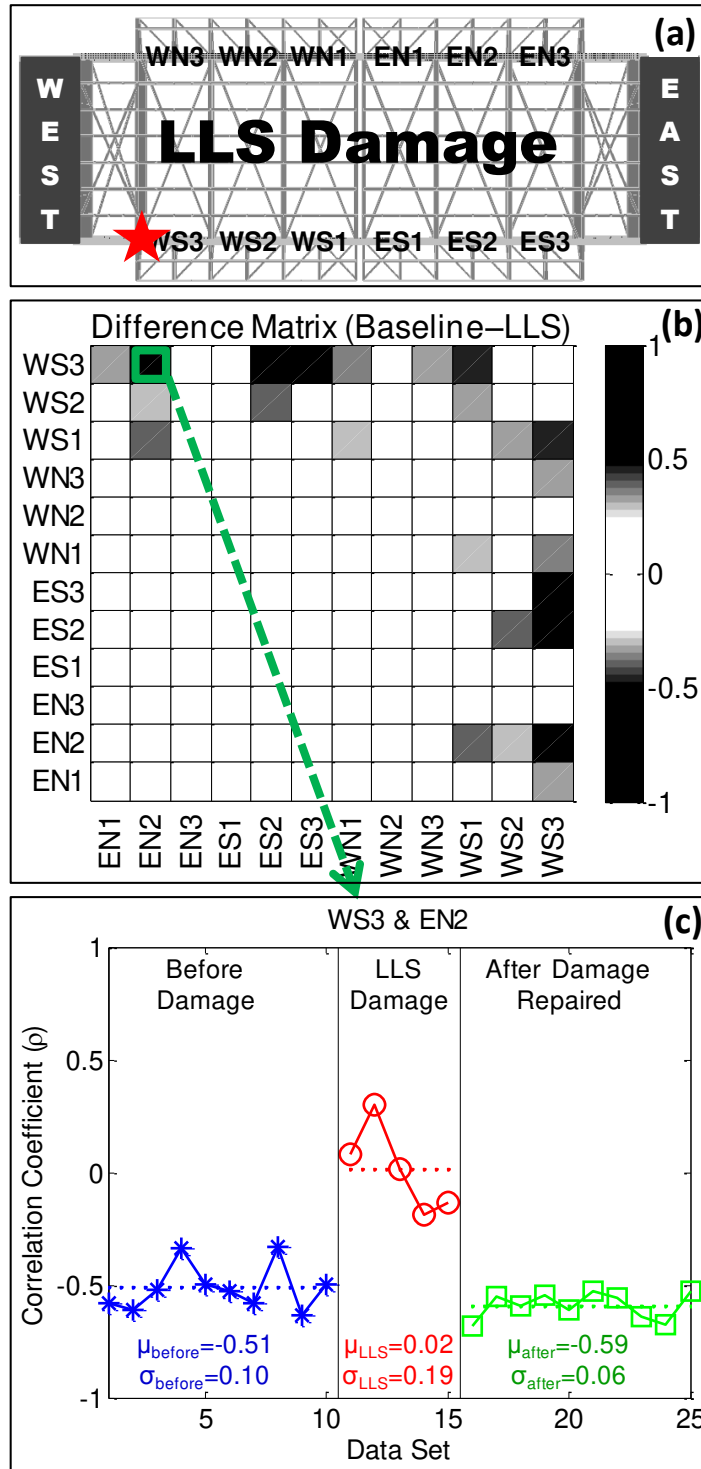
Figure 39: Damage locations (a), difference matrix between baseline and LLS damage (b), and sample correlation data used for the corresponding cell of WS3 and EN2 strain gages (c)
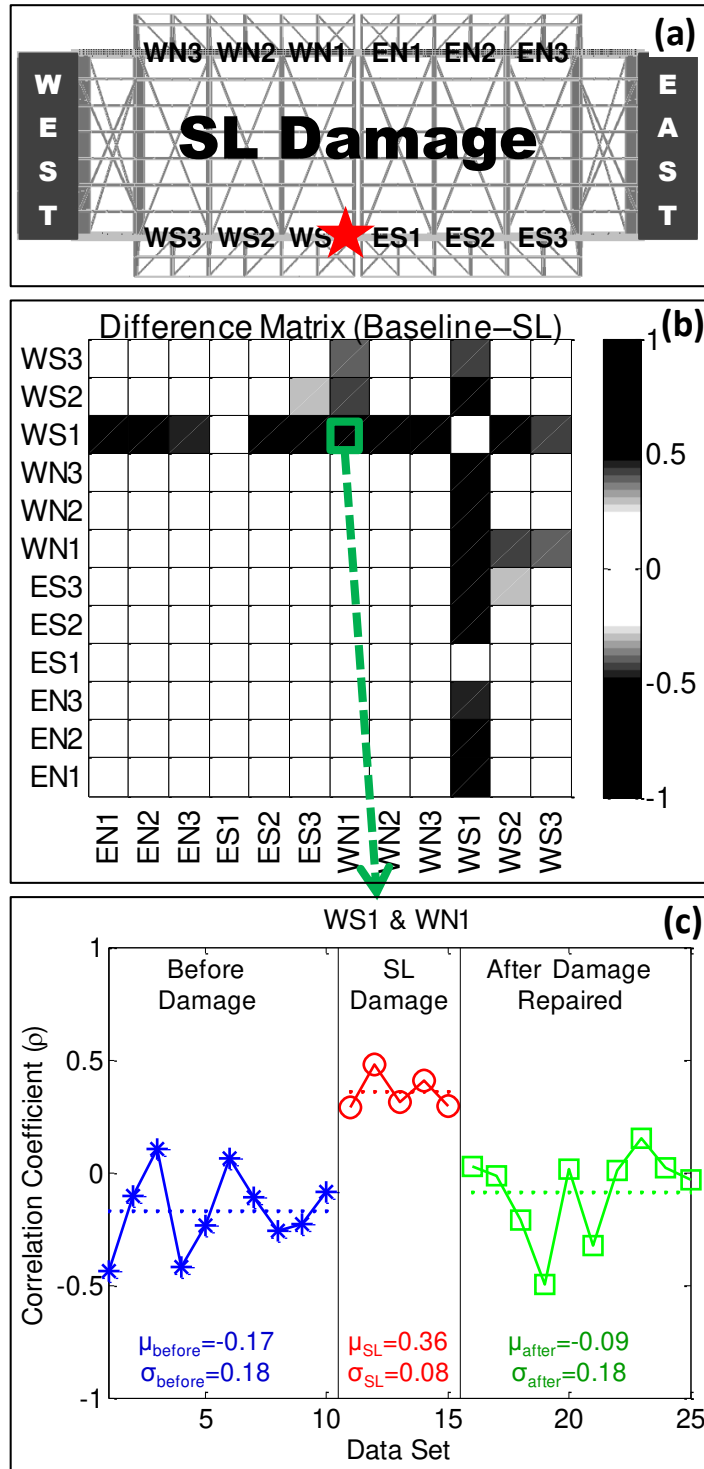
Figure 40: Damage locations (a), difference matrix between baseline and SL damage (b), and sample correlation data used for the corresponding cell of WS1 and WN1 strain gages (c)
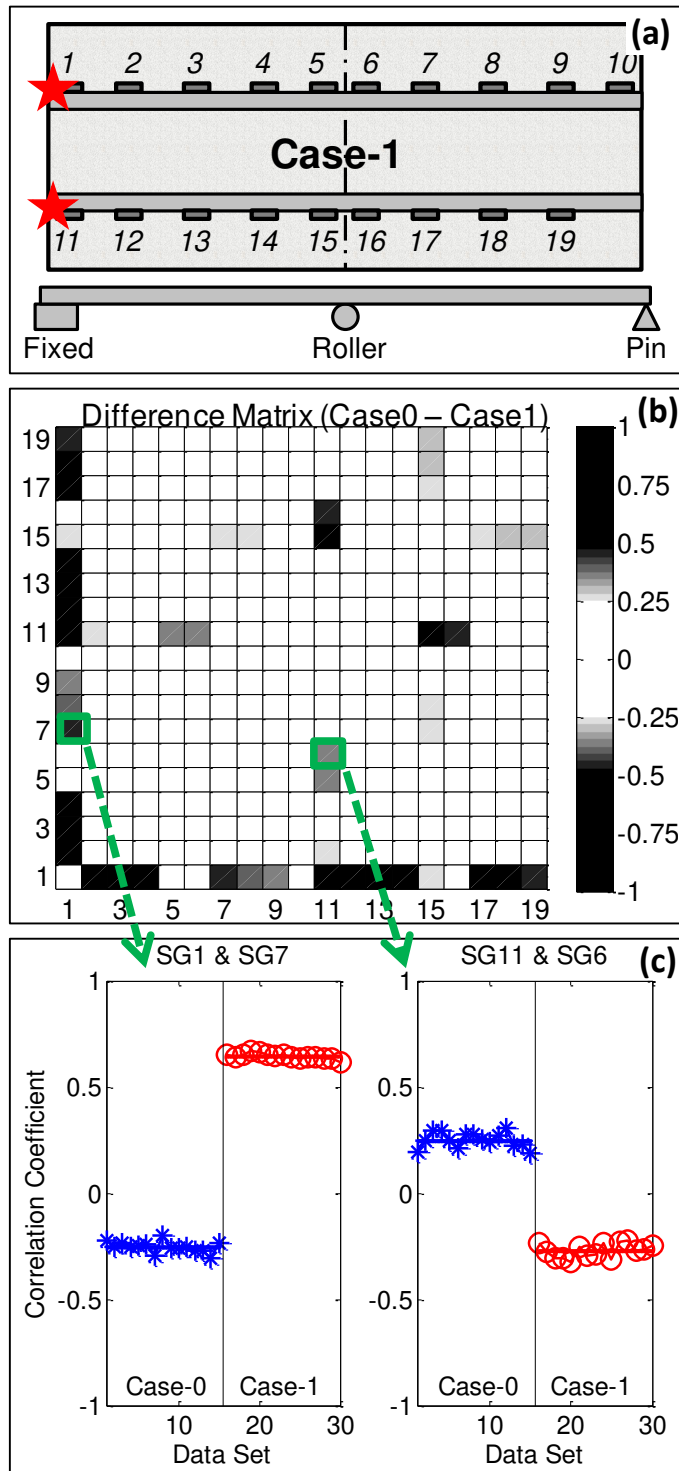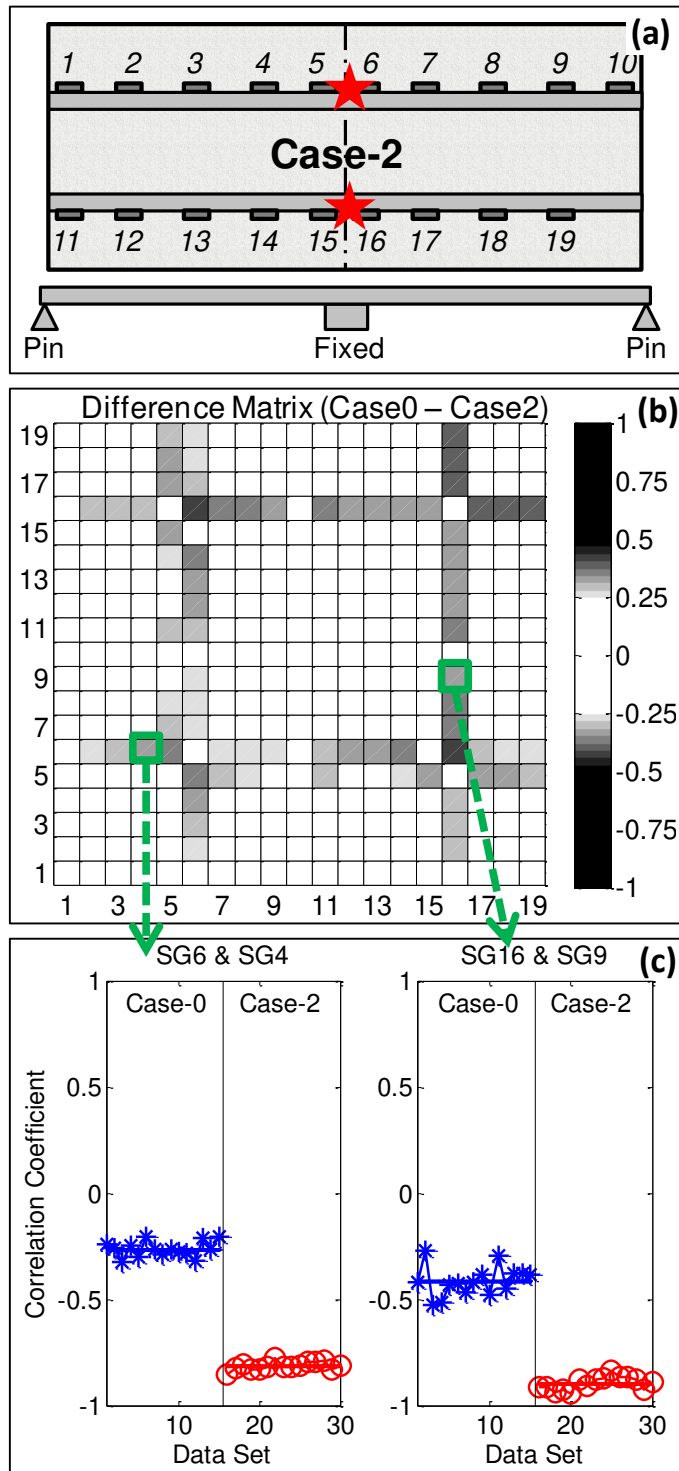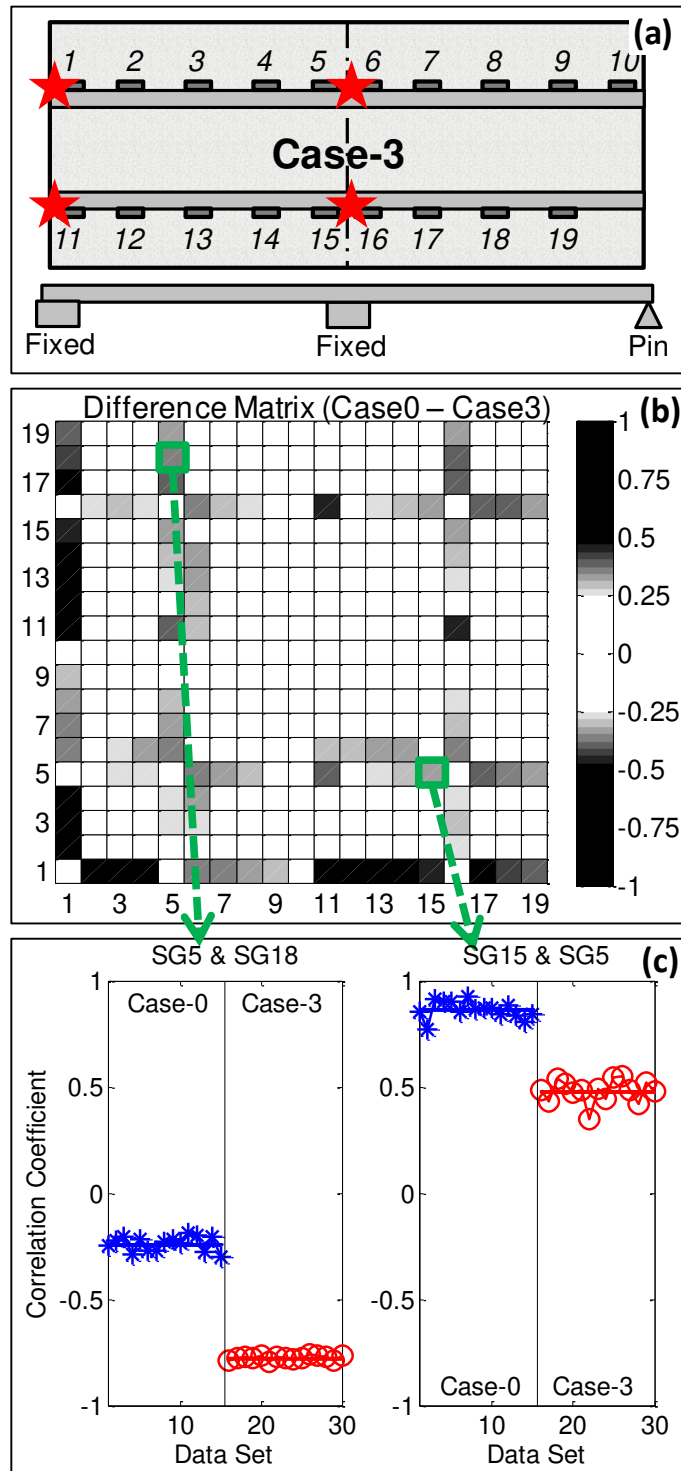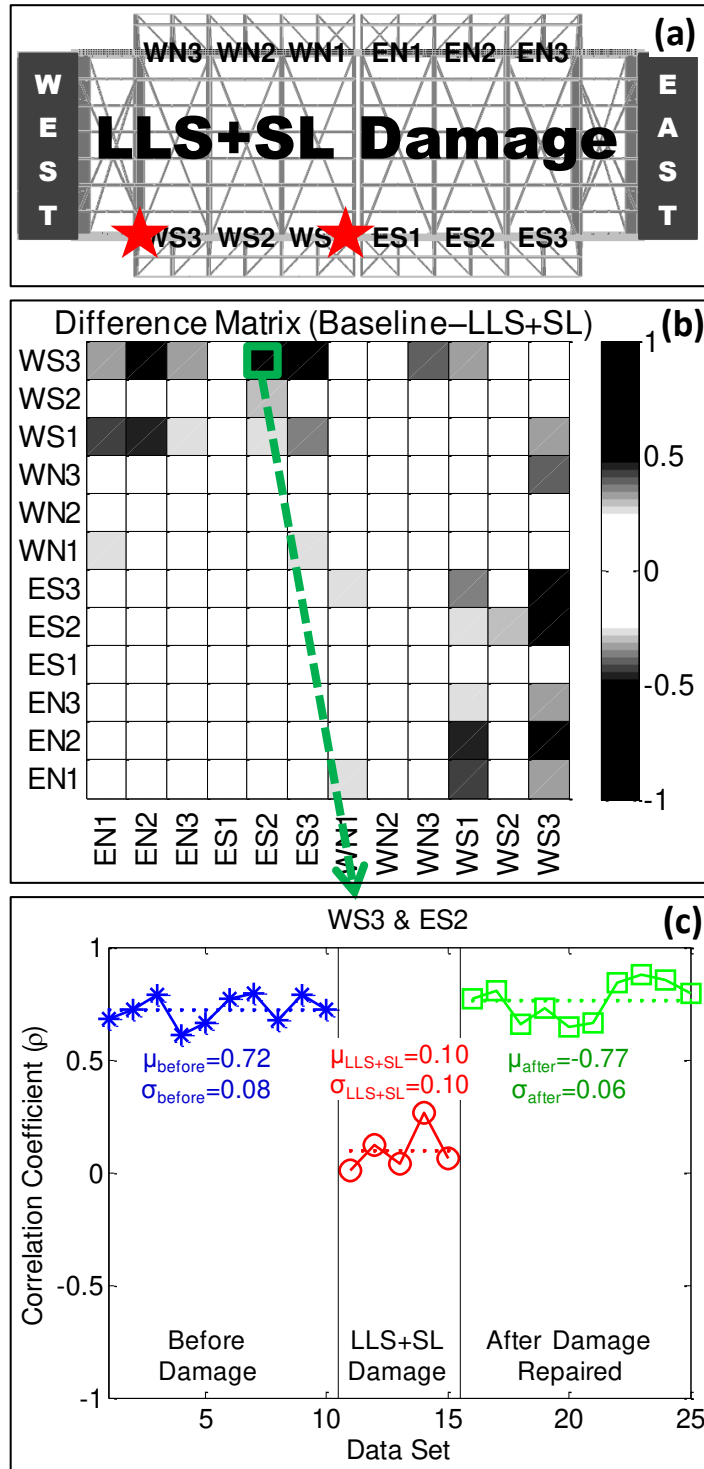
Figure 41: Damage locations (a), difference matrix between baseline and LLS+SL damage (b), and sample correlation data used for the corresponding cell of WS3 and ES2 strain gages (c)

One of the important issues to be discussed is the separation of the mean difference levels for a substantial change that can confidently be attributed to a structural change. Table 4 shows level of change illustrations from the three different damage cases shown in Figure 39c, Figure 40c, and Figure 41c.

Table 4: Level of change illustrations for cases shown in Figure 39c, 40c, and 41c

Sample Cases Compared from the following	$\Delta\mu$ (ρ-difference)	σ_i	σ_j	$\Delta\mu/\sigma_i$	$\Delta\mu/\sigma_j$
Before Damage & LLS	0.53	σ_{BD}=0.10	σ_{LLS}=0.19	5.3	2.8
LLS & After Damage	0.61	σ_{LLS}=0.19	σ_{AD}=0.06	3.2	10.2
Before Damage & SL	0.53	σ_{BD}=0.18	σ_{SL}=0.08	2.9	6.6
SL & After Damage	0.45	σ_{SL}=0.08	σ_{AD}=0.18	5.6	2.5
Before Damage & LLS+SL	0.62	σ_{BD}=0.08	σ_{LLS+SL}=0.10	7.8	6.2
LLS+SL & After Damage	0.67	σ_{LLS+SL}=0.10	σ_{AD}=0.06	6.7	11.2

Higher ($\Delta\mu/\sigma$) ratios express more confidence for change/damage between the cases compared. It is seen in most of the cases that separation is very high (as high as $\Delta\mu\approx11\sigma$), indicating there is virtually zero overlap between the correlation coefficients between different cases. This separation can be confidently attributed to a change between the observed conditions. On the other hand the lowest separation observed is $\sim2.5\sigma$ between the SL damage and after SL damage repaired cases as presented in Figure 42a. Probability of overlapping or in other words separation level between the two cases can be easily identified as presented in Figure 42b. For the lowest case ($\Delta\mu\approx2.5\sigma$), uncertainties in the separation indicate that almost 99% of the data points are separated. Therefore, all the results show sufficient separation.

83

$$SeperationLevel = \Phi\left[\dfrac{\mu_i - \mu_j}{\sqrt{\sigma_i^2 + \sigma_j^2}}\right] = \%99$$
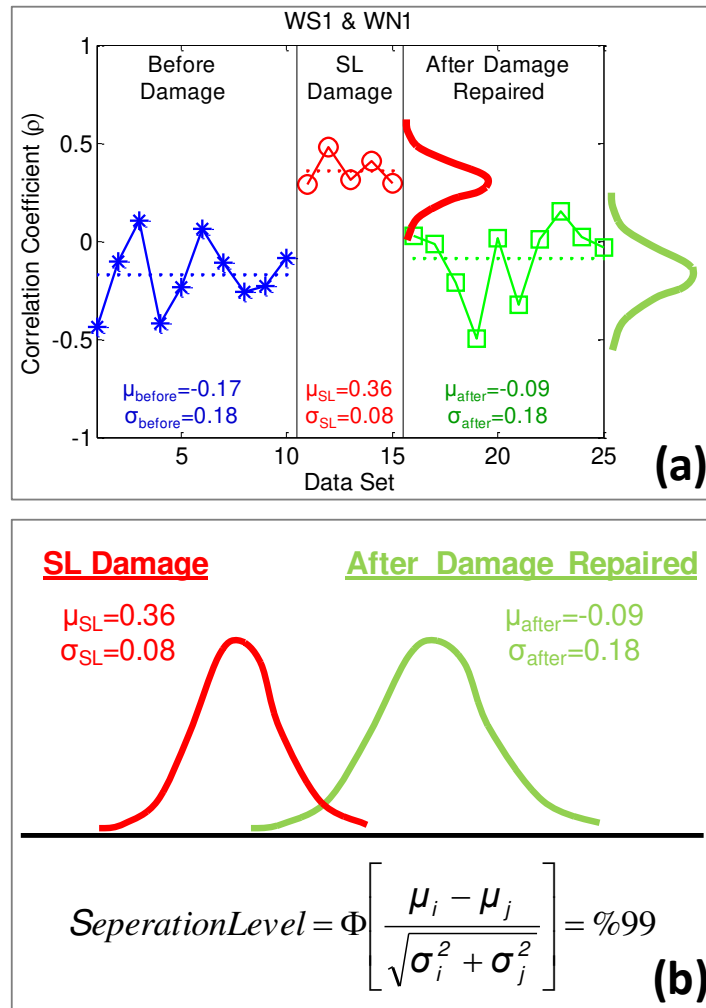
Figure 42: Uncertainty in separation between span lock damage and after damage repaired

3.5. Summary

The statistical analysis of large structural health monitoring data help the engineer or researcher handle large amounts of data more efficiently, especially in the case of extensive SHM applications with high spatial resolution generating data continuously. In addition, statistical features of the data can be attributed to structural behavior, and change in the descriptive statistics can be attributed to structural changes, damage, and/or deterioration. As

mentioned earlier, in some situations, measured data may exist, but it is not always possible to have prior or calibrated models in the structural identification framework. In this chapter, an effective nonparametric data analysis methodology, which is based on the correlation of the strain-time histories from different sensor locations for structural change/damage detection, is demonstrated on a laboratory test structure and on a real-life bridge. Cross correlations of the strain measurements indicate a level of correlation among different sensor pairs, and the correlation coefficients are tracked for extracting the information about structural change. It is seen that the correlation-based methodology can identify and locate the damage for both structures, which are monitored under normal and damaged conditions.

In long-term monitoring applications, data size is a challenging issue, but the correlation analysis considerably reduces the data size to provide useful information from large amounts of strain data; thus, the methodology is computationally efficient. Furthermore, the presented approach eliminates the need for loading information (magnitude and placement) for strain-monitoring applications. Strain-time histories used for the data analysis are obtained from arbitrary operating traffic conditions. Moreover, from the maintenance point of view, it is also shown that the method can be utilized to evaluate the effectiveness of maintenance (including repair) by checking the variations of the correlation coefficients before and after the maintenance application. Consequently, this methodology has the potential to be easily applied by engineers to different kinds of civil infrastructure that require condition monitoring and maintenance. For instance, when the LLS and SL are fixed, it is seen that the correlation levels return to the previously observed levels as shown in Figure 39c.

CHAPTER 4.
PARAMETRIC STRUCTURAL ASSESSMENT: LAB DEMONSTRATION

4.1. *Introduction*

Complex analysis and design of structures, especially landmark structures such as long-span bridges, have been conducted by many engineers and researchers (Abdel-Ghaffar and Housner 1978; Abdel-Ghaffar and Nazmy 1991; Imai and Frangopol 2002; Frangopol and Imai 2004; Masri et al. 2004; Catbas et al. 2007; Catbas et al. 2008b). With advances in sensor technologies, utilization of monitoring data for assessment of bridges has also gained increased attention over the last decade or so. This approach and technique, which is termed Structural Health Monitoring (SHM), can be used for improving the condition evaluation of existing structures by means of advanced sensing devices, data acquisition systems, and communication technology. SHM applications include structural condition assessment, parameter identification, model development and updating, geometric model calibration, and real-time monitoring.

Building upon the theoretical and experimental studies that have been carried out over the last several decades, it is possible to collect monitoring data in greater quantities and with greater precision with the current advances in sensing technologies at significantly reduced costs. Novel approaches such as wireless sensing, distributed networking, and Internet-based data acquisition have been more widely available. It is now very feasible and efficient to acquire data for structural responses such as strain, displacement, vibration, and environmental effects (i.e., wind speed, temperature, and earthquake excitation) (Catbas et al. 2004a). To objectively evaluate the condition of existing structures and to design better structures, novel sensing technologies and analytical methods can be used to rapidly identify the onset of structural damage. SHM offers an

automated method for tracking the health of a structure by combining damage-detection algorithms with structural monitoring systems (Lynch and Loh 2005; Catbas et al. 2008b; Gul and Catbas 2009; Yun and Masri 2009; Frangopol 2011a; Gul and Catbas 2011; Okasha et al. 2011; Zaurin and Catbas 2011).
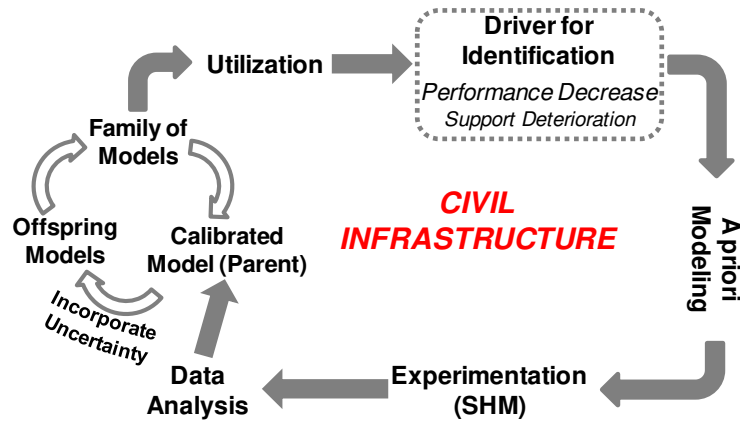
Figure 43: Use of uncertainty-incorporated family of models for St-Id of a laboratory structure due to performance decrease

In addition, it is also very feasible to develop complex analytical models with large degrees of freedom using current computer systems. Advanced geometric models such as FEMs can be utilized to determine the load-carrying capacity of bridges, to simulate damage and deterioration, and to predict the probability of failure. The difficulty of developing models and predictive analysis is further compounded due to the complexity of large-scale structures, such as long-span suspension bridges (Imai and Frangopol 2001) and long-span truss bridges (Catbas et al. 2007; Catbas et al. 2008b). While the mathematical developments and sophistication of the probabilistic approaches are well established, predictions using geometric models can be improved with the continuous utilization of monitoring data and the incorporation of uncertainties from the models and the data. In this chapter, a family-of-models approach with

parent and offspring models will be investigated for predicting the performance of a laboratory structure due to performance decrease as illustrated in Figure 43.

4.1.1. *Uncertainties*

For a large and complex system, data from all critical components become important, especially for system-level assessment and prediction. The reliability of a system depends on the reliability of the components, which is closely related to the structural configuration (based on failure mechanisms of primary and secondary elements) and redundancy (possible survival paths in the structure) of the system (Ghosn et al. 2010; Okasha and Frangopol 2010). It should also be indicated that although monitoring is expected to provide data for calibrating FEMs leading to more accurate reliability predictions, uncertainty still exists in the data as well as in the models, and this uncertainty needs to be incorporated even in the calibrated models.

One of the most significant studies to consider uncertainty in model development was presented by Smith and Saitta (2008), who explored factors for uncertainties affecting the model updating process using multiple models by combining dimensionality reduction (principal component analysis) and clustering (K-means). An important aspect of this methodology is the generation of a population of candidate models, which can be defined as identified FEMs. Moreover, several software packages are also developed for uncertainty analysis, such as NESSUS and DAKOTA developed by the Southwest Research Institute and Sandia National Laboratories, respectively. These attempts mainly address the aleatory uncertainty and are not powerful enough for the epistemic uncertainty quantification (Moon and Aktan 2006a). The main sources of uncertainties are shown in Table 3.

88

4.1.2. *Objectives*

The main objective of this chapter is to explore the impact of uncertainty in predicting the system reliability obtained by a one-time, initially calibrated FEM and a family of models that are continuously calibrated with SHM data. When analyzing structures and predicting the probability of failure by using 3-D FEMs, a number of different approaches are possible for the consideration of data and model uncertainties, as summarized in Figure 44.

Nominal FEM	Initially Calibrated w/ SHM	Continuous Calibration w/ SHM	Continuous Calib. w/ SHM + Uncertainty Incorporation
① Input	① SHM Data $\varepsilon_{exp}, \delta_{exp}, \theta_{exp}$	① SHM Data $\varepsilon_{exp}, \delta_{exp}, \theta_{exp}$	① SHM Data $\varepsilon_{exp}, \delta_{exp}, \theta_{exp}$
② Nominal FEM	② FEM Calibration	② FEM Calibration	② FEM Calibration (Parent)
③ Response $\varepsilon_i, \delta_i, \theta_i$	③ Input	③ Input	③ Incorporate Uncertainty of Variables μ_E / σ_E, μ_I / σ_I, μ_k / σ_k
④ Reliability Prediction β_i	④ Calibrated FEM	④ Calibrated FEM	④ Population of Offsping FEMs ……
	⑤ Response $\varepsilon_i, \delta_i, \theta_i$	⑤ Response $\varepsilon_i, \delta_i, \theta_i$	⑤ Input μ_P / σ_P
	⑥ Reliability Prediction β_i	⑥ Reliability Prediction β_i	⑥ Response Distributions $\mu_\varepsilon / \sigma_\varepsilon$, $\mu_\delta / \sigma_\delta$, $\mu_\theta / \sigma_\theta$
		⑦ New SHM Data $\varepsilon_{exp}, \delta_{exp}, \theta_{exp}$	⑦ Reliability Prediction β_i
		Repeat Steps 1-7 w/New SHM Data	⑧ New SHM Data $\varepsilon_{exp}, \delta_{exp}, \theta_{exp}$
			Repeat Steps 1-8 w/New SHM Data

Figure 44: Different approaches for utilizing FEMs for reliability prediction of bridges

The first column of Figure 44 illustrates that a complex yet nominal 3-D FEM can be employed for preliminary analysis of the structure. With the availability of SHM data, it is also possible to calibrate this model as shown in the second column and then use it for different analyses, such as various simulations including damage and deterioration scenarios, and reliability prediction by taking the advantage of uncertainties in loads, inertias, areas, etc. defined in the literature. While the use of SHM data improves the level of confidence from the simulations, it needs to be recognized that a critical assumption in most analyses is that the structural responses remain stationary, observable, and reasonably linear during the course of the monitoring. In real life this is not the case, and the data used for model calibration provide information from a particular time window from the life cycle and operation of the structure. Monitoring data, especially for long-span bridges, show the existence of a change in structural behavior mainly due to environmental effects. As a result, it is intuitive to realize that models have to be continuously updated with monitoring data to give better representations of structural behavior, as shown in column three of Figure 44. At this point, it is critical to consider that there are still uncertainties as indicated in Table 3. Consequently, even a "calibrated model" will have to account for the uncertainties coming from these different sources. The idea of continuously calibrating models with the consideration of the uncertainties yields a family of models as illustrated in the last column of Figure 44. Such models can be employed for different simulations as well as for the prediction of the system reliability. This chapter of the dissertation provides a framework and a fundamental study to quantify the difference from predictions of reliability when the uncertainties are incorporated with a family of models as compared to an initially calibrated model.

90

4.2. Lab Studies

4.2.1. *Experimental Setup*

Laboratory studies are essential to explore new concepts and methodologies before more expensive field tests are performed. For this reason, a test structure that is simple to construct and test, yet has specific characteristics leading to quantification of uncertainties as part of this fundamental demonstration is decided to design for this section. From a redundancy point of view, the characteristics of this test setup were inspired by the I-40 Bridge, which had two girders as main load-carrying elements connected with crossbeams. The I-40 Bridge was extensively analyzed, tested, and characterized by Farrar et al. (1994).

The steel test setup "Double-H-Frame (DHF)" is designed as a basic bridge model with four structural elements. In Figure 45a, DHF components can be seen with a reliability block diagram of a combined series-parallel system. Two of the structural elements are the main elements (denoted as 1 and 4 in Figure 45a), whereas the others are the secondary elements (denoted as 2 and 3 in Figure 45a). For the construction of the DHF, S3x5.7 section (AISC Steel Manual, 2006) with yield strength of 250 MPa is used and the net span length of the structure is 1.5 m. For the undamaged case (baseline), triangular prisms are used to support the beam at the boundaries, restraining vertical deflection but not preventing rotation.
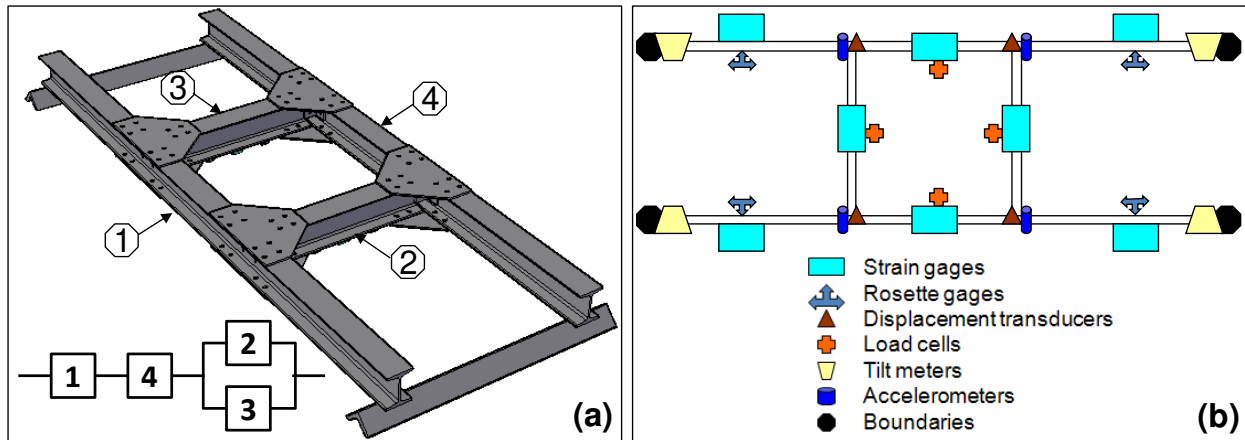
Figure 45: DHF, reliability block diagram (a) and sensor locations (b)

4.2.2. *Instrumentation Plan*

DHF is instrumented with eight strain gages, four rosette gages, four displacement transducers, four load cells, four tilt meters, and four accelerometers. The sensor locations are shown in Figure 45b. Strain gages are used to obtain the critical moment values, whereas the rosette gages are used to find the shear values near the supports. On the other hand, load cells are needed to closely monitor the load since the hydraulic actuator capacity is 445 kN, and the maximum load applied to the structure is 27 kN, which is determined from preliminary finite element analysis based on the yielding stress criteria with a safety factor of 1.5. Moreover, displacement transducers are used for checking the deflections for the local calibration of the model. In addition, the tiltmeters are also attached to the support points for the boundary condition tests to observe the support rotations. Last, the accelerometers are used for the impact hammer and ambient vibration tests for further studies. It should be noted that for this chapter of the dissertation only strain and displacement measurements are used for the calibration of the

FEMs for each boundary condition, and strain measurements are used for the reliability calculations.

4.2.3. *Experimental Plan*

In this section, different types of support deterioration simulation tests are carried out. In Figure 46, the test setup and the data acquisition system are shown. The main idea behind the static tests is to calculate the system reliability index due to the support degradation. For this reason, several tests are conducted with the loading up to 6 kips level for the changing boundary conditions (Figure 47). In these tests, one of the supports is selected, and then the number of elastomeric pads at that boundary is changed to simulate the support deterioration. In the test nomenclature, "M" corresponds to mid-loading, which means the middle points of the components are loaded, and "P" corresponds to the number of pads (Figure 47). After creating each test setup for boundary conditions with no elastomeric pad (pin), one elastomeric pad, three elastomeric pads, and five elastomeric pads, the same loading is applied in all cases.
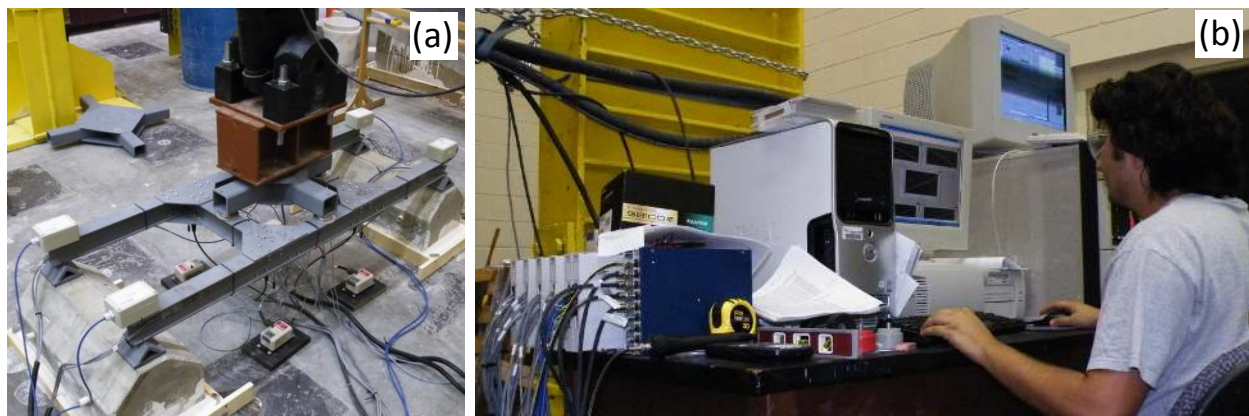
Figure 46: DHF test setup (a) and data acquisition (b)
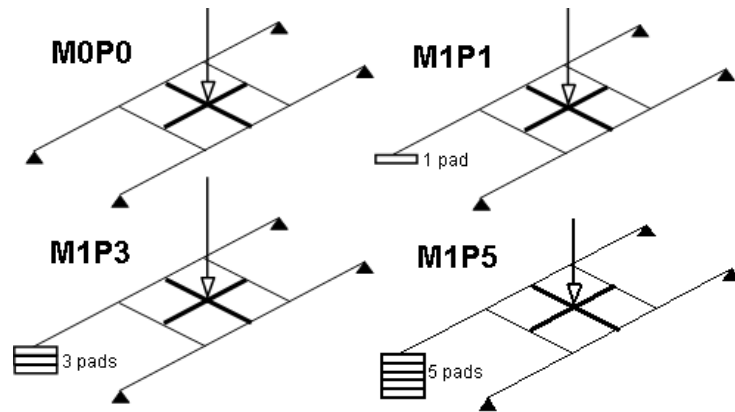
Figure 47: Loading of DHF under different boundary conditions

In addition, compression tests of the elastomeric pads are performed in order to obtain stiffness values and their distributions (Figure 48). These stiffness values are then used in the finite element models. Compression tests also help to identify the behavior of material properties for individual pads as well as pads stacked together vertically. The laboratory data for the elastomeric pads are also employed to determine the distribution type and parameters such as mean and standard deviation for the spring stiffness.
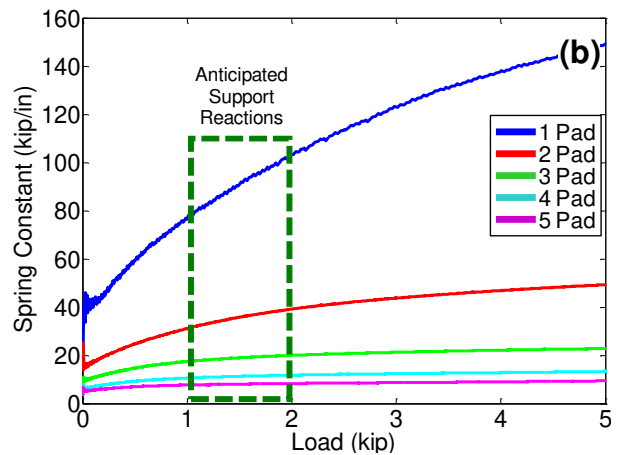
Figure 48: Compression tests of duro-50 pads using a universal testing machine (a) and spring constants at the anticipated support reaction interval (b)

Probabilistic modeling of the structural capacity and load effects requires determination of the statistical parameters representing the uncertainties in the calculation of each parameter. Sources of variability are generally categorized as material factor (material properties), fabrication factor (imperfections), and analysis factor (assumptions, approximations) (Ellingwood et al. 1980). The mean value and the variance (or standard deviation, or coefficient of variation) should be known for reliability analysis. In this chapter, probability distributions are used for the random variables. Table 5 shows the probabilistic parameters (i.e., main descriptors of random variables) used in this framework, which is demonstrated on a laboratory structure. It should be noted that the level of uncertainty for real-life structures can be different and in most cases higher depending on the structure. In the following chapters, the challenges and refinement of this framework for real-life implementations are explored.

Table 5: Main descriptors of random variables

Parameter	Modulus of Elasticity (E)	Moment of Inertia (I)	Load (P)	Spring Stiffness (k)
Mean	29000 ksi	3 in^4	Depends on the location	Depends on number of pads
Assumed Coefficient of Variations	5%	5%	5%	5%
Distribution Type	Lognormal	Lognormal	Lognormal	Uniform

4.3. *ANN-Based FEM Calibration*

SHM data can be used to calibrate FEMs using various methods for calibration, and different methodologies can be used for this process. There are a number of studies available in model calibration and geometric parameter identification. For example, Sanayei et al. (1997) and

Santini et al. (2007a) determined the geometric parameters for model calibration by means of an error function minimization technique between the measurements and the FEM. In these studies, a MATLAB-based parameter estimation program developed by Sanayei (1997) was employed to obtain critical properties such as moment of inertia at complex connections.

In this dissertation, Artificial Neural Networks (ANN) is utilized for FEM calibration. Briefly, ANN learns from the existing patterns and then makes a prediction for the patterns that are not considered during learning. Therefore, the success of a network is measured by its generalization performance. If the difference between the actual and computed output by ANN is within an acceptable level, then the network can be used for prediction in the similar domain, which exhibits certain common characteristics with the existing patterns. The prediction performance of a network usually depends on the network parameters and the topology chosen. The best performance is generally achieved by extensive parametric study on the different network using a trial-and-error approach. In each trial, the performance of the network is evaluated. This process is repeated until the best architecture with the right network parameters is obtained.

A common approach for FEM calibration is the manual calibration approach based on trial and error, which can be time consuming. Since the objective in this chapter is to explore uncertainties by means of a family of models, these different models generated based on an automated calibration approach provides good coverage of the distributions of different parameters. Therefore, it is feasible to develop these models and also utilize them for a neural-network-based solution strategy for easy and practical calibration of these models.

In the beginning of the calibration process, a preliminary FEM of the DHF is developed using the nominal structural parameters and material properties. Next, sensitivity studies are conducted to determine the governing parameters affecting the static response of the DHF, as well as to determine the sensitivity range of each parameter. Afterward, a set of training patterns incorporating a selected number of DHF parameters (spring constant, modulus of elasticity, and moment of inertia) and responses (strain and displacement) are constituted by considering different values/combinations of these parameters generated randomly within their sensitive ranges. The input parameters (E, I, k) and responses (δ and ε) are illustrated in Figure 49.
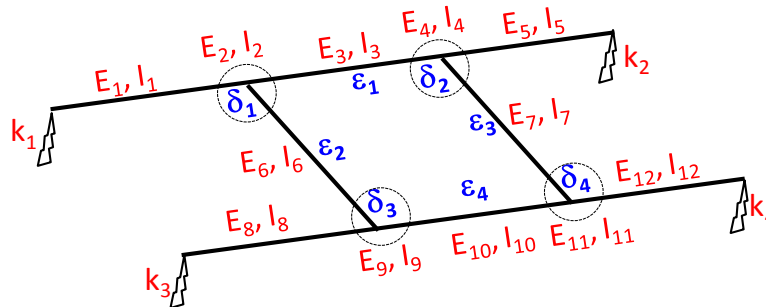
Figure 49: Input parameters and output responses for the ANN-based calibration

In the ANN-based calibration process, the Levenberg-Marquardt algorithm (Levenberg 1944; Marquardt 1963) is used for the learning rule of the ANN, and the sigmoid function is used for the activation function. Since Levenberg-Marquardt requires less time and epochs to converge, it performs more efficiently compared to other learning rules, which in turn makes it ideal for the trial of different networks (Yonaba et al. 2010). The use of the sigmoid function requires that the input and output data be scaled to the range 0–1. In this application, the input and output data are scaled to a somewhat narrower range between 0.2 and 0.8, resulting in a

considerable improvement in learning speed due to increased sensitivity of the sigmoid function within this range.

The network architecture consists of an input layer of eight nodes (four axial strain values and four displacement values), an output layer of 28 nodes (four stiffness values at supports, 12 elasticity values eight of which are member elasticity and four of which are joint elasticity, and 12 moment-of-inertia values eight of which are moment of inertia and four of which are joint moment of inertia), and one hidden layer of 28 nodes. Each is found to be the appropriate network.

A total of 2,000 FEMs are created randomly with these input parameters and output responses are collected for the network training process. ANN is then trained to learn the relationship between the DHF parameters and responses in reverse direction, such as the inputs are the strains and displacements, whereas outputs are the spring stiffnesses, moduli of elasticity, and moments of inertia. These training data are divided into three sets, namely, the training set, the cross-validation set, and the test set. The training set contains 1,300 patterns and is used to detect any relationship between the DHF parameters and the responses. The cross-validation set contains 300 patterns and is used to avoid the problem of over fitting. The test set contains 400 patterns and is used to evaluate the performance of the networks. Based on defined network parameters, the effect of the number of hidden layers and the number of processing elements in hidden layers as well as in output layers are observed using several architectures.

After the completion of training of each network, the performance of the network is tested using the test patterns that are not used during the training phase. The performance is measured by the average maximum error in the testing set. This process is repeated for each

network design. In this way, many networks that are capable of generalization at different levels are obtained. The best network is selected from among them. After network selection, experimental readings (strains and displacements) are fed into the trained neural-network system to predict the values of structural parameters for each boundary condition. These structural parameters, which are predicted from network analysis, are then used to create the calibrated FEMs for each boundary condition.

A comparison between the experimental and analytical response of the DHF is conducted. If these two sets of parameters differ significantly, then the ANN model is re-trained. The re-training procedure is continued until the difference between the measured and calculated responses is less than 10%. This calibration could have targeted an even lower difference between the network results and the measurements. However, it was shown that 10% root mean squared error (RMSE) between models of long-span bridges and local measurements such as strain and displacement can be considered quite satisfactory (Catbas et al. 2007). The flowchart of the ANN-based calibration process is summarized in Figure 50.

1) FEM Input Constants-Loads (P_i)
2) FEM Input Variables (E_i, I_i, k_i)
3) FEM Output Variables & ANN Training Inputs $(P_i, \epsilon_i, \delta_i)$
4) Hidden Layers
5) ANN Outputs (E_o, I_o, k_o)
6) Experimental Results $(P_{exp}, \epsilon_{exp}, \delta_{exp})$
7) Calibrated Model Parameters $(E_{cal}, I_{cal}, k_{cal})$
8) Loads (P_{exp})
9) FEM Results $(\epsilon_{cal}, \delta_{cal})$
10) FEM Results & Experimental Results Comparison
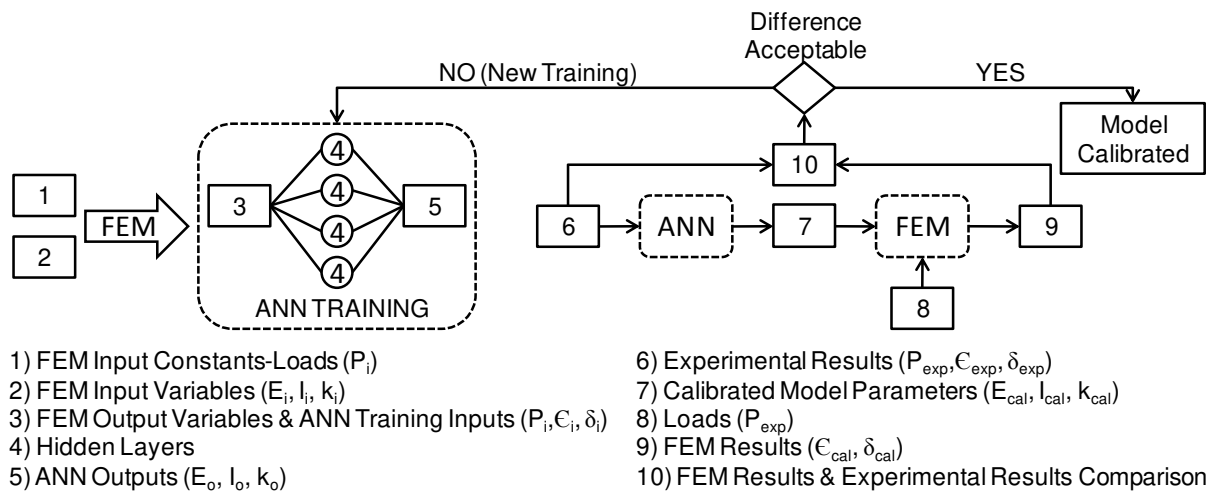
Figure 50: Flowchart of the calibration process

The calibration methodology is applied for each boundary condition (Figure 47), and four calibrated FEMs (zero pads, one pad, three pads, and five pads) are created as parent FEMs. In Table 6, experimental readings versus ANN-based calibrated FEM outputs for different test setups are shown with the error percentages. Each calibrated FEM has less than 7% RMSE, which can be considered as a realistic difference as discussed above.

Table 6: Network inputs and FEM outputs comparison for different test setups

		Input To Network	Output From Calibrated FEM	Difference (%)			Input To Network	Output From Calibrated FEM	Difference (%)
0-Pad	ε_1 (µε)	634	582	8.2	1 Pad	ε_1 (µε)	531	504	5.0
	ε_2 (µε)	241	221	8.3		ε_2 (µε)	269	258	4.0
	ε_3 (µε)	130	127	2.3		ε_3 (µε)	132	128	3.2
	ε_4 (µε)	630	576	8.6		ε_4 (µε)	698	666	4.6
	δ_1 (in)	0.121	0.114	5.4		δ_1 (in)	0.143	0.137	4.1
	δ_2 (in)	0.122	0.116	5.0		δ_2 (in)	0.129	0.124	3.8
	δ_3 (in)	0.126	0.123	2.6		δ_3 (in)	0.139	0.132	5.1
	δ_4 (in)	0.123	0.121	1.3		δ_4 (in)	0.138	0.135	2.1
Root Mean Square Error: 5.9%					Root Mean Square Error: 4.1%				
3 Pads	ε_1 (µε)	507	474	6.5	5 Pads	ε_1 (µε)	476	441	7.5
	ε_2 (µε)	285	270	5.2		ε_2 (µε)	306	275	9.9
	ε_3 (µε)	133	126	5.3		ε_3 (µε)	131	135	3.1
	ε_4 (µε)	723	657	9.1		ε_4 (µε)	762	745	2.3
	δ_1 (in)	0.282	0.264	6.3		δ_1 (in)	0.426	0.414	2.9
	δ_2 (in)	0.195	0.211	8.0		δ_2 (in)	0.275	0.296	7.9
	δ_3 (in)	0.139	0.136	1.8		δ_3 (in)	0.149	0.135	8.8
	δ_4 (in)	0.138	0.133	3.8		δ_4 (in)	0.143	0.135	5.9
Root Mean Square Error: 6.1%					Root Mean Square Error: 6.6%				

4.4. *Family of Models*

Even after calibration of the FEMs for each boundary condition, uncertainties from different sources need to be incorporated. Considering possible distributions of critical

parameters yields a family of models. The calibrated FEMs (total of four FEMs, one for each boundary condition) are considered as *parent* models, from which a set of *offspring* models are generated. The number of offspring models that will be used for simulations is decided based on the following error associated sample size given by Ang and Tang (1984):

$$\% \, error = 200 \times \sqrt{\frac{1 - P_f}{n \times P_f}} \tag{4.1}$$

where P_f is the structure's estimated probability of failure and n is the sample size. A total of 10,000 offspring FEMs are to be created for each test setup (i.e., zero pads, one pad, three pads, and five pads). In each group of 10,000 FEMs, variables (moment of inertia, modulus of elasticity, load and spring constant) are generated based on the distributions given in Table 5. Finally, these offspring models are analyzed, and the distributions of the strain values are obtained to calculate the system reliability. Figure 51 illustrates the process of generating offspring FEMs from the parent FEMs by incorporating the uncertainty of variables.
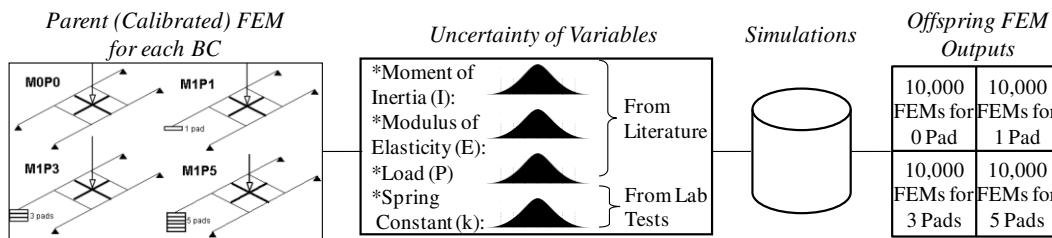
Figure 51: Incorporating uncertainty of variables into the offspring models

The simulations with offspring models yield a distribution for the responses of the structure. In Figure 52, it is shown that the responses obtained from the monitoring data fall into the distributions generated from the simulations. It is seen that the response distributions from the offspring models encompass the measured responses with the monitoring system. The

response distributions incorporate the uncertainties that are described in Figure 51. As discussed above, the parent model and the offspring models calibrated continuously using monitoring provide a better estimate of the structure's probability of failure than models calibrated once with monitoring data. The prediction difference between an initially calibrated FEM and a family of FEMs that are continuously calibrated with SHM data approaches will be quantified next for the DHF as conceptually illustrated in Figure 53.
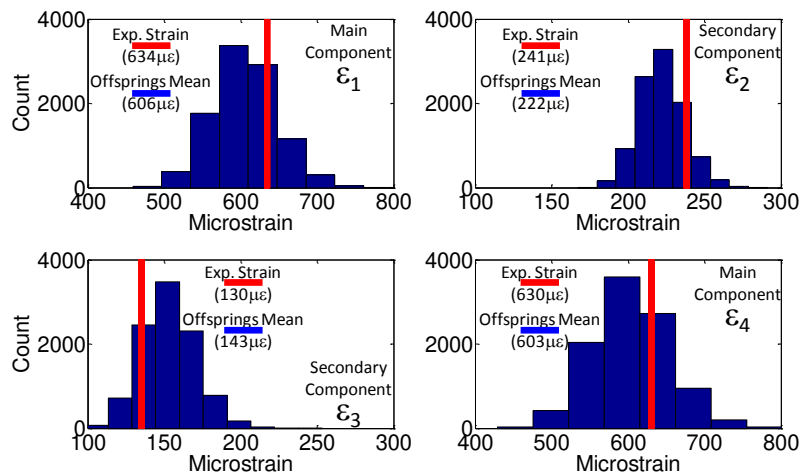
Figure 52: Experimental strain and simulation strain histogram comparison for the zero pads case
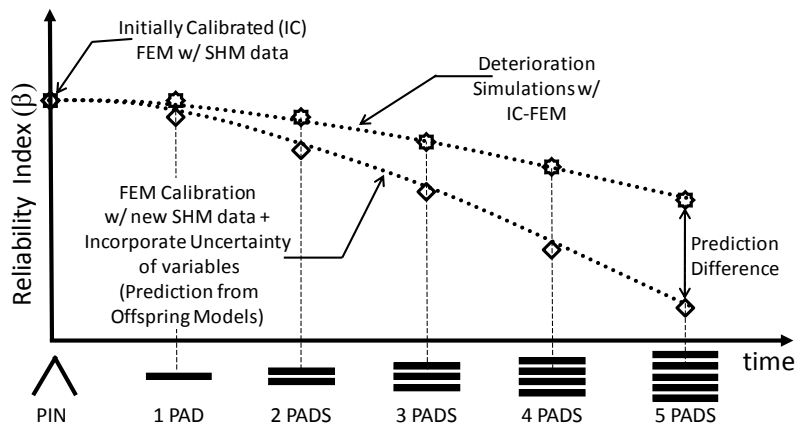
Figure 53: Reliability prediction comparison of initial and continuous calibration

4.5. *Component and System Reliability*

Calculation of the system reliability of a structure, which was explained in the second chapter of this dissertation, requires the component reliabilities and selection of an appropriate system model. A system can be modeled as parallel, series, or a combination of parallel-series connected components. Component reliabilities, or in other words, reliability indices of individual members, are obtained separately based on yielding strain criterion from the following limit state function:

$$g = \varepsilon_y - \varepsilon_d$$

(4.2)

where ε_y is the yielding strain of steel and ε_d measured is the measured strain obtained from monitoring during different boundary deterioration stages. The system model of the four-element DHF, which is presented in (Figure 45a), is created by considering the types of elements such as main and secondary components. The analogy here is main components can be considered as a main girder of a bridge, whereas the secondary components can be considered as floor beams of a bridge. Therefore, according to this system model, failure of any main component will fail the system or failure of both secondary components will fail the system. More details about some of the possible system configurations can be found in (Catbas et al. 2012a).

For the DHF, the strain response of the structure and the corresponding component reliabilities, which are determined using the limit state function given in Eq. (4.2), are illustrated in Figure 54 as a function of the number of pads. In this figure, the responses of the main components (components 1 and 4) vary, while the responses of the secondary components (components 2 and 3) remain relatively constant with the change in boundary conditions. The

addition of pads relaxes the stresses of component-1, which is supported by the elastomeric pads, while component-4 is to resist the applied loading thereby experiencing an increase in stresses. Furthermore, Figure 54 shows that none of the four components exceeds the yielding strain, and the minimum component reliabilities are calculated for component-4.
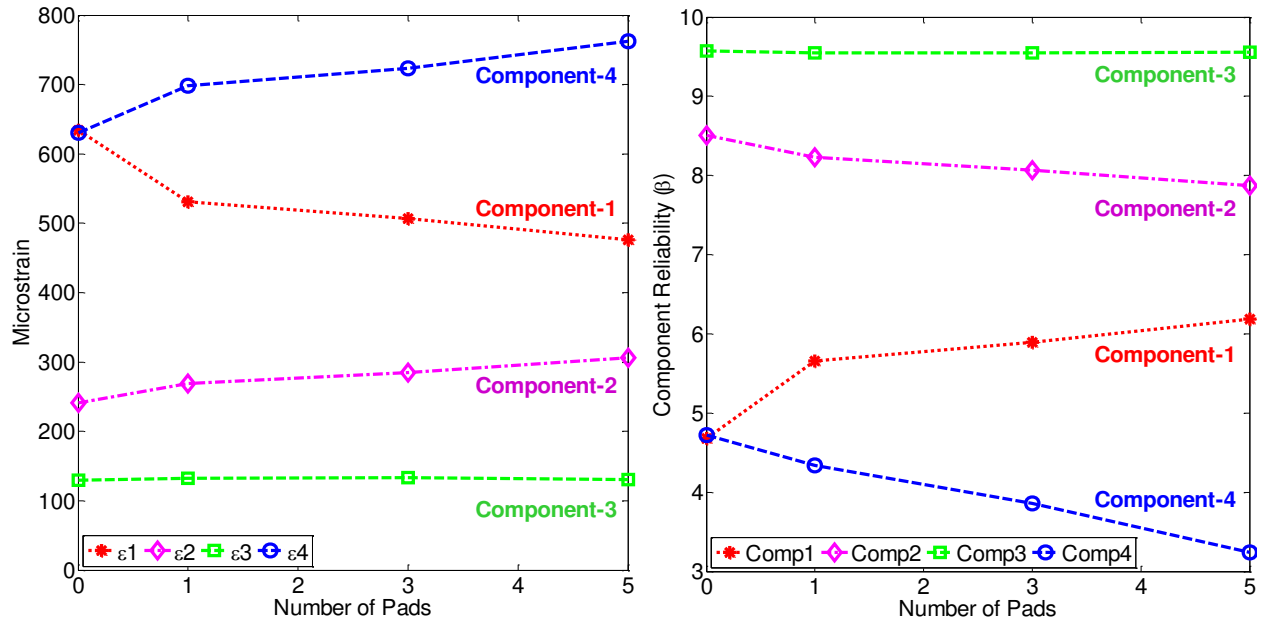
Figure 54: Experimental strain values and corresponding component reliabilities

As mentioned in previous sections, a major objective of this chapter is to demonstrate the quantification of uncertainty in terms of the reliability prediction difference between a one-time initially calibrated FEM and continuously calibrated models (parent and offspring models) for different situations where boundary conditions are changed. For this purpose, DHF is employed using the system configuration given in Figure 45a. The results of the initially calibrated FEM and continuously calibrated family of FEMs are presented in the following.

A complex yet nominal (uncalibrated) FEM or an (initially) calibrated FEM is commonly used for identifying the structural performance under certain damage and deterioration scenarios,

104

as well as to predict the probability of the failure (or reliability) of the structure. In order to quantify the prediction difference between such a case with continuously calibrated models, these two cases are evaluated on the laboratory structure.

The reliability of the system is determined based on the given yielding performance function in Eq. (4.2). First, the FEM is calibrated for pinned support condition, and this model (initially calibrated FEM) is then used for the system reliability calculation. For the subsequent deterioration scenarios (for one pad, three pads, and five pads cases), this initially calibrated FEM model is modified with the spring constants coming directly from the laboratory tests of the elastomeric pads to obtain prediction curves using this initially calibrated FEM. This approach is analogous when a model is employed for reliability prediction where any visually observed condition such as damage or deterioration is simulated using the model. As a result, no monitoring data after the zero-pad condition are used for calibration except for the spring constants that are determined as shown in Figure 48.

Ideally, the FEMs should be continuously calibrated and these models should also consider the uncertainty that still exists within the entire process. To demonstrate this case, the FEM is calibrated for each particular boundary condition by using the ANN-based model calibration approach. As described earlier, such a model is called the parent FEM from which 10,000 offspring FEMs are generated by incorporating the uncertainties, considering the distributions of critical parameters. Consequently, the strain responses of the offspring models, which are obtained as random variables from the offspring model outputs, are employed in reliability computations.

It should be noted that the use of parent-offspring FEMs becomes more important especially when critical parameters cannot be well-defined. The boundary conditions at the very beginning can be characterized as pin support, which can be effectively modeled as compared to elastomeric pads. When the elastomeric pads are stacked on top of each other, the vertical stiffness associated with this support condition cannot be defined simply with a constant coefficient, as can be observed from the laboratory tests shown in Figure 48. As a result, it is seen in Figure 55 that the prediction of reliability from the two cases become separated over time with increased boundary condition changes by adding elastomeric pads at the supports.
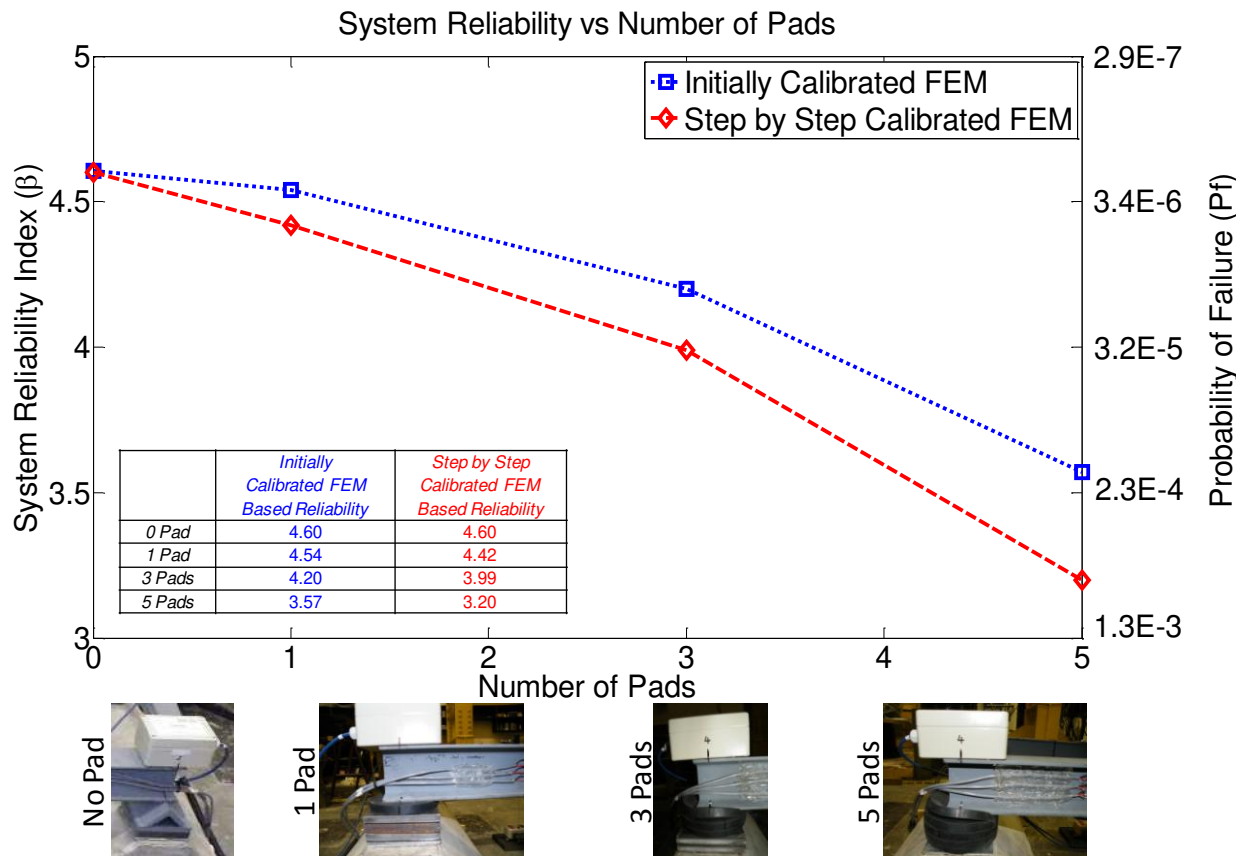
Figure 55: Reliability indices for initially calibrated and step-by-step calibrated family of models

106

The system reliability index of the DHF with pin support (no pads) is predicted as 4.60 by both the calibrated FEM and the family of models since the main uncertainty from the boundary conditions can be modeled effectively. With the addition of the elastomeric pads, the difference in the predictions becomes more and more apparent, especially when five pads are used. In this case, the initially calibrated FEM, which is updated with spring stiffness values from the compression tests, gives a system reliability index of 3.57. However, the continuously calibrated parent model and its offspring yield a reliability index of 3.20. In terms of the probability of failure, the difference in the predictions can be as high as an order of magnitude. This illustrates the importance of calibrating models continuously and incorporating uncertainties with a family of FEMs to better predict the reliability of structures.

4.6. *Summary*

This chapter explores the impact of uncertainty in predicting the system reliability by using a single model as well as using a family of models, whose concept is presented in previous chapters. For the demonstration of system reliability determined by field-calibrated models, a single FE model, which was calibrated initially using the monitoring data, is compared against results obtained from a family of models, which are continuously calibrated with monitoring data. In this chapter, uncertainty types and sources are discussed as these uncertainties are incorporated in the models. In order to illustrate the uncertainty effects, a laboratory structure called Double-H Frame (DHF) is built with a series-parallel system configuration. This test setup is instrumented with different sensors and monitored under changing the boundary conditions in a controlled environment. The changing boundary conditions simulate support deterioration by

using a number of elastomeric pads. The uncertainty due to boundary conditions increases by adding pads at the support. The monitoring data is employed to calibrate FEMs by means of an ANN-based approach.

The calibrated FEMs are considered as parent models, from which a set of 10,000 offspring models are generated, and the offspring models incorporate the uncertainties due to different parameters, which are characterized as random variables. It should be noted that the use of parent-offspring FEMs becomes important especially when critical parameters that have impact on the models cannot be well-defined. The simulations with offspring FEMs yield responses of the structure as distributions rather than single, deterministic values. It is seen that the monitoring data are represented with the offspring models, and the offspring models provide different results for the structural reliability, and this difference increases especially as the structure deteriorates over time, which is simulated by increasing the elastomeric pads at one support location.

In terms of the probability of unsatisfactory performance, the difference in the predictions (obtained using the initially calibrated FEM and a family of FEMs continuously calibrated with monitoring data) can be as large as an order of magnitude. This illustrates the importance of calibrating models continuously with monitoring data and incorporating uncertainties with a family of FEMs to better predict the reliability of structures.

CHAPTER 5.
PARAMETRIC STRUCTURAL ASSESSMENT:
REAL-LIFE DEMONSTRATION-I

5.1. *Introduction*

It is accepted that structural identification (St-Id) applications inevitably involve uncertainties in the measurement and modeling, but such uncertainties can be reduced with improved knowledge. The uncertainty types and sources have long been investigated by many researchers (Ang and Tang 1984; Ang and De Leon 2005; Ellingwood 2005; Moon and Aktan 2006a; Catbas et al. 2008b; Frangopol 2011a). Since the St-Id applications are directly affected by both measurement and modeling uncertainties along with the time-variant characteristics of civil structures, it may not always be reasonable to use a single FEM to represent a structure with this model for various applications. A single FEM calibrated using a set of data may reproduce that data set accurately within acceptable limits, however, another prediction might not be accurate as a result of uncertainties in the data and model, as well as the non-stationarity and nonlinearity of the structure.

The use of population of models has been proposed in the literature in order to consider uncertainty in model development. Papers by Beck and Katafygiotis (1998) and Katafygiotis and Beck (1998) are some of the pioneering efforts in using a set of structural models via Bayesian framework for model updating. In these studies, they mainly discussed identifiability of multiple calibrated models and illustrated a Bayesian probabilistic framework on identification of a two-degree-of-freedom linear planar shear building to update the robust reliability using measured response data. It should be noted that for Bayesian inference applications, new data is needed to

obtain the posterior distributions, but this type of future data may not exist for making long-term predictions in some cases. In a study by Papadimitriou et al. (2001), Bayesian methodology-based system identification of a very simple beam model is combined with probabilistic structural analysis to update the assessment of the robust reliability based on dynamic test data and the difficulties of evaluating the total probability theorem unless only a small number of modal parameters are involved. Bayesian probabilistic approaches are also investigated for identification of structural damage via SHM (Sohn and Law 1997; Papadimitriou et al. 2000; Ching and Hsieh 2009).

In recent years, selection of a population of candidate models with the help of a stochastic global search was presented by Robert-Nicoud et al. (2005b). In that study, it was shown that the increase of sensor information can reduce the number of candidate models, which directly affects the system identification process. In a study by Smith and Saitta (2008), a combined data-mining technique (based on principal component analysis and k-means clustering) was investigated for finding the candidate models. This new methodology was demonstrated on a real-life structure (Schwandbach Bridge) and the usefulness of data-mining techniques for grouping models into clusters for better St-Id was demonstrated. Moreover, different optimization methods, such as global search for obtaining the initial sensor locations for a monitoring system and greedy strategy for finding the locations for damage identification, were presented on two different bridges by Kripakaran and Smith (2009) with the multi-model approach considerations. In a different study, multi-models of Langensand Bridge in Lucerne were used for displacement, rotation, and strain predictions by considering the modeling and measurement uncertainties (Goulet et al. 2010). While such studies provide concepts of multiple models, the use of

110

numerous models for determining some of the practical engineering concepts, such as load rating

of bridges, or more advanced concepts, such as system-level reliability with the consideration of

correlation of different components with each other, were not explored for real-life structures.

In the previous chapter, the impact of uncertainty was explored for predicting the system

reliability obtained by a one-time, initially calibrated FEM and also by a family of FEMs

continuously calibrated with monitoring data (Catbas et al. 2012a). The importance of using

multiple models, the effects of using single models for performance prediction, and the

advantages of continuous calibration with new SHM data were discussed and demonstrated on a

simple laboratory structure.
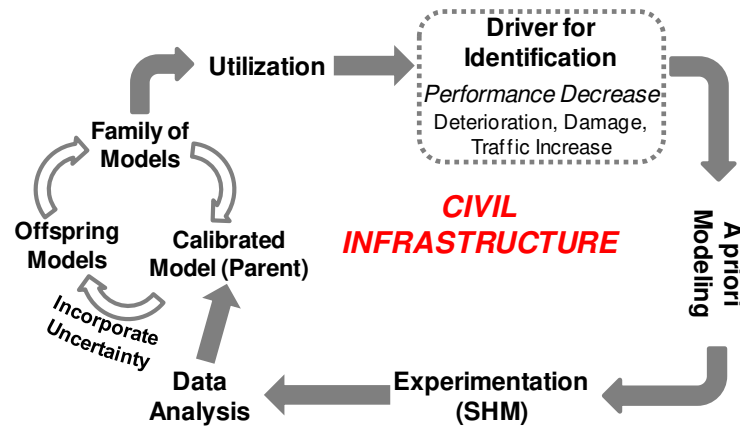
Figure 56: Use of uncertainty-incorporated family of models for St-Id of a movable bridge due to performance decrease

In this chapter, a family-of-models approach with parent and offspring models will be

investigated for predicting the performance of a real-life structure due to performance decrease

(Figure 56). St-Id is employed by means of developing models, utilizing field measurements for

model calibration, and decision making for load-carrying capacity and reliability of the structural

system. The uncertainty in the data collected by means of intermittent testing or monitoring, limitations of the models, and non-stationary nature of structural behavior need to be considered. These uncertainties can be incorporated by using a family of models that can be described as parent and offspring models.

The significant contributions of this chapter may be summarized as follows. The multiple models (offspring models) are created to incorporate the uncertainties. A single calibrated model is not used because a perfect single model cannot be obtained using the SHM data as commonly seen in the literature. Implementation of multiple models for performance prediction under damage and deterioration is rarely tackled in previous studies. The inclusion of the real SHM data for calculating the reliability index is also not commonly seen in the literature. In this chapter, load rating is presented with a probabilistic approach along with the structural reliability analysis of the Sunrise Boulevard Bridge. As a result, the performance of the bridge is evaluated using these commonly used performance metrics. In this case, load rating is given with a distribution with the inclusion of uncertainties. For the system reliability approach, the bridge is modeled with different system configurations, and the analyses are conducted based on (1) SHM data, which provide the traffic stresses due to heavy vehicle traffic and temperature cycles, and (2) family-of-model simulations in which a traffic flow is generated with different vehicles. In order to consider some common issues related to this specific bridge type, time-dependent deterioration models that include corrosion of the girders along with live load increase over time and a damage case are investigated to demonstrate the implementation of St-Id with a family of models for performance prediction. Such results are expected to provide a set of solutions for the performance of a structure for optimum decision making.

5.2. Case Study: Sunrise Boulevard Bridge and Monitoring System

Sunrise Boulevard Bridge is employed to demonstrate the use of a family of models incorporating uncertainty for structural identification due to performance decrease. Details about the bridge description and the monitoring system were discussed in the second chapter of this dissertation. For this chapter, three months' worth of monitoring data from the high-speed and slow-speed strain gages, which are located at the bottom flange sections of the main girders, is used for the investigation of the structural identification process by considering deterioration, damage, and traffic increase. A total of 12 high-speed strain gages are utilized for capturing traffic events, and a total of 12 slow-speed strain gages are utilized for capturing environmental events on the bridge.

The nomenclature for strain gages and the corresponding three-month traffic-induced strain and temperature-induced daily strain cycle histograms obtained using the monitoring data are given in Figure 57. In this figure, histograms for heavy-traffic-induced strain and temperature-induced daily strain cycle for the East-North (EN) main girder sensor locations are shown along with the fitted lognormal distributions. It should be noted that these measured data will be used for the reliability calculations of the bridge in the later sections of this chapter. As seen in the traffic strain histograms, the higher strain values are observed at EN3, which is close to the boundary location called live load shoes. Due to the cantilever behavior of the Sunrise Boulevard Bridge leaves, the lowest traffic-induced strains are recorded at the tip location (EN1). More details about the bridge and its monitoring system can be found in Catbas et al. (2011) and Gokce et al. (2012a).
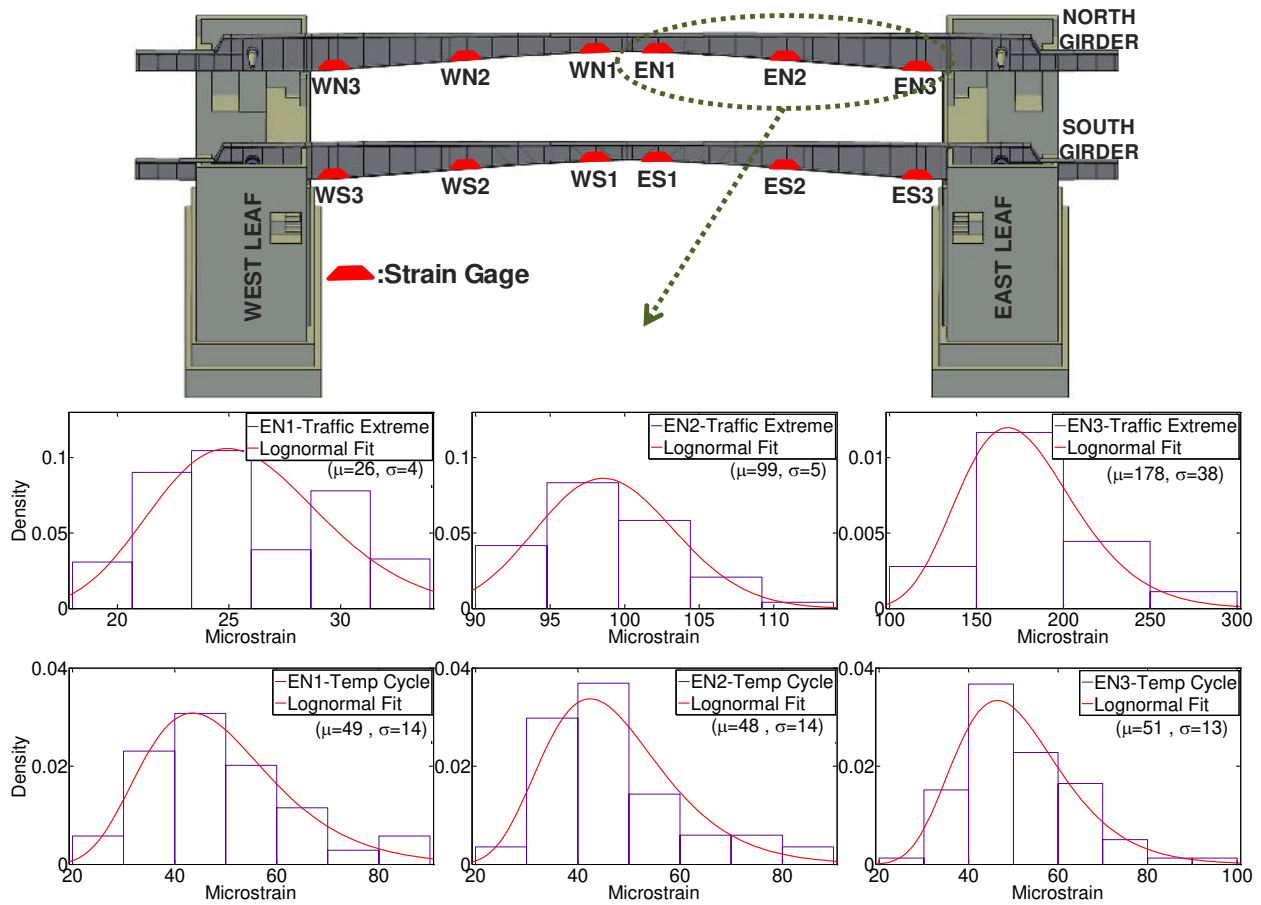
Figure 57: Location nomenclatures and representative traffic- and temperature-induced strain histograms for different locations of the east-north girder

5.3. *Family of Models*

The importance and reasons of using a family-of-models approach was discussed in the second chapter. In this section, a family-of-models approach is described for a movable bridge. In the following subsections, uncertainties, artificial neural network (ANN) based calibration strategy by utilizing multiple objective functions, and parent and offspring models are discussed. A flowchart that summarizes chapter five is presented in Figure 58.
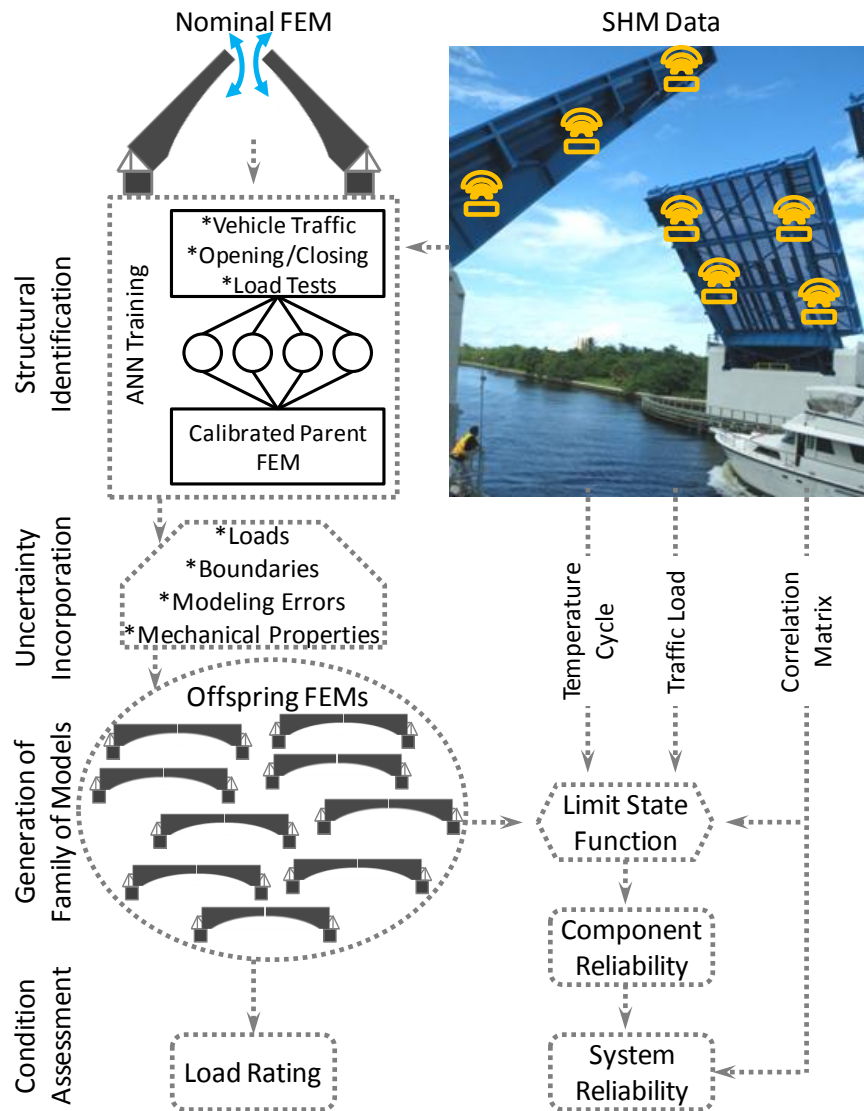
Figure 58: Flowchart that summarizes chapter five

5.3.1. *Uncertainties Considered for the Case Study*

Characteristics and sources of uncertainties need to be identified and defined as carefully as possible for the reliability analysis. Although many sources of uncertainty may exist, they are generally categorized as either aleatory uncertainty, which is associated with randomness, or

epistemic uncertainty, which is associated with imperfect knowledge due to lack of data or crude models (Ang and De Leon 2005). It should be noted that the effect of epistemic uncertainty can be reduced with more information, which can be obtained with health monitoring systems. In a paper by Kiureghian and Ditlevsen (2009), the categorization of uncertainties as aleatory or epistemic is mainly discussed, and it is mentioned that this categorization depends on the uncertainty model builder by considering the context and application.

Sources of uncertainties, which are visualized in Figure 59, are classified into three different groups: (1) Associated with modeling: boundary conditions, material properties, section properties, loads, deterioration, and damage; (2) Associated with measurement: data acquisition accuracy, sensor resolution, and field test design; (3) Associated with data post-processing: failure modes, correlation, and assumed distributions. Distribution types and coefficients of variation of these uncertainties are provided in Figure 66.
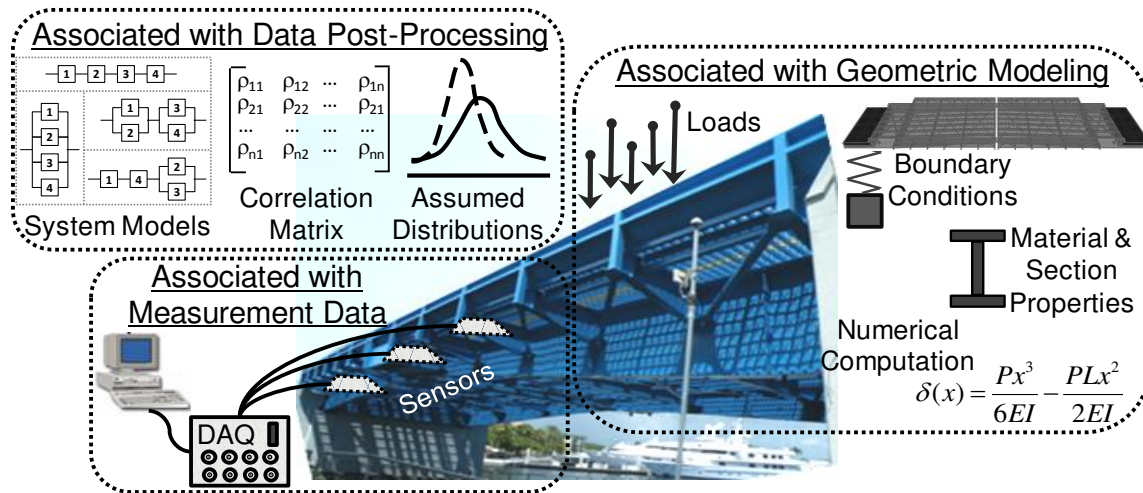
Figure 59: Uncertainty sources considered in this chapter

5.3.2. *ANN-based FEM Calibration and Parent Model*

Different model updating/calibration studies from different researchers are presented in the introduction. In this study, Artificial Neural Networks (ANN) are utilized for FEM calibration. Briefly, ANN learns from the provided patterns and then makes a prediction for the patterns that are not provided during learning. A flowchart is presented in Figure 60 to summarize the ANN-based model calibration strategy for the Sunrise Boulevard Bridge model.

In the beginning of the calibration process, first a preliminary frame model of the bridge, which consists of 1,084 frames, 720 shells, 32 solids, and 963 rigid links, is developed using the nominal structural parameters and material properties. Next, a total of 2,000 FEMs are created randomly by using the uniformly distributed modulus of elasticity, moment of inertia, and spring stiffness parameters generated by the parameter pool. The strain outputs of these FEMs are collected at 12 different locations. Then, ANN is trained to learn the relationship between the bridge responses and model parameters by using the Levenberg-Marquardt learning algorithm (Levenberg 1944; Marquardt 1963). Eq. (5.1) shows the basic algebraic equation for each layer of an ANN that is used in this study.

$$a_j = f\left[\sum w_{ij}u_i + \theta_j\right]$$

(5.1)

where a_j is the output of neuron j; w_{ij} represents the weight from neuron i to neuron j; u_i is the input signal generated for neuron i; θ_j is the bias term associated with neuron j; and the nonlinear activation function $f(x)$ is assumed to be a sigmoid function as:

$$f(x) = (1 + e^{-x})^{-1}$$

(5.2)

1) Model Parameters Pool (E_i, I_i, k_i)

2) Randomly Generated FEMs

3) FEM Outputs & ANN Training Inputs (P_i, ϵ_{FEM})

4) Hidden Layers

5) ANN Outputs (E_o, I_o, k_o)

6) Experimental Strains from Load Test
(P_{EXP}, ϵ_{EXP})

Trained ANN from 3,4 and 5

7) Calibrated Model Parameters (E_{cal}, I_{cal}, k_{cal})
Check if the predicted parameters are realistic

8) Axle Loads from Load Test (P_{EXP})

9) FEM Results (ϵ_{cal})

10) 1st Objective: Truck Load Test
Check difference if within acceptable limits.

11) 2nd Objective: Dead Load Test
Check difference if within acceptable limits.

12) 3rd Objective: Regular Traffic Load
Check difference if within acceptable limits.

13) Obtained Parent FEM

Figure 60: Flowchart of ANN-based calibration process

The network architecture consists of an input layer of 12 nodes (12 axial strain values), an output layer of 32 nodes (8 stiffness values at supports, 12 modulus of elasticity values, and 12 moment of inertia values) and one hidden layer of 32 nodes. In this training procedure, data coming from 2,000 models is divided into three sets, and the first set is the training set, which contains 1,300 patterns to detect the relationship between inputs and outputs. The second set is

the cross-validation set, which contains 300 patterns to avoid the problem of over fitting or in other words to avoid memorization of the patterns. The last set is the test set, which consists of 400 patterns and is used to evaluate the performance of the networks by checking errors between the real and the ANN-predicted values.

After the completion of network training, experimental strain readings coming from load test are fed into the trained neural network system to predict the values of structural parameters (moments of inertia, moments of elasticity, and spring stiffnesses). These structural parameters predicted from network analysis are first checked whether the parameters are realistic and then are used to create the preliminary calibrated FEM.

Then, using a multi-objective evaluation, which utilizes data from different tests, the validity of the ANN training is checked to confirm if a calibrated model is obtained. It should be noted that the truck loading corresponds to static field tests conducted on the bridge, which were explained in second chapter. In addition, dead load is obtained by the strain differences during opening-closing events. Lastly, the regular traffic load is collected by the automated monitoring system during rush hours. More information about these loadings can be found in (Catbas et al. 2011).

The acceptable root mean squared error for 12 locations is selected as 10% because it was shown that this much difference between local measurements (strains or displacements) and analytical models of bridges can be considered quite satisfactory (Catbas et al. 2007). In this multi-objective evaluation, a comparison between the experimental and analytical response of the bridge is conducted. If these two sets of parameters differ significantly, then the ANN model is re-trained. The re-training procedure is continued until the difference between the measured

and calculated responses assures the target criteria. In Figure 61, a comparison of test and calibrated FEM outputs under different objectives is presented with root mean squared errors for different locations. These errors indicate that the preliminary calibrated FEM can be accepted as a parent model (Figure 62) from which the offspring models are generated as discussed in the following.
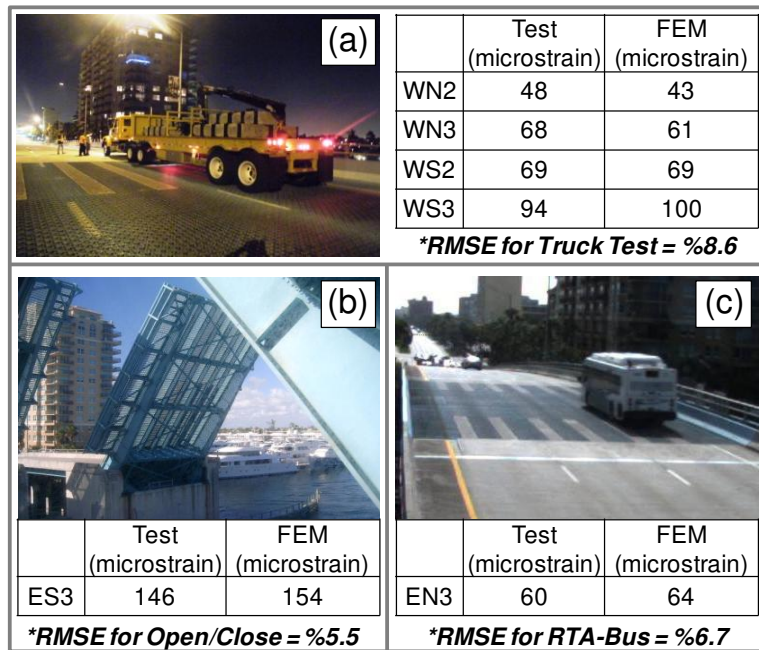
Figure 61: Comparison of measured strains and calibrated model results for truck load (a), dead load (b), and bus load (c)
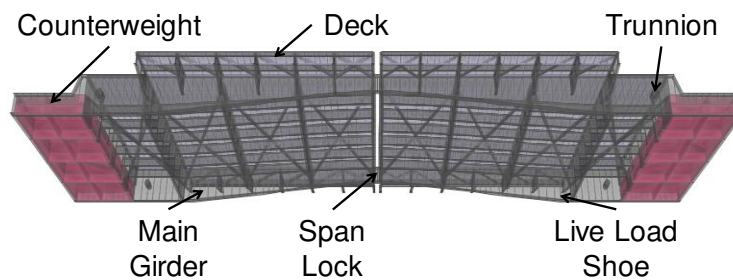
Figure 62: Sunrise Boulevard Bridge parent model and some typical movable bridge components

5.3.3. *Deterioration and Damage*

As mentioned in the second chapter, movable bridges undergo certain deterioration effects due to normal aging and operation. For maintenance operations and bridge safety, it is crucial to estimate the future condition of these bridges. Corrosion penetration and associated section loss can be considered as the main factor in capacity degradation over the lifetime of the bridge. Section loss due to corrosion is a major cause of deterioration for steel profiles, especially at locations closer to salt water and with high humidity. The following corrosion penetration model given by Albrecht and Naeemi (1984) is used in the family-of-models application to define the degradation effect over time:

$$C(t) = A \times t^B$$

(5.3)

where $C(t)$ is the corrosion penetration depth in 10^{-6} m, t is time in years, and A (normal distribution, mean=34.0, coefficient of variation=0.09) and B (normal distribution, mean=0.65, coefficient of variation=0.10) are statistical random variables (Albrecht and Naeemi 1984). The corrosion penetration is assumed to follow the pattern shown in Figure 63. According to this pattern, due to pooling, the corrosion progresses along the top surface of the bottom flange and ¼ of the depth of the web. A similar example was also presented by Estes and Frangopol (1999). The section loss can be calculated based on the corrosion penetration function and the corrosion pattern. The mean value and standard deviation for the moment of inertia and section modulus at WS3 are evaluated with respect to time for all girder members of the parent FEM (Figure 63). Finally, the long-term deterioration effects due to corrosion are modeled as statistical variables. It is noted that the uncertainty in the model increases with time as expected. The parent FEM discussed above is selected to represent the current condition (0 year) of the Sunrise Boulevard

Bridge. By considering the time-dependent corrosion models, five more parent FEMs are created for demonstration of the condition of the bridge for 15, 30, 45, 60, and 75 years. In this study, no maintenance for corrosion was assumed over the 75 years as shown in Figure 63.
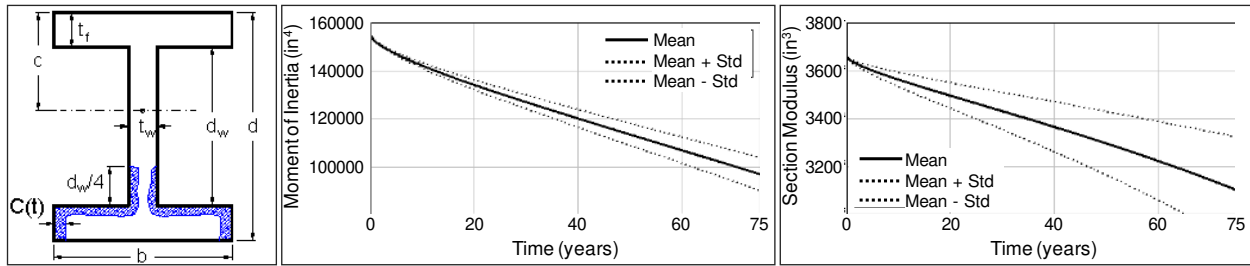
Figure 63: Corrosion penetration model, moment of inertia, and section modulus change over time for WS3 section

Movable bridges constantly suffer from the wearing effect of opening/closing operations such as the breakdown of the span lock and its drive system (Figure 64). In addition to the deterioration that gradually occurs over time, instantaneous damage is another problem in these types of kinematic structures. Therefore, the effects of span-lock failure, which was identified as one of the problematic components in the second chapter, are also investigated as a sudden performance decrease. In the literature, the effect of span-lock failure was investigated from the load distribution point of view by Catbas et al. (2011), but in this chapter this effect is explored from a performance metric point of view.

The span-lock bar locks the two leaves of the double-bascule spans, providing a safer load distribution and preventing excessive deflections and vibrations. For this purpose, another parent model with south span-lock failure is created for 0 years to compare the effects of performance loss between the deterioration and damage. To represent the span-lock damage in

122

the parent model, the continuity condition of the south girders was removed for the damage simulation.
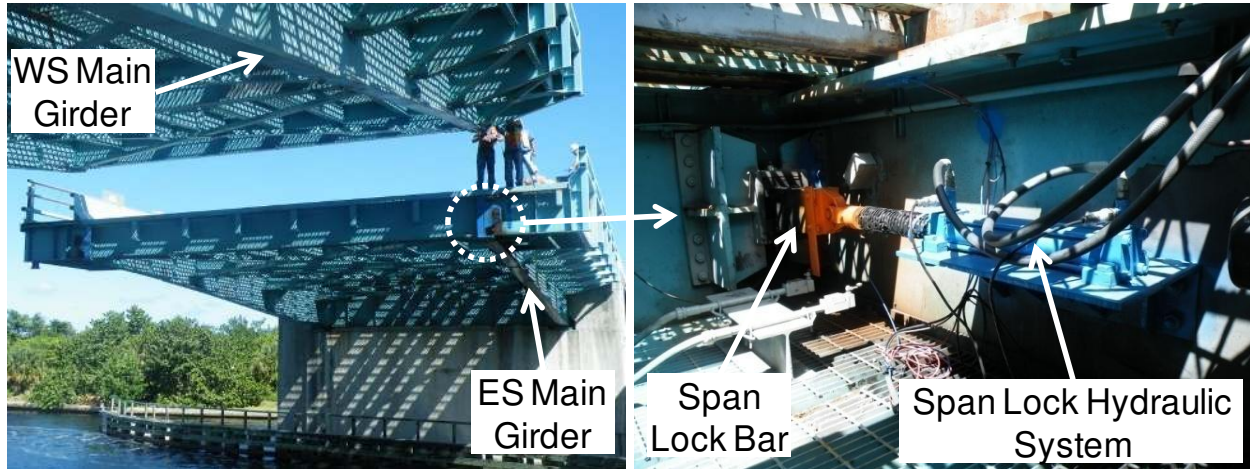
Figure 64: Movable bridge span lock and its components

5.3.4. *Live Loads and Live Load Increase*

The parent model of Sunrise Boulevard Bridge is loaded with different types of vehicles for two types of performance evaluations, i.e., load rating and system reliability. Calculations of these performance analyses are presented in the following sections in more detail. For the load rating evaluation, two HL-93 trucks and lane load are used as shown in Figure 65a. These positions of the two HL-93 trucks are selected to give the most critical load rating case which was identified based on a previous study by Gokce et al. (2011). In addition, a total of 14 vehicles which consist of the buses and firetrucks are also used for loading the model in the right and left lanes for the system reliability evaluation (Figure 65b). The idea behind the loading numbers of heavy vehicles is to create traffic flows from the offspring models, which are described in the next section. It should be noted that these two specific heavy vehicles are

selected since their presence on the bridge is very likely due to the bus route and proximity of a fire station to the bridge.
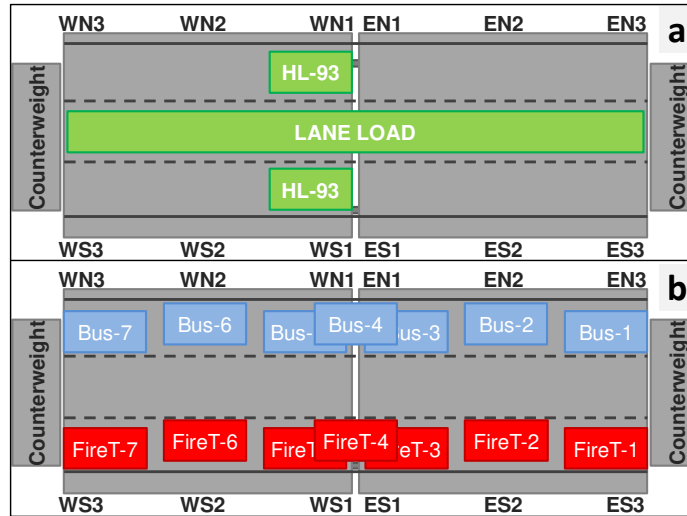
Figure 65: HL-93 (a) and heavy truck (b) loading for the parent model of the movable bridge

For the parent models representing the aged bridge (15, 30, 45, 60, and 75 years), a traffic load increase over time is also considered based on the following equation given by Nowak (1999):

$$\Delta = \mu_{traffic} + 5.33 \times \sigma_{traffic}$$

(5.4)

where Δ is the expected 75-year maximum traffic load, $\mu_{traffic}$ and $\sigma_{traffic}$ are the mean and the standard deviation of the current traffic load based on the three months daily maximum data, respectively. This increase is reflected directly to the applied loads (bus and firetruck) in the offspring models of different ages by considering the live-load uncertainties. Finally, a total of seven parent models are developed: one for the baseline condition (0 year), five for deterioration simulations over 75 years (15, 30, 45, 60, 75 years), and one for the span-lock damage case (0 year-SL).

5.3.5. *Offspring Models and Traffic Generation*

This section presents the generation of offspring models based on the parent models (total of seven) by considering the adapted uncertainties (Nowak and Collins 2000), which are presented in Figure 66. The number of offspring models that will be used for simulations is decided based on the Eq. (4.1), which was error associated sample size proposed by Ang and Tang (1984).

In each offspring model, variables such as moment of inertia, modulus of elasticity, dead load, live load, spring constants for boundaries, and yield stress are incorporated based on the coefficients of variation as given in Figure 66 to create the offspring models from each parent model. As described in previous chapters, this manipulation is accomplished by a visual basic code that was developed by researchers that interacts with the finite element code and randomly changes the variables with the defined distributions in the text files of the parent models. Moreover, the analyses of the offspring models are completed with a batch file that automatically opens and analyzes the model and then saves the outputs in a defined format under the defined loads for interested locations.

	Coefficient Of Variation	Distribution
*Moment of Inertia (I)	18%	Normal
*Modulus of Elasticity (E)	10%	Lognormal
*Dead Load (D)	10%	Normal
*Live Load (P)	18%	Normal
*Spring Constant (k)	10%	Normal
*Yield Stress (F_Y)	10%	Lognormal
*DAQ and Sensor (η)	2%	Uniform

Parent (Calibrated) FEM for each year: 0 year, 15 year, 30 year, 45 year, 60 year, 75 year, 0 year-SL

Offspring FEM Generation based on Uncertainty of Variables

Simulations with Offspring FEMs

Offspring Outputs for each group: 0-y, 15-y, 30-y, 45-y, 60-y, 75-y, 0-y SL

Figure 66: Incorporating uncertainty of variables into the parents to generate offspring models

125

Several other computer codes are also developed to collect and tabulate the data from numbers of offspring models. One important code is for the traffic flow generation from the offspring outputs. As mentioned earlier, 14 different heavy vehicles (bus or firetruck) are loaded in each offspring model, and a traffic flow is generated for each family of models with a random selection process based on the following probabilistic assumptions:

- In 60% of the situations, only one vehicle will be on one lane. For example, there are 14 pre-defined spots, which cover almost all of the locations in right and left lane, and randomly one of the vehicles (bus or firetruck) will be on one of these spots.

- In 30% of the situations, which yields 3,000 out of 10,000 simulations, two vehicles will be on two different lanes.

- In 10% of the situations, two vehicles will be on the same lane. As an illustration, one bus and one firetruck can be on the right lane. The third assumption is a rare one, but it is likely to be seen right after an opening/closing event when vehicles simultaneously start after short durations of stopped-vehicle traffic.

Finally, these outputs of offspring models are analyzed, and the histograms of the responses are obtained along with the appropriate distribution fits. The distributions are obtained to calculate the load-rating distributions and system reliability and can be seen for the ES and WN main girder locations for 0 year in Figure 67. For all of the locations, it is seen that the best distribution fit is chosen as Generalized Extreme Value (GEV) distribution function given in Eq. (5.5), and this selected distribution type is used in the system reliability calculations.

$$f_x(x) = \frac{1}{\sigma}\left[1 + \xi \times \left(\frac{x - \eta}{\sigma}\right)\right]^{-1/(\xi-1)} \times \exp\left(-\left[1 + \xi \times \left(\frac{x - \eta}{\sigma}\right)\right]^{-1/\xi}\right) \qquad (5.5)$$

where $f_x(x)$=probability density function (PDF) of the GEV distribution; ξ=shape parameter of $f_x(x)$; σ=scale parameter of $f_x(x)$; η=location parameter of $f_x(x)$.
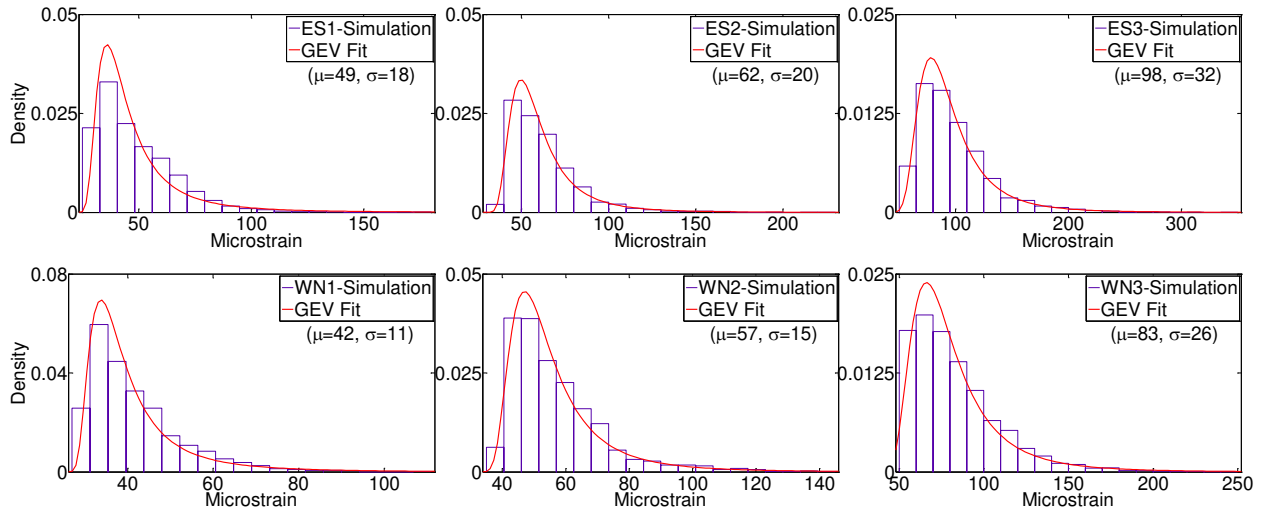
Figure 67: Representative offspring output histograms coming from the generated traffic flow for WN and ES main girder locations for Year 0

5.4. *Bridge Performance Predictions*

5.4.1. *Load Rating*

In the second chapter, details of the load rating calculation were discussed, and formulation was given in Eq. (2.1). In this section, the load rating of the movable bridge is calculated by following the AASHTO Guide (AASHTO 2004) and using the offspring model outputs, which are loaded by two HL-93 trucks and HL-93 lane load (0.64 kip/ft) as given in Figure 65a. The load factors change according to the type of load rating, i.e., inventory or operating load rating, and only the inventory load ratings are presented in this section for the sake of brevity.

127

The weakest link for the inventory load rating is found to be the WS3 location under HL-93 loading from the offspring models outputs. In Figure 68, the load rating values from single models (parent models) and load rating distributions from the family of models are compared for different cases.

Load Rating	Parent FEM	Family of Models mean ; c.o.v
Current cond. (0 years)	2.11	2.21 ; 9%
Predicted cond. at 30 years	1.88	1.76 ; 15%
Predicted cond. at 75 years	1.15	1.06 ; 35%
0 year with SL Damage	1.40	1.47 ; 17%
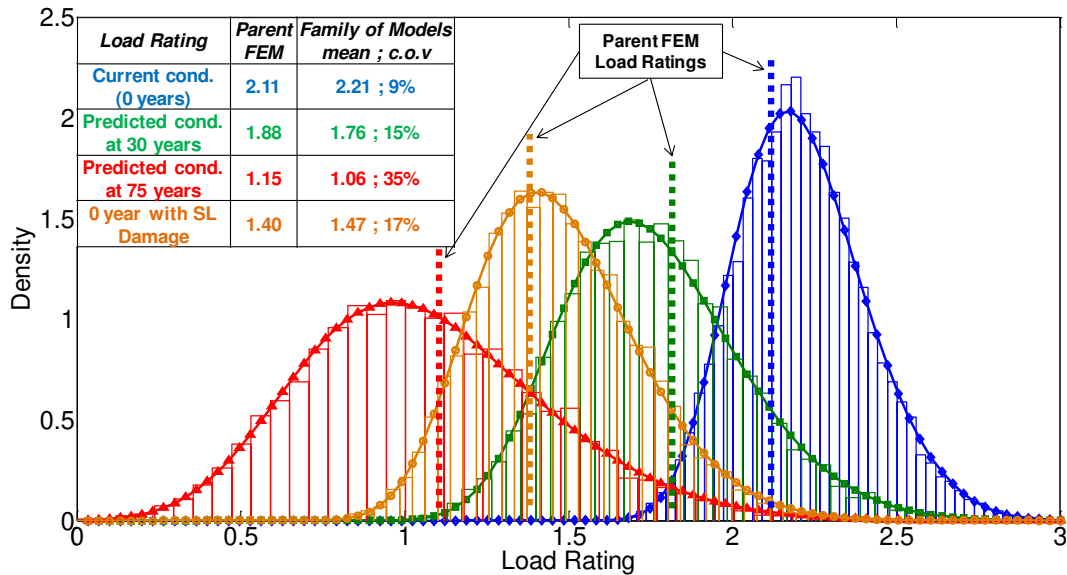
Figure 68: Comparison of load rating at WS3 obtained using a family of models and parent models

For the current condition of the bridge, the parent model gives a load rating of 2.11, whereas the offspring model outputs give a distribution with a mean of 2.21 and a standard deviation of 0.20. Furthermore, under deterioration, the predicted parent-model load rating for 75 years is 1.15, and the predicted family-of-models load rating distribution has a mean of 1.06. These deviations in the predicted load rating values can be reduced if SHM data is employed to update the models as proposed in the fourth chapter of this dissertation. Moreover, it is observed that some of the parent-model load ratings are slightly higher than the mean of the distribution for future cases, implying that non-conservative values may be obtained when parent models are

128

used. This can be attributed to the increase in uncertainty bounds as presented in Figure 63 for deterioration conditions. Next, Figure 68 also indicates that span-lock damage is a very critical issue for bascule type movable bridges because this phenomenon directly affects the load distribution on the bridge. The offspring model outputs show that the mean load rating for 0 year is decreasing from 2.21 to 1.47 due to span-lock failure. This specific damage can be considered to be equivalent to a 45-year deterioration effect in terms of the load rating of the bridge.

With the family-of-models approach, it is also possible to explore the probability of not meeting a certain level of load rating for a structure. In this discussion, this probability is deemed as risk. In a study by Catbas et al. (2012c), the uncertainty impacts were found to be considerable when simplified methods used for load rating calculations as followed in the current practice. Since it is known that uncertainties cannot be totally eliminated, it is important to incorporate them in the analysis and also to quantify the risk from these models. In Figure 69, load rating results of parent and offspring models are presented along with the quantified risk of having a load rating less than one for the span lock failure case.

Based on the AASHTO Guide (AASHTO 2004), the load rating of a bridge should be higher than 1.0. In this study, load rating is calculated as 1.40 from the parent model whereas the mean of the load rating coming from the offspring models is calculated as 1.29. Both results are acceptable from a bridge engineering perspective. Based on family-of-models approach, the probability ("risk") for having a load rating less than 1.0 is calculated as 1.6%. As a result, family-of-model approach not only provides the bounds and distributions of load ratings in a non-deterministic manner by considering different uncertainty sources but also quantifies the risks for structures.

129

Load Rating	Parent FEM	Family of Models mean ; c.o.v.
0 year with SL Damage	1.40	1.47 ; 17%

Parent Model
(SL Damage)
LR=1.40

Risk
0.016

Offspring FEMs
$\mu_{LR} = 6.87$
$\sigma_{LR} = 1.29$
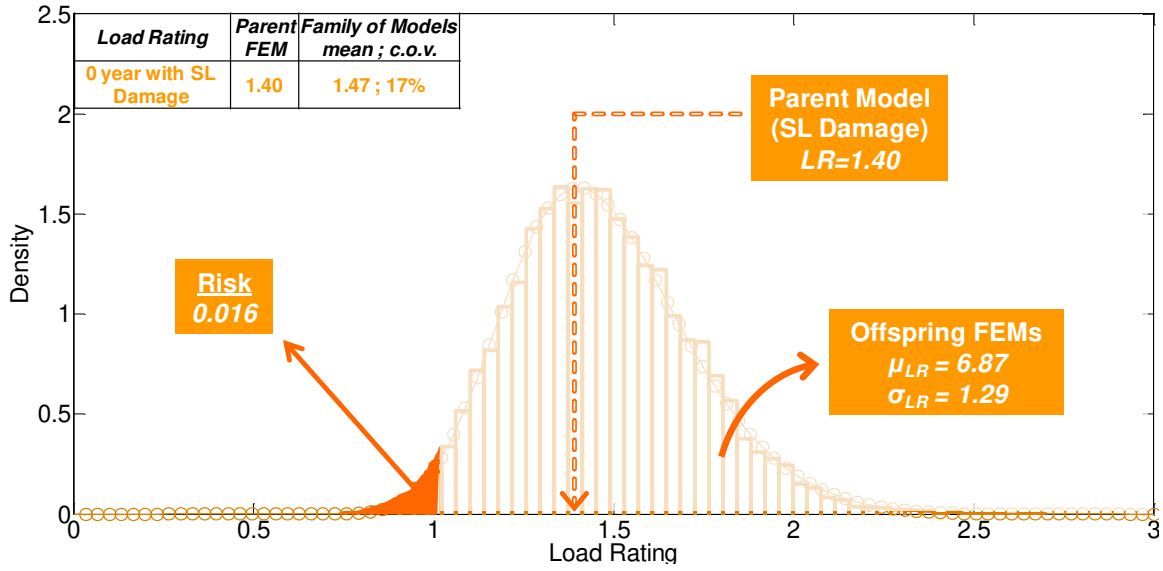
Figure 69: Load rating results of parent and offspring models for the span-lock failure

5.4.2. *Component and System Reliability*

The second bridge performance metric demonstrated in this chapter is the reliability index that can be defined as probabilistic modeling of capacities and demands under a given limit state. As explained in the second chapter of the dissertation, prior to applying the system reliability approach, the limit state functions for the components are defined; the correlation between responses of different components and the system models are generated. In this section, Sunrise Boulevard Bridge is analyzed with respect to yield strain of 12 different failure modes. Component reliabilities of the bridge are obtained mostly from SHM data, which are presented with histograms in Figure 57, by using the following limit state function:

$$g = \left(0.9 \times \varepsilon_y\right) - \varepsilon_{dead}^{offspring} - \varepsilon_{live}^{offspring} - \varepsilon_{lane}^{SHM} - \varepsilon_{temp}^{SHM} \tag{5.6}$$

The given limit state function consists of the capacity and demands. For the strain capacity (ε_y), a multiplier 0.9 is assumed for the given limit state to be within linear range. On

130

the other hand, demand has different components such as dead load ($\varepsilon_{dead}^{offspring}$) obtained from self weight of the offspring models, heavy vehicle load ($\varepsilon_{live}^{offspring}$) obtained from off-spring models (Figure 65b), lane load (ε_{lane}^{SHM}) obtained from SHM data (Figure 57) and temperature induced strain cycles (ε_{temp}^{SHM}) obtained from SHM data (Figure 57). It should be noted that using only SHM data may produce higher reliability indices (or lower probabilities of failure) because the mean of the SHM data will offer lower strain values due to the light traffic caused by cars which can be insignificant for reliability applications. For this reason, real data is used as a lane load. Component reliability results for South main girder locations at t=0 year can be seen in Figure 70.
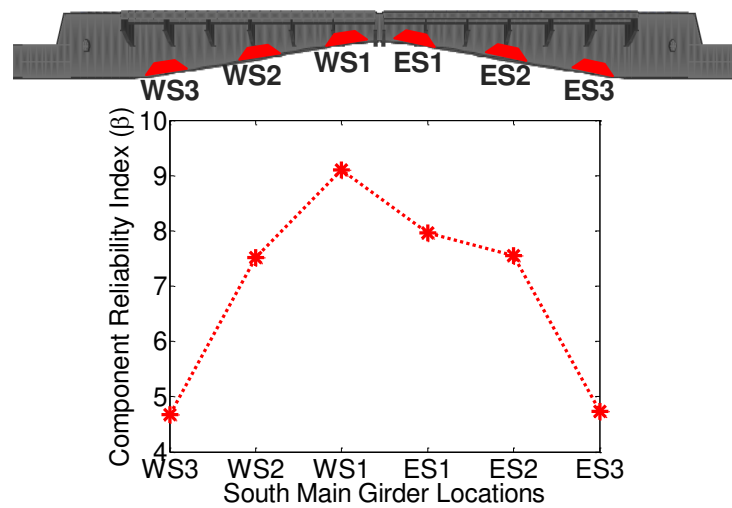
Figure 70: Component reliability index results for south main girders locations at t=0 year

As mentioned earlier, due to the cantilever behavior of the bridge, lower reliability indices are seen for locations close to boundaries (such as ES3 and WS3) which are near the live load shoes of movable bridges. On the contrary, ES1 and WS1, which are closer to the span locks (tips of the cantilever), show the lowest stresses (strains) and as a result, they have the

highest reliability indices. It should also be mentioned that there is a difference in the component reliability of the symmetric ES1 and WS1 due to the slightly different response of these components as seen in the monitoring data.

Four different system models (Figure 71), which describes the relationship of the components and behavior of the system, are generated to cover possible failure modes of the bridge and these models are as follows:

- Series system: Failure of any component will fail the system.

- Parallel system: Failure of all components will fail the system.

- Combined System-1: Failure of any two main girder components will fail the system.

- Combined System-2: Failure of all components any main girder will fail the system.

Series and parallel systems are considered to provide upper and lower reliability bounds whereas two different combined systems are presented to offer a more realistic system models by mainly considering the failure of each main girder.
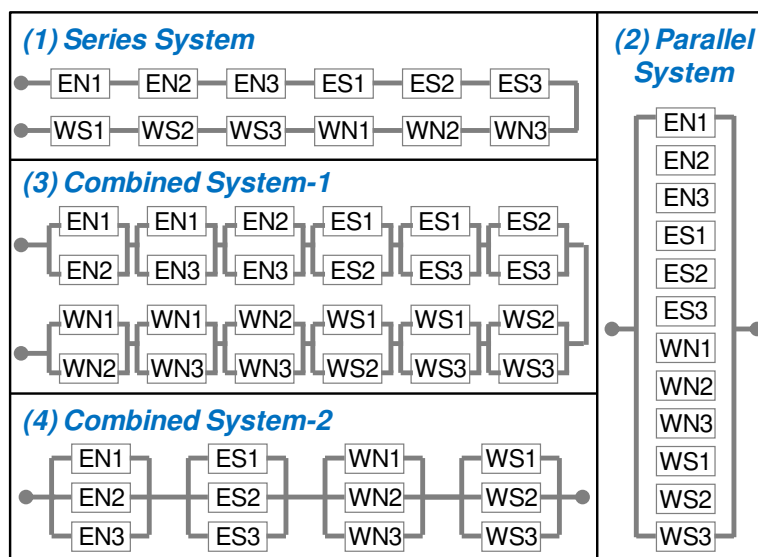
Figure 71: Series, parallel and combined system models for the movable bridge

132

The system reliability of any system depends also on the correlation among the safety margins of the components. The two extreme cases are: (a) perfectly correlated safety margins, and (b) independent safety margins. Due to the lack of data regarding correlation among the random variables (capacities, dead loads, live loads, and temperature loads) involved, the following considerations were assumed. Load and resistance are separately correlated with each other but not correlated together. Moreover, there are four types of loads that are separately correlated with each other. For example: correlation coefficient between dead loads can be 1.0 or 0.5 but correlation coefficient among dead load and live load is always considered as 0. Considered three correlation cases are as follows: (1) capacities and all the loads are independent ($\rho=0$), (2) capacities are perfectly correlated ($\rho=1$) and each type of load is separately perfectly correlated ($\rho=1$), (3) capacities are partially correlated ($\rho=0.5$) and each type of load is separately partially correlated ($\rho=0.5$). All these cases were considered for each assumed system.

The reliability analysis of the bridge was conducted by using the reliability software RELSYS (Estes and Frangopol 1998). RELSYS can compute reliability of generic series/parallel systems other than single components. In order to compute system reliability, RELSYS needs to reduce the systems to one equivalent component by solving the parallel components first and then the series components. The calculation of the system probability of failure was presented in the second chapter of the dissertation.

Upper and lower bounds of the system reliability indices are illustrated in Figure 72. For a series system, the system safety is maximum when the safety margins of components are perfectly correlated and minimum when they are independent. For a parallel system, the system safety is maximum when the safety margins of components are independent and minimum when

133

they are perfectly correlated. As a result, the upper reliability bound is the parallel configuration of the system with zero correlation variables and the lower bound is the series configuration with zero correlation. In these system reliability calculations, failure modes with very high reliabilities (i.e., $\beta_{sys} > 10.0$) are taken as 10.
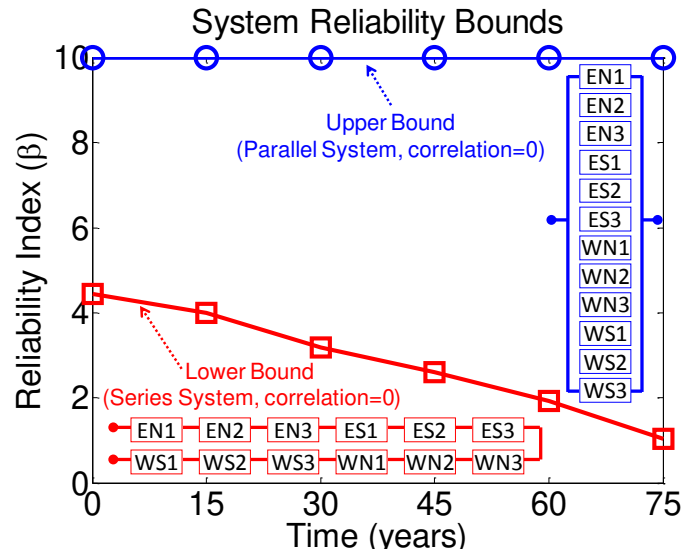
Figure 72: System reliability upper and lower bounds for the movable bridge

Figure 73 shows the system reliability results of combined system models over time for different correlation cases, which are defined previously. As expected system reliabilities of combined system-1 are less than those of system-2 due to the assumed differences in system models. In addition, it is observed from these results that no correlation yields smaller probabilities of failure of the structural system over years. Moreover, partial or perfect correlation does not make too much difference for system reliability indices in combined system-1 while for the more redundant system model (combined system-2); the effect of correlation is

more pronounced. Finally, the reliability values for the different systems lie between the upper and lower bounds as expected.
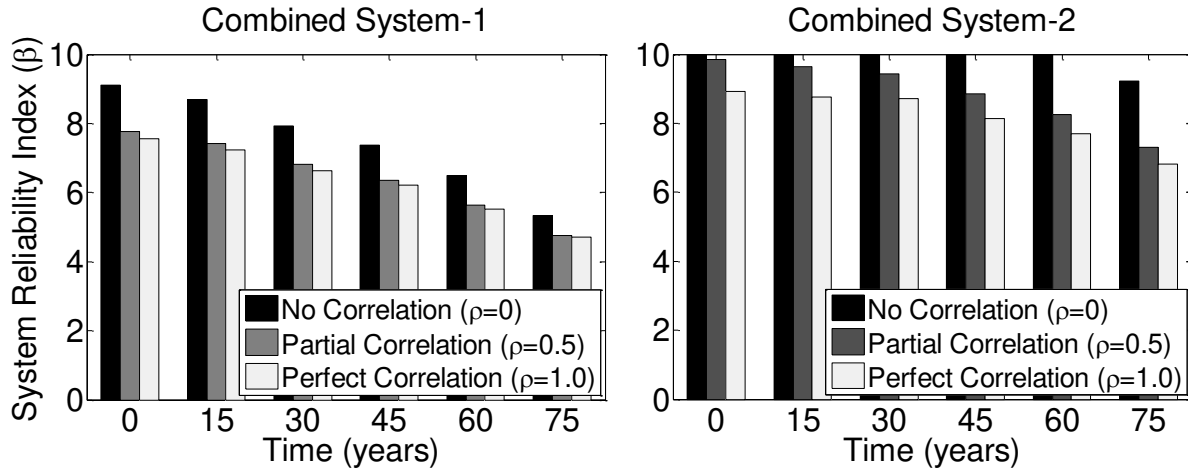
Figure 73: System reliability results of combined system models of the movable bridge for different correlation cases over time

Apart from the deterioration cases, system reliability results for the damaged and undamaged condition are presented for the current year in Table 4. From this table, it is seen that a span lock failure in the bridge will decrease the reliability index to a 30-45 year deterioration effect which is also similar to the findings for the load rating analysis. During span lock damage, importance of the correlation in combined system-1 can be observed by comparing the reliability index results for the no correlation case with the perfect correlation case. This difference in the system reliability index corresponds to a substantial increase of the failure probability. These results show that the configuration of the bridge and the correlation of variables are important factors for system reliability calculations.

Table 7: System reliability indices during a span lock failure for different system models of the movable bridge under different correlation values

	System Type	No Correlation	Partial Correlation	Perfect Correlation
	Series	4.45	4.45	4.58
t=0	Combined-1	9.12	7.77	7.56
	Combined-2	10.00	9.86	8.92
t=0 with Span Lock Damage	Series	3.07	3.07	3.16
	Combined-1	7.02	6.07	5.94
	Combined-2	10.00	9.28	8.98

5.5. *Summary*

This chapter presents a structural identification implementation by means of a family of calibrated models for performance evaluation of a movable bridge due to deterioration, damage, and traffic increase. Performance metrics, load rating, and reliability are predicted using the family-of-models approach, which considers the possible uncertainties associated with modeling, measurement, and data post-processing. For the calibration of the nominal model, an ANN-based calibrations methodology is employed using different monitoring data with multiple objective functions. The application of the new and effective calibration methodology, which was presented in previous chapters, is also validated with a real-life application.

As a demonstration of the family-of-models approach, a real-life movable bridge performance is evaluated for a 75-year period with the inclusion of deterioration (corrosion of steel members) and sudden damage (span-lock failure typical for movable bascule bridges). In addition, the traffic increase is also anticipated and included in the predictive analysis. A single FEM that is calibrated using a set of data may reproduce that data set accurately within

acceptable numerical limits, however, another prediction might not be accurate as a result of uncertainties in experimental data, structural model assumptions, and non-stationary and nonlinear behavior of real-life structures. While previous studies provide concepts of multiple models, the use of many models for determining some of the practical engineering concepts, such as load rating of bridges, and more advanced concepts, such as system-level reliability with the consideration of the correlation of different components with each other, are explored for real-life structures.

The load rating from parent models and load rating distributions from offspring models are compared for different cases. With the inclusion of uncertainties, the load rating of the bridge is presented with a distribution rather than a deterministic value. As expected, the load rating decreases over time along with an increased coefficient of variation. Also, an instantaneous damage simulated for the span lock reduces the load rating to a considerably deteriorated condition. The system reliability of the bridge is considered by using four different system models. Perfectly correlated safety margins, partial correlation, and independent safety margins are considered, and the reliability of the system is predicted within bounds over a period of time. A careful selection of the system model and the use of monitoring-based correlation among the safety margins of different components can be used for reliable performance predictions as well (Frangopol 2011b). Reliability studies in this chapter show the importance of data post-processing and how the results can be affected due to various system, model, or correlation assumptions.

CHAPTER 6.
PARAMETRIC STRUCTURAL ASSESSMENT:
REAL-LIFE DEMONSTRATION-II

6.1. *Introduction*

Structural system damage and deterioration is a complex problem that affects system performance over the life cycle of the structure. Bridge performance problems due to damage and deterioration have become a national concern. Some reasons behind the deterioration of bridges are aging of materials, excessive loading, environmental changes, lack of proper condition based maintenance. Consequently, maintenance actions such as retrofit, repair, rehabilitation and replacement need to be taken to ensure the safety of the public.

Before making any decisions about maintenance operations it is desirable to simulate the conditions of the structure with analytical models. Different types of models with varying complexity are developed for the analysis and design of structural retrofit while performance enhancement can be determined by modeling of unretrofitted and retrofitted systems. There are also several uncertainties that need to be considered for better understanding retrofit effects on structural performance. To develop more accurate models by considering uncertainty may be carried out by using calibrated models with monitoring data. This will help to better characterize the existing system and to predict future performance of the structure more adequately. As a result, field calibrated finite element models (FEMs) are very critical for understanding the maintenance and retrofit effects on the performance of a structure, and in this chapter, retrofit effects on structural performance of a long span cantilever truss bridge is investigated.

Throughout history, dramatic steel bridge collapses have been observed due to lack of redundancy and those failures cost human lives. These unfortunate incidents initiate research towards safer structures for these observed failures as well as produce new vocabulary such as fracture critical members. Among several bridge collapses, Silver Bridge, US (1967), Mianus River Bridge, US (1986) and the Latchford Bridge, Canada (2003) are illustrative for fracture critical members. The Silver Bridge, which spanned the Ohio River, was built in 1928. The joint of the eyebar at west of the Ohio tower of this suspension bridge failed in 1967 and then, the collapse continued with failure of the West Virginia tower and the middle portion of the center span (Lichtenstein 1993). The Mianus River Bridge, which was carrying the I-95, was built in 1958. Due to a rusted hanger–pin connection, the hanger failed in 1983 and two lane of the roadway fell into the river below (Little 2002). As a final example here, in 2003, the Latchford Bridge over the Montreal River settled 2 m when a truck was crossing the bridge due to failure of upper connection of the hanger (Biezma and Schanack 2007).

After these collapses, many hanger elements, which became a new concern of bridge engineers and researchers, were closely inspected, evaluated and retrofitted for increased redundancy. As seen from the examples given, hanger elements can be defined as fracture critical members for structural systems because failure of these elements can lead to collapse of the overall system. Although retrofitting applications of hanger elements are very common; load rating, component and system reliability changes before and after this procedure have not been explored extensively in the literature.

Some representative studies related to hanger element include the following: possible different hanger systems (Kondoh et al. 2001), investigation of stress spikes in hanger elements

due to misalignment loading (Mehta 2001) and testing full scale retrofitted truss bridges in the field and in the laboratory (Azizinamini 2002; Ermopoulos and Spyrakos 2006). Additionally, major efforts were made on the seismic retrofit of bridges where different retrofit schemes and damper systems were proposed (Ingham et al. 1997; Sarraf and Bruneau 1998; Murphy and Collins 2004; Pollino and Bruneau 2007; Casciati et al. 2008; Hoang et al. 2008). Moreover, fragility of bridges after retrofit application (Padgett and DesRoches 2007), life cycle cost analysis of retrofit applications (Padgett et al. 2010) and nonlinear modeling and analysis of a steel truss bridge (Nagavi and Aktan 2003) were reported in the literature.

In this chapter of the dissertation, performances of a long span cantilever truss bridge before and after retrofit applications are investigated with a calibrated model and family of models approach. The suspended span of a cantilever truss bridge is carried by four hanger elements and as a result, the axial forces on these fracture critical members are extremely high (Aktan et al. 2000a). The hangers can be retrofitted by adding additional retrofit members around the hanger members to increase the redundancy and also to decrease the dead load forces on these elements by pre-stressing the retrofit members.

The scope of this chapter is as follows: First, the bridge and its monitoring system are explained. Afterwards, a-priori, calibrated and retrofitted finite element models (FEMs) are discussed. Then, family of models is used to evaluate the load rating and reliability of the bridge with emphasis on the uncertainties. Finally, the results from single models (a-priori, calibrated and retrofitted) and family of models are presented in a comparative fashion to quantify the uncertainty effects on structural performance metrics such as load rating and system reliability.

Schematic presentation of the identification process is presented for use of a-priori model and uncertainty incorporated family of models in Figure 74 and Figure 75, respectively.
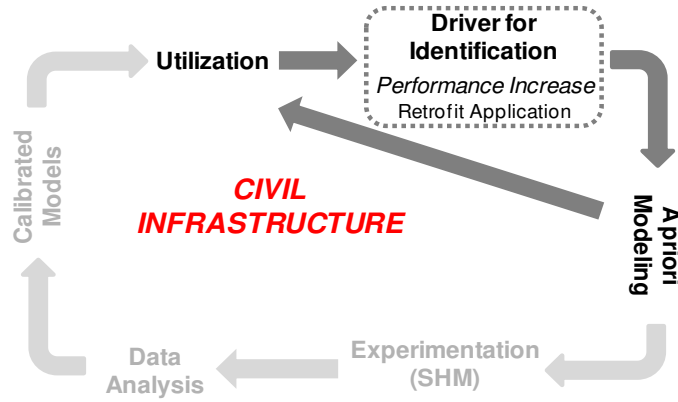
Figure 74: Use of a-priori model for St-Id of a long span bridge due to performance increase
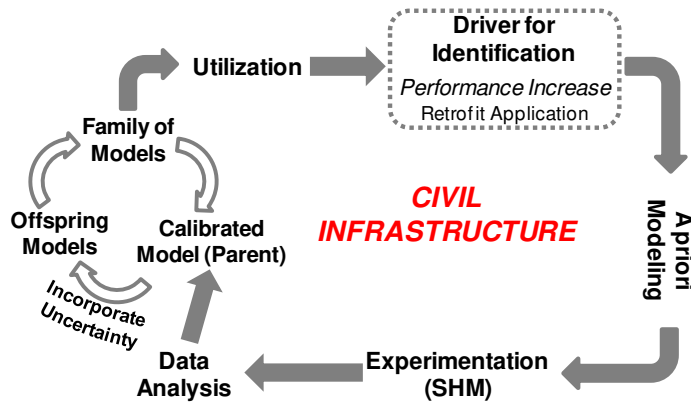
Figure 75: Use of uncertainty-incorporated family of models for St-Id of a long span bridge due to performance increase

6.2. *Case Study: Long Span Cantilever Truss Bridge*

The longest cantilever truss bridge in the US is selected as a case study to demonstrate the retrofit effects on structural performance (Figure 76). The bridge, which was opened to traffic in 1974, is spanning over Delaware River near Philadelphia with a main span length of 1,644 ft

and a total length of 13,912 ft, carrying five traffic lanes, serves more than six million vehicles annually. The substructures of the through-truss contain four reinforced concrete piers which were constructed on pile foundations. The two main trusses of the through-truss are spaced 72.5 ft apart. Each main truss has 73 panel points spaced at 45.7 ft intervals. Welded box sections are used for the top and bottom chords of the trusses and a combination of welded box and I-sections is used for the vertical and diagonal truss members. Lateral bracing is provided by K-bracing at the top and bottom chord levels, and by portal and sway frames located at various panel points throughout the structure. The suspended span of the bridge is connected to the cantilever arms via vertical hangers, which are pinned at their upper and lower extremities. Truss members with axial and rotational releases transition the top and bottom chords between the suspended span and the adjacent cantilever arms. The floor system of the bridge is an 8 in thick lightweight reinforced concrete deck that is composite with 9 steel beams laterally spaced at 6.9 ft. The beams are continuous over the floor beams in either four span or five span increments. An important characteristic of this bridge is that the suspended span is hung between the cantilever spans with four fracture critical hanger elements, making them non-redundant. More details about the bridge can be found in Aktan et al. (2000a).

Figure 76: Long span cantilever truss bridge

6.2.1. *Monitoring System and Field Tests*

The bridge was extensively instrumented and monitored in order to track different inputs such as traffic, wind and temperature and structural responses such as vibrations and strains. In addition, vibrations and strains provided by the monitoring system are used for characterizing the global and local bridge behavior of the FEMs. The monitoring system includes video cameras, weigh in motion (WIM) systems, weather stations, strain gages, accelerometers, tiltmeters, crackmeters and vibrating wire gages. In this chapter of the study, only temperature induced strain data coming from vibrating wire gages and wind speed and direction data coming from wind stations are used for the performance evaluations of the bridge. Measured temperature cycle, temperature induced strain and wind data, which are presented in Figure 77, Figure 78, and Figure 79, respectively, are included in the reliability analysis. It should be noted that vibrating wire strain gages used in the monitoring are temperature compensated (stress-induced strains) by adjusting the thermal expansion coefficients of the strain gage wire and the steel member that the strain gage is attached to (Levi 1997).
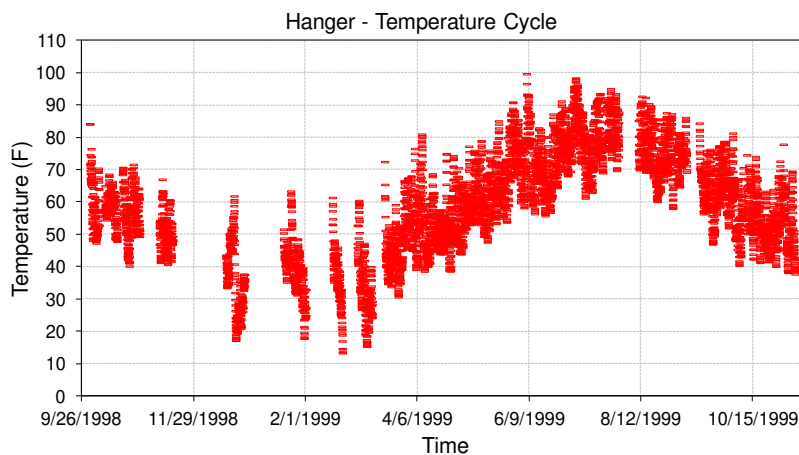
Figure 77: Measured temperature variations for the hanger

143
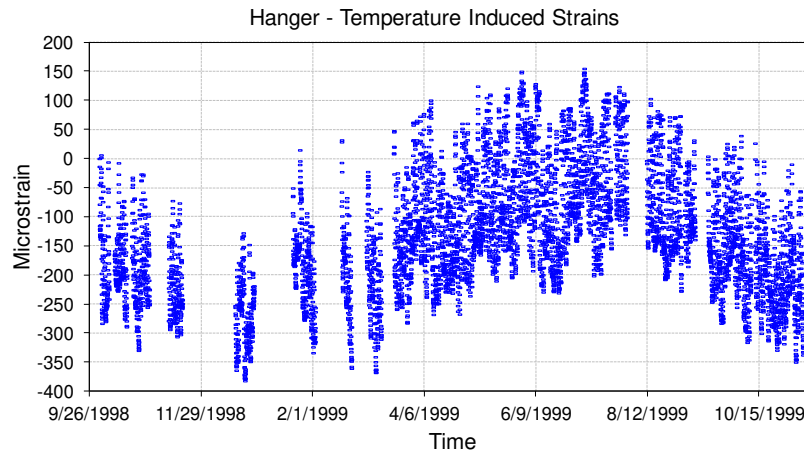
Figure 78: Measured temperature induced strain variations for the hanger
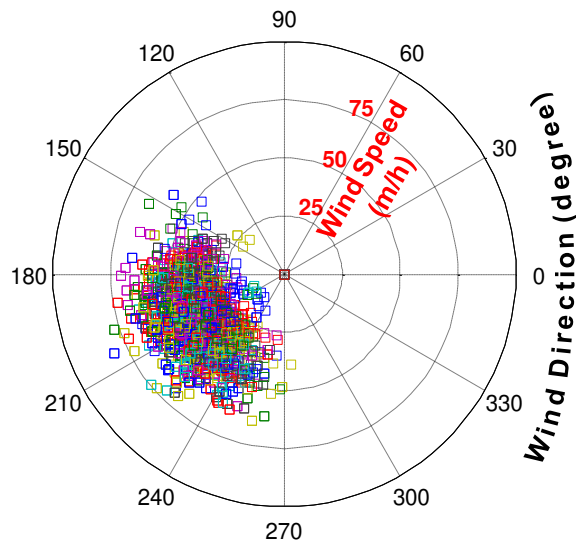
Figure 79: Measured wind direction and wind speed data

The other important part of the experimental program on the bridge was the ambient vibration and truck load tests conducted on the bridge to provide additional data to calibrate the FEM at global and local levels. Ambient vibration data was collected from various locations and directions via 45 accelerometers on the through truss in order to identify dynamic properties

(frequency, mode shapes) for the structure. The data obtained from the ambient vibration surveys at the bridge was used for global level FEM calibration of the through truss spans. Controlled load tests were performed using two cranes of known weight (108 kip each) on the through truss spans and the deck truss and stringer approach spans in order to obtain strain data (via 52 high-speed strain gages) necessary for local level calibration of the FEM. The concepts of global and local level FEM calibration and how these were performed in this study are described in the following section.

6.2.2. *A-Priori and Calibrated FEMs*

Development and calibration procedure of a 3-D FEM can take several stages. First, the relevant design drawings and calculations for the long span bridge need to be obtained. Based on the design drawings and photographs, a 3-D CAD model of the structure is constructed and then, the drawing files are imported to the finite element software for obtaining the general geometry of the bridge. Next, the material properties, section properties, releases and constraints are assigned to the structural elements. Finally, the initial boundary conditions are created based on design drawings. It should be noted that a-priori modeling, field experimentation and model calibration steps for the St-ID of the long span bridge were accomplished through the studies conducted by Drexel Intelligent Infrastructure and Transportation Safety Institute (DI3) researchers and extensive studies related to these steps can be found in the literature (Aktan et al. 2000a; Aktan et al. 2000b; Catbas and Aktan 2002; Catbas et al. 2007). Based on the calibrated model utilized for the previous studies, a retrofitted model, which is explained in the next section, is created.

The structural elements of the bridge were modeled using a combination of shell and beam elements, with rigid links as well as body constraints to represent the actual 3-D geometry of the interfaces and connections. In-plane and out-of-plane deformations of the deck slab were simulated by discretizing the slab into 2,966 rectangular shell elements with six degrees of freedom at each node. 3-D beam elements represented the upper chords, lower chords, verticals, diagonals, floor beams, out-of-plane truss members, bracing, and roadway stringers. A model using bar elements for the through truss elements was developed, however, due to actual end connections and the test data, beam elements were found to perform better. The piers were modeled with 3-D frame elements in a smeared manner for computational efficiency. The total number of frame elements utilized in the model was 6,047. General view of the a-priori model is presented in Figure 80.
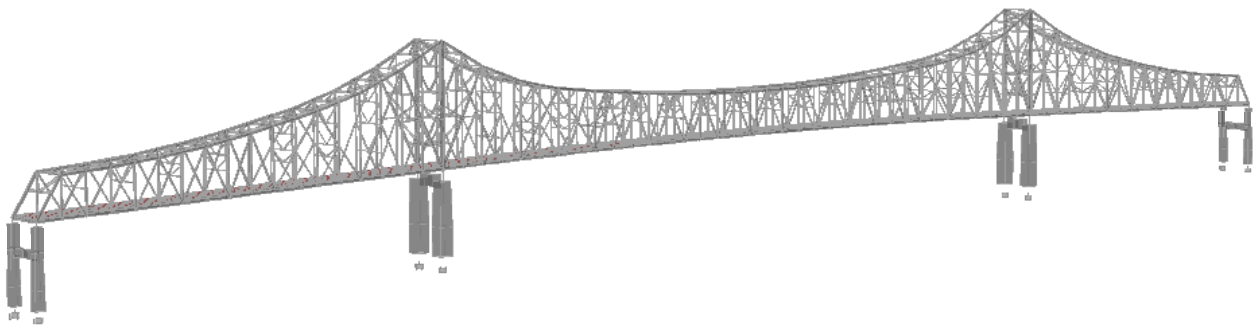
Figure 80: A-priori model of the long span cantilever truss bridge

Before calibration, any possible human errors in input have to be eliminated by quality assurance and control measures developed for large scale models, since analyses may be carried out and global equilibrium may be maintained even with the presence of many errors at the local level. A-priori model was verified by checking the static equilibrium, checking the dead load

forces with the design calculations and checking the preliminary mode shapes for local connection problems.

In order to calibrate the models, data is needed at both global and local levels and these data sets were obtained from experimental data collected when the field tests were performed on the bridge. The first step of the calibration process is the global calibration of a-priori model and this was achieved by using global vibration characteristics of the bridge. Ambient vibration test data and data analysis results were utilized for this purpose. Since modal properties (frequencies and mode shapes) are a function of parameters such as the mass, stiffness, damping of a structure, differences in the identified modal properties from the experiment and the FEM can be attributed to differences in these parameters. Moreover, the a-priori model was calibrated by modifying its boundary conditions or by idealizing its some structural elements. When the mode shapes were similar, and the frequency difference between the model and experiment results was minimized, it could be concluded that the model represents the measured responses in a global sense.

The second step of the calibration process is the local calibration of the a-priori model and controlled load test data was utilized for this purpose. If there was an unacceptable level of difference between the experimental results and model predictions, the stiffness of the model in specific locations or regions was adjusted. It is important to note that parameters that are adjusted during the local calibration process should reflect a physical situation. Incorporating a non-physical condition that satisfies a purely numerical correlation between experimental and analytical results was avoided. The details about the model development and calibration processes can be found in Catbas et al. (2007).

6.2.3. *Retrofitted FEM*

The importance of the hanger element was discussed in the previous sections. For the case study here, all four hanger elements of the bridge mostly carry the dead loads and these hangers transmit the forces from the suspended to the cantilever spans. Failure of any one of the hanger elements may lead to the overall system failure of the bridge. 3-D FEM and conceptual representation are presented with different spans in Figure 81.
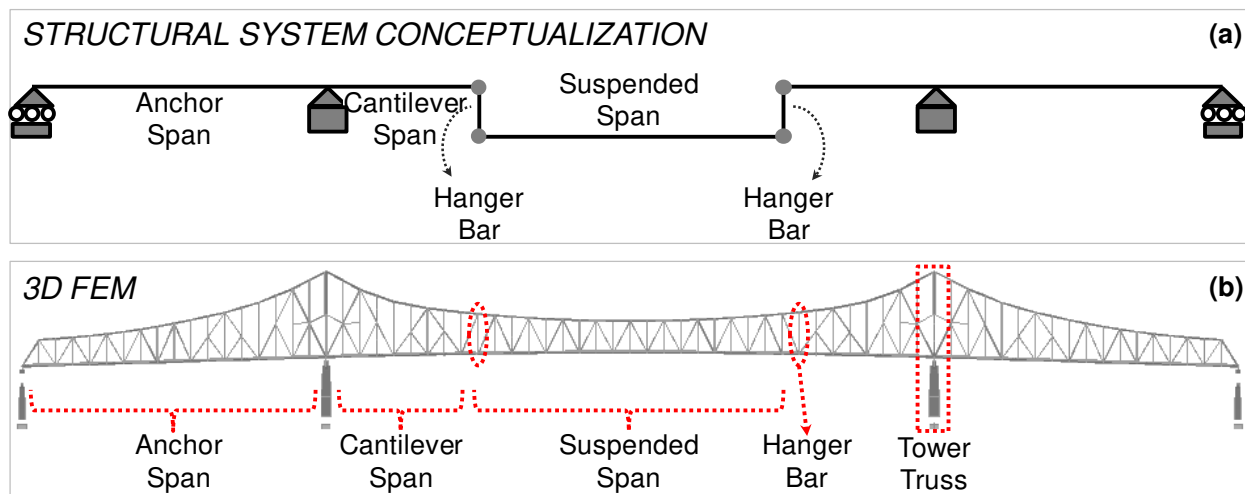
Figure 81: Structural system conceptualization representation (a) and 3-D FEM of the long span cantilever truss bridge (b)

To increase the redundancy of hanger elements as well as to increase the overall system reliability, these bridges generally are subjected to retrofit applications. The goal of the retrofit application on pin-hanger system is to reduce the dead load forces on these elements by adding an auxiliary support system around each hanger element. In this particular application, this auxiliary support system consists of four 7.5 in diameter stainless steel rods, four spreader beams located at the upper and lower truss chords, splice couplers, nuts, and washers. Rods extend

vertically from the upper chord of the cantilever arm to the lower chord of the suspended span and these rods are pre-tensioned to remove 50% of the dead load from the hanger bar. Some pictures and a schematic representation of the auxiliary system are shown in Figure 82.

Figure 82: Retrofitted hanger and auxiliary system photos and drawings (Catbas et al. (2003) and photo credit to Dr. Kirk Grimmelsman)

As described previously, the main components of an auxiliary system are the stainless steel rods and the steel spreader beams. These members are added to the calibrated model by using frame elements with the appropriate dimensions and material properties. Then, the spreader beams are connected to the hanger element by using rigid links, which can transfer the load through the auxiliary system. Afterwards, post-tensioning of the rods is simulated with temperature loads until 50% of the dead load removed from hanger members. Modal frequencies of the experimental results, a-priori model, calibrated model and retrofitted model are presented in Figure 83 and it is seen that the addition of the auxiliary system to the calibrated model do not

affect the frequencies significantly. In addition, axial forces due to dead load are presented in Figure 84 for the a-priori model, calibrated model and retrofitted model. Axial force of the hanger element due to dead load is found to be 3,708 kips, 3,199 kips and 1,584 kips for the a-priori, calibrated and the retrofitted model, respectively. The retrofitted model, which is developed using the calibrated model is utilized as the parent model for the family of models for the investigation of performance change by considering uncertainties.
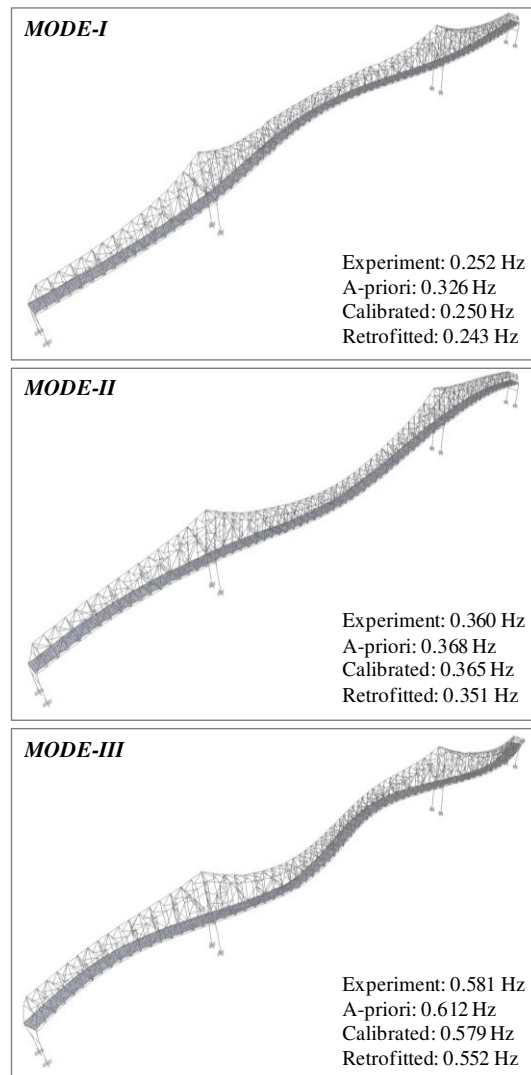
Figure 83: Experimental, a-priori model, calibrated model and retrofitted model frequencies
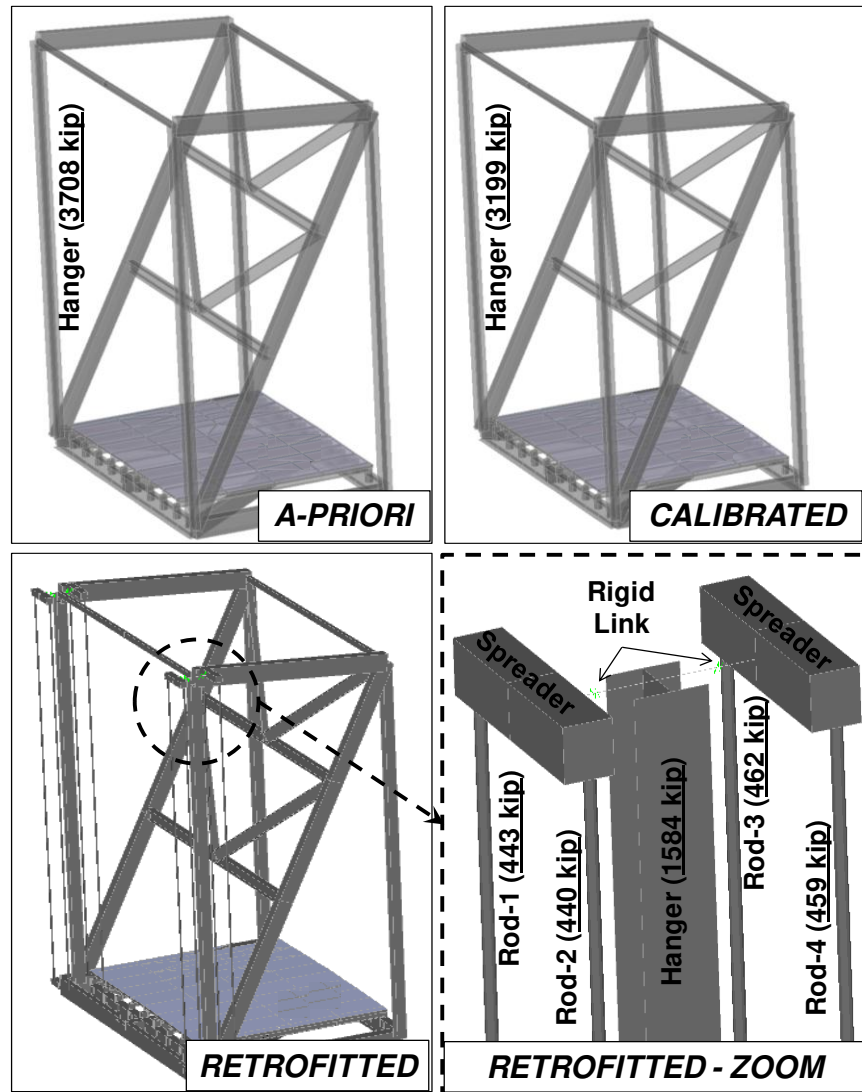
Figure 84: Axial forces under dead load for a-priori, calibrated and retrofitted models

6.3. *Family of Models*

Family of models approach concept and its advantages are discussed in the previous chapters. The retrofitted FEM is considered as the parent model and from this parent model, a set of offspring FEMs are generated. The number of offspring FEMs that are used for simulations is selected as 10,000 based on the following error associated sample size given by Eq. (4.1).

Dead, live, wind and post-tension loads for the parent model are defined before the offspring model generation process. The self weight of the structure is defined as the dead load whereas the HL93 loading which includes lane and truck loading is used as a live load. For this study, all five lanes of the bridge are loaded with 0.64 kip/ft HL93 lane load and 72 kip HL93 truck load as defined in the AASHTO (2004) specifications. A preliminary moving load analysis is also conducted to find the critical loading condition for the hanger elements since only one HL93 truck loading per lane is used. In addition, to define the wind loading in the finite element software, mean of the wind loading parameters (Figure 79) coming from the monitoring system are utilized along with the exposure type, importance factor, gust factor, pressure coefficient, velocity pressure exposure coefficient and topographic factor. Finally, another preliminary analysis is carried out to obtain the needed temperature value to be applied to the rods to simulate the dead load transfer by means of post-tensioning of the rods.

The offspring models of the long span cantilever truss bridge are generated from the parent model, which is mainly the calibrated FEM with an additional auxiliary system on the hanger elements. A summary of the family of models procedure is presented in Figure 85.
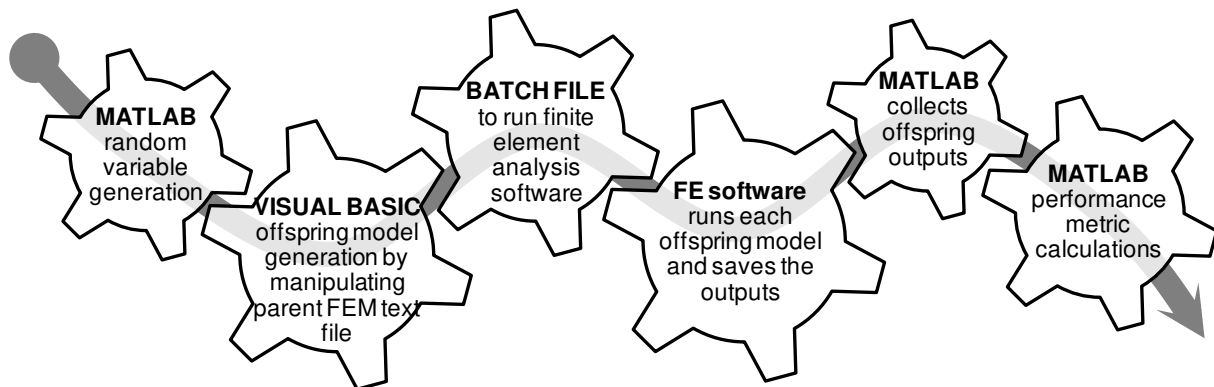
Figure 85: Schematic summary of the family of models procedure

The generation of family of models incorporates the variables such as the loads, section properties and mechanical properties based on the distributions obtained from the studies found in the literature. In Table 8, statistical parameters such as bias factor, coefficient of variation and distribution types are given for the random variables along with the sources.

Table 8: Statistical parameters for the random variables

	Bias (λ)	C.O.V.	Dist. Type	Source
Dead Load (DL)	1.05	0.10	Normal	(Ellingwood et al. 1980)
Lane Load(LL)	1.20	0.18	Normal	(Ellingwood et al. 1980)
Truck Load (TL)	1.20	0.18	Normal	(Ellingwood et al. 1980)
Post-Tension(PTL)	1.00	0.10	Normal	Assumed
Elasticity (E)	1.00	0.06	Lognormal	(Ellingwood et al. 1980)
Yield Stress (F_y)	1.05	0.11	Lognormal	(Ellingwood et al. 1980)
Area (A)	1.00	0.05	Lognormal	(Haukaas and Der Kiureghian 2007)

Based on the data generated using random variables, uncertainties are incorporated in the offspring models by means of the different programs and files (Figure 85). Different load variables (dead, live, wind and temperature for post-tensioning), elasticities, yield stresses and cross-section areas are assigned for each offspring model. Next, a batch file (command file) is employed to automatically analyze and save the results from these offspring FEMs. Then, the values of interest are collected from the saved results and combined into a matrix format. Afterwards, the performance metrics, which will be described in the next section, such as load rating, component and system reliabilities are calculated via the given formulations. Lastly, histograms for capacity, dead load, live load and wind load are obtained to calculate the load rating distributions and system reliability. Representative axial strain histograms and distribution fits for the hanger and one of the stainless rods are shown in Figure 86 and Figure 87,

respectively. These figures clearly indicate the importance of the dead loads in long span bridges when compared to other types of loading such as live and wind loads.
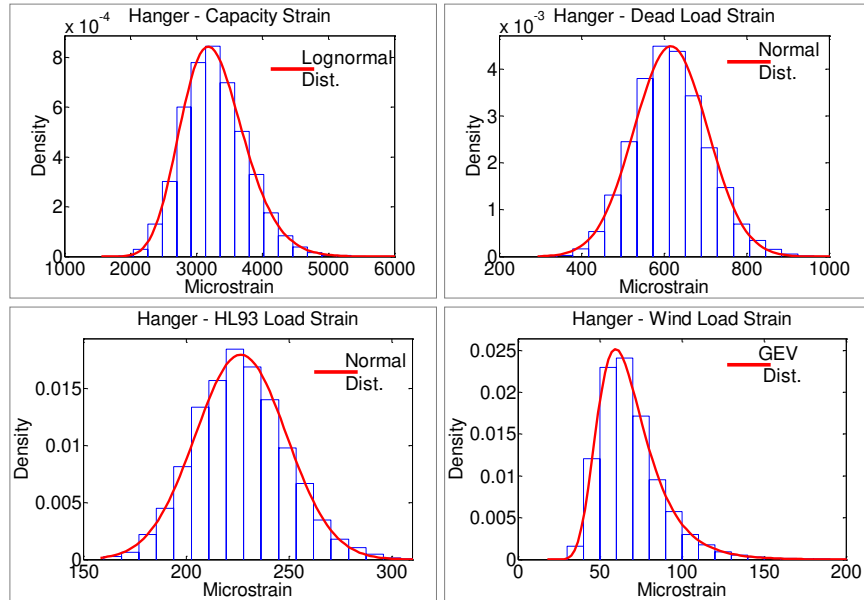
Figure 86: Representative offspring output histograms and distribution fits for the hanger bar
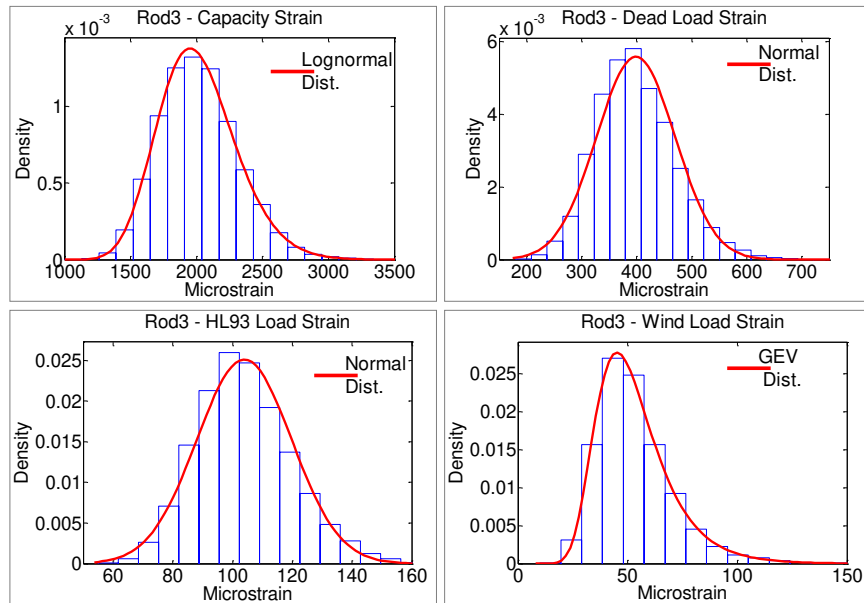
Figure 87: Representative offspring output histograms and distribution fits for Rod-3

6.4. *Bridge Performance Prediction*

6.4.1. *Load Rating*

Load rating of a bridge can be expressed as the factor of the critical live load effect to the available capacity for a certain limit state. Load rating can be carried out for a number of critical locations and components on the structure. For this study, the load rating of the hanger and the auxiliary system are calculated by following the AASHTO (2004) guide and using the a-priori model, calibrated model and family of models (parent and offspring models). The general formulation to calculate the rating factor is given in Eq. (2.1).

Since 3-D models are used, axle loads are defined as individual point loads (8 kip − 32 kip − 32 kip) for the truck loads and lane loads are defined as distributed load at 0.64 kip/ft as defined in the AASHTO code. The yield strength is given as 100 ksi for the steel hanger and 50 ksi for the stainless steel rods as given in the design drawings. The capacities of the sections are calculated based on the axial strain capacity. The cross-section area (A) of the hanger is 94.13 in^2 while it is 44.18 in^2 for a single rod. The dynamic impact factor is used as 33% for calculating load ratings.

For the comparative evaluation, first, the load rating is calculated from the capacity, dead load and live load values of the a-priori model and calibrated model, which do not have the auxiliary system or in other words do not have the retrofits. It should be noted that the a-priori model was created to capture the design load calculations. From the a-priori without retrofit and calibrated without retrofit models, hanger load rating is found as 2.46 and 2.85, respectively with the dead load forces, which are presented in Figure 84.

155

Hanger load rating results after the addition of the auxiliary system is presented in Figure 88. Load ratings of the hanger element become 5.86 for the a-priori model with retrofit, 7.66 for the calibrated (parent) model. In addition, the mean and the standard deviation of the load rating distribution coming from the offspring models are found to be 6.87 and 1.29, respectively. These results indicate that the design load rating coming from the nominal model is almost tripled when compared to the calibrated (parent) model after the retrofit application.
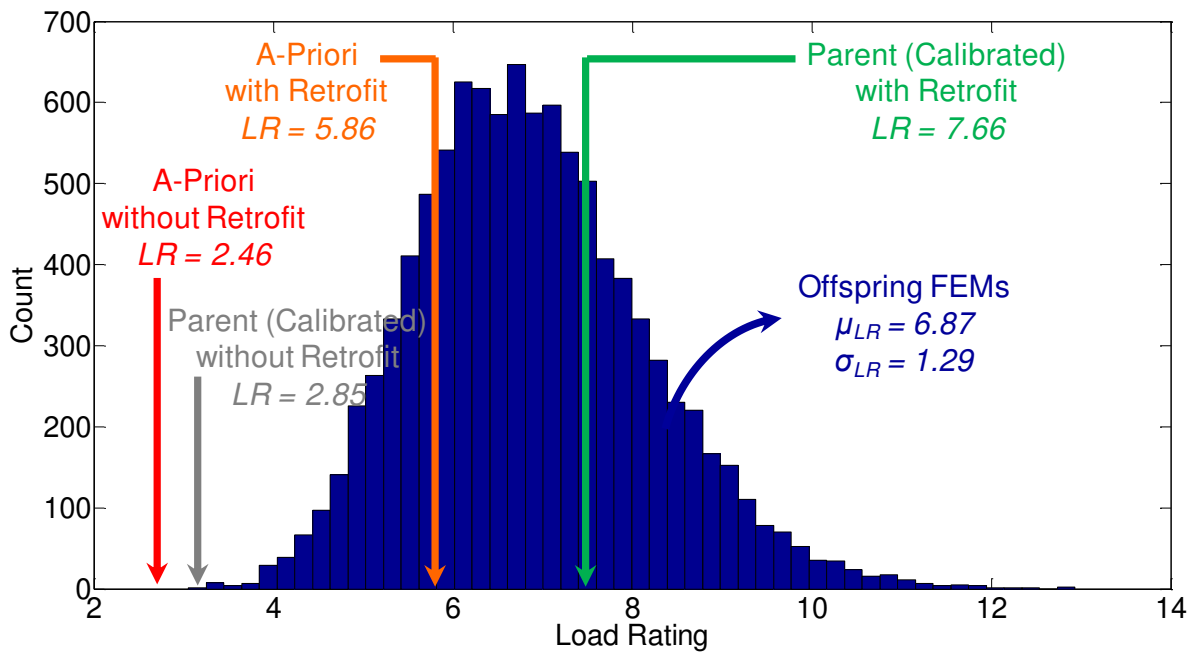
Figure 88: Comparison of hanger element load ratings for a-priori, a-priori with retrofit, calibrated, calibrated (parent) with retrofit and offspring models with retrofit

It is observed that the parent FEM load rating is slightly higher than the mean of the distribution coming from the offspring models due to the effects of uncertainties. The difference in load rating between the parent model and the mean of the offspring models is about 0.80 and this indicates that the uncertainties can lead to a load difference as much as 0.80 times the

defined live load (HL-93 loading). Moreover, the load rating ratio between the parent model with retrofit (LR=7.66) and the offsprings with retrofit (LR=6.87) is calculated as 90%, in other words the reduction in load carrying capacity is found as 10% independent of the loading.

Another important load rating difference between the a-priori model with retrofit and parent (retrofitted and calibrated) model is determined to be 1.80 and this clearly illustrates that the a-priori model can produce underestimated results in this case which may yield to unreliable decision making. From the performance ratio calculation, the load carrying capacity reduction is found as 25% between the a-priori model with retrofit and the parent model with retrofit. It should be noted that the load rating of the a-priori and parent models simulating retrofit application are in the $\pm\sigma$ range of the load rating distribution of the offspring models.

The other components of the auxiliary system are the stainless steel rods. The load rating results for the a-priori, parent and offspring models are presented in Figure 89 for the 4 rods. The load ratings of the rods are varying between 6.94 - 7.71 for the a-priori model with retrofit, 8.59 - 9.53 for the parent model. Mean values of the offspring model load rating histograms for different rods are changing between 7.90 – 8.83 with a standard deviation interval of 1.85 – 2.07.

Finally, the family of model approach offers to see the bounds and distributions of load ratings in a non-deterministic manner by considering different uncertainty sources. The probabilistic results provided by family of models approach promises more informed decision making for different purposes such as replacement or maintenance by identifying the risk associated for different alternatives.
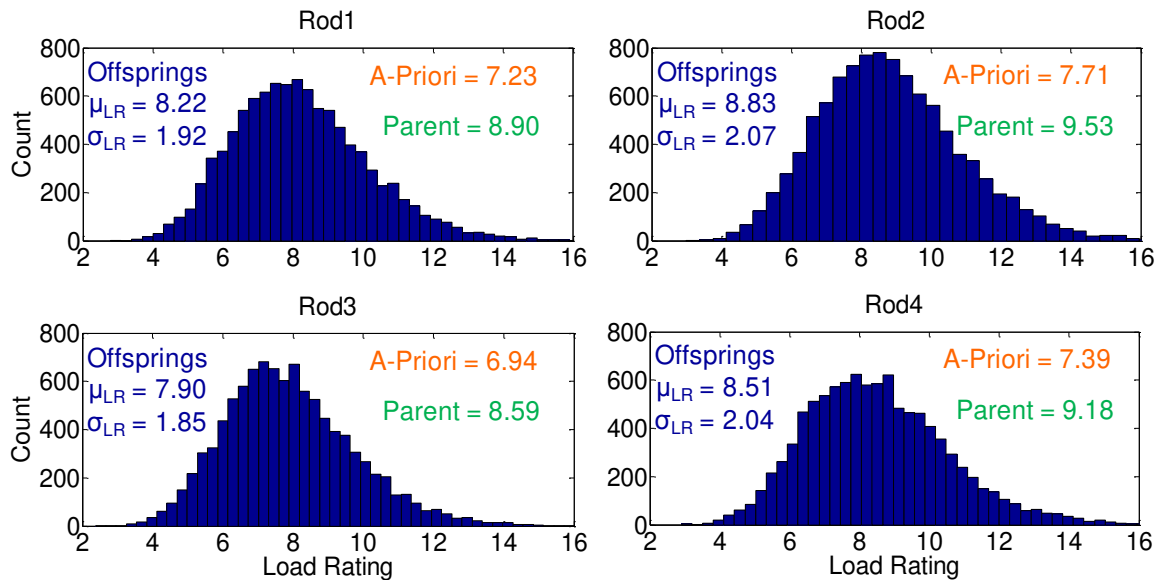
Figure 89: Comparison of rod element load ratings for the a-priori, parent and offspring models

6.4.2. *Component and System Reliability*

Structural reliability analysis can be defined as the modeling of capacities and demands as random variables for predicting the probability of failure under a given limit state function. The probability of failure and the reliability index are related metrics and they are interchangeably used for the same condition. It should also be noted that "failure" does not necessarily mean structural collapse, rather not fulfilling the defined limit state condition for a structural component or for the entire structural system. In this dissertation, structural reliability is employed as a decision metric in addition to load rating for the case studies involving bridges. From an application perspective, the load rating is more commonly used bridge engineer practice as load rating is more explicitly defined in bridge design and assessment codes for decision making. Also, the need of intense mathematical knowledge in the reliability approach makes it more difficult to be utilized in regular bridge decision making (Estes and Frangopol 2005).

A system reliability approach requires the capacity and demand random variables, correlation of these variables and finally a system model, in other words, a failure mechanism. In this study, a long span bridge is analyzed with respect to yield strain of 5 different elements under the limit state based on the axial capacity and loading. Component reliabilities of one hanger and four rods are obtained from FEM and SHM data by using the limit state equation:

$$g = \left(0.75 \times \varepsilon_y\right) - \varepsilon_{DL} - \varepsilon_{LL} - \varepsilon_{WL} - \varepsilon_{TL}$$

(6.1)

For the strain capacity (ε_y), a multiplier 0.75 is assumed for the given limit state to be within linear stress-strain range. The demand has different components, which are dead load strain (ε_{DL}), live load strain (ε_{LL}) coming from HL93 loading, wind load strain (ε_{WL}) and the temperature induced strain (ε_{TL}). As already mentioned in previous sections, wind speed and wind direction data from the monitoring system are used in the finite element analysis for the wind loading calculations. In addition, temperature induced strains coming from vibrating wire measurements (Figure 78) are used for the reliability calculations by obtaining the maximum strain differentials, which were calculated in Catbas et al. (2008b). The correlation values between the random variables are assumed as zero. Hanger subsystem models that are related to the hanger elements and the retrofit rods are defined for the comparative evaluation of the performance before and after retrofit application as presented in Figure 90.
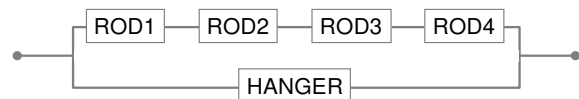
#	SYSTEM MODEL	MODEL DESCRIPTION
(A)	HANGER	Hanger subsystem before retrofit
(B)	ROD1 — ROD2 — ROD3 — ROD4 / HANGER	Hanger subsystem after retrofit

Figure 90: Subsystem models and descriptions

159

Before retrofit application, hanger subsystem contains only the hanger element (Figure 90-A). After retrofit application, the auxiliary system will increase the redundancy with the addition of four rods in parallel to the hanger subsystem (Figure 90-B). The idea is that four rods will reduce the load demand on the hanger and even in the case of hanger failure; the rods will be able to carry their share of load coming from the load of the suspended span.

Component reliabilities can be calculated for the hanger before a retrofit application. For this purpose, a-priori and calibrated models are used and the reliability indices for the hanger are calculated as 1.97 and 2.61, respectively for the given limit state function. When the auxiliary system is added to the hanger region, the component reliability of the hanger element is increased to 6.28 for the parent model, which is the calibrated model with the retrofit rods. Also, a family-of-models is generated with the inclusion of the uncertainties defined previously for this particular case study. It is observed that the reliability index of the hanger is found to be 4.68 when the hanger is retrofitted with 4 rods. It should be noted that the uncertainties coming from Table 8 are directly used in reliability calculations for single model, whereas these uncertainties are incorporated in the offspring model with a Monte Carlo approach and the reliability indices are calculated from the output distributions of the offsprings.

The increase in component reliability index of the hanger is mainly due to the significant decrease in the dead load strains. Half of the dead load is transferred to the rods through auxiliary system and the component reliability indices of the rods are calculated as 3.96, 4.15, 3.81 and 3.98. The component reliability indices for a-priori without retrofit, calibrated without retrofit, parent (calibrated with retrofit) and offspring models with retrofit are presented in Table 9.

Table 9: Summary of the component reliability indices and corresponding probability of failures for a-priori, calibrated, parent and offspring models

	A-PRIORI (no retrofit)		CALIBRATED (no retrofit)		PARENT (retrofitted)		OFFSPRINGS (retrofitted)	
	BETA(β)	Pf	BETA (β)	Pf	BETA (β)	Pf	BETA (β)	Pf
ROD1	-	-	-	-	5.10	1.7E-07	3.96	3.7E-05
ROD2	-	-	-	-	5.36	4.1E-08	4.15	1.6E-05
ROD3	-	-	-	-	5.00	2.9E-07	3.81	7.0E-05
ROD4	-	-	-	-	5.21	9.6E-08	3.98	3.5E-05
HANGER	1.97	2.4E-02	2.61	4.5E-03	6.28	1.7E-10	4.68	1.4E-06

The results show a tremendous decrease in probability of failure, thereby, increase in structural reliability index of the hanger as shown in Table 9. While the reliability indices both for parent model and the offspring models are quite high, the incorporation of the uncertainties in the offspring model has a major impact in the final results for these two cases when analyzed in a comparative fashion.

After the component reliability evaluation, the subsystem reliability is also investigated in order to quantify the system reliability with the inclusion of uncertainties in the offspring models. To compute the system reliability, first, the component reliabilities are calculated and then, cut-set information is provided to the reliability analysis software. The system reliability results of hanger subsystem are shown in Table 10. When hanger bar is combined with four rods as presented in Figure 90-B, the subsystem reliability index of the parent model with retrofit increases to β=8.25 as expected due to the redundancy by auxiliary system increases the and also due to significant decrease in the dead load forces on the hangers. As stated before, the use of family of models approach gives lower results when compared to the single parent model as a result of the combined effect of the uncertainties. As an illustration, the system reliability of the

hanger subsystem is calculated as β=6.25 from the offspring models outputs. It should be noted that the performance and survival of the long span bridge mainly depend on the performance of the system of the hangers and retrofit bars.

Table 10: Summary of the system reliability indices for hanger subsystem

	PARENT (retrofitted)		OFFSPRINGS (retrofitted)	
	BETA (β)	Pf	BETA (β)	Pf
SUBSYSTEM (Figure 90-B)	8.25	7.9E-17	6.25	2.0E-10

The implication of the consideration of the uncertainties may be more critical if all the elements of the system are analyzed to evaluate the system reliability of the entire bridge as described in Catbas et al (2008) where all upper chord elements, vertical, diagonal and lower chord elements are employed for the structural system reliability computations. In this dissertation, the scope is limited to the performance evaluation of the hanger retrofit for a hanger subsystem (hanger and retrofit rods). It is seen that a reasonably designed and constructed retrofit for such bridges increases the system reliability of the hanger system practically to the highest level for a limit state that employs the axial strain capacity. The subtle point here is that the impact of uncertainty can play a major role irrespective of the high reliability indices as can be seen here when the parent model and offspring models are considered.

6.5. Summary

Historically, bridge collapses have always been unfortunate and unforgettable incidents that not only cost human lives but also resulted in economical losses. Pin and hanger systems (as

fracture critical members) are one of the reasons for several bridge failures in history. In the literature, pin-hanger systems were closely investigated from a seismic application point of view but not fully examined from an auxiliary system application point of view. In this chapter of the dissertation, performance increase is studied for a long span cantilever truss bridge after the pin and hanger system is retrofitted. Although the retrofit application is very common for these types of structures, load rating, component reliability and system reliability changes due to the applications have not been fully studied.

First, the bridge and its monitoring system are explained. Then, the field tests including ambient vibration and load testing are presented. Afterwards, a-priori, calibrated and retrofitted models are discussed. Second, family of models is used to evaluate the load rating and reliability of the bridge with emphasis on the uncertainties. Finally the results from single models (a-priori, calibrated and retrofitted) and family of models are presented in a comparative fashion to quantify the uncertainty effects on structural performance metrics such as load rating and system reliability.

Load rating calculations show that load rating of the hanger element is 2.46 for the a-priori model without retrofit. After adding the auxiliary system to the a-priori model, the load rating dramatically increased to 5.86 due to the significant reduce in the dead load forces on the hanger element. In addition, load rating of the hanger bar is calculated as 7.66 for the parent (calibrated with retrofit) model whereas the mean and the standard deviation of the load rating distribution coming from the offspring models are found to be 6.87 and 1.29, respectively. The effect of the uncertainties causes a difference of 0.8 in load rating and this indicates that the uncertainties can lead to a difference around 0.8x(8kips+32kips+32kips)=57.6 kips of a live load.

163

Additional retrofit members around the hanger members are not only increasing the redundancy but also decreasing the dead load forces on these elements. Therefore, component and system reliability results are also presented in a comparative fashion for the different models of the bridge including a-priori model without retrofit, calibrated model without retrofit, parent model with retrofit and offspring models with retrofit. The component reliability index of the hanger element is increased due to the significant decrease in the dead load strains.

In addition, the impact of uncertainties in hanger component reliability is also clearly seen from the difference ($\beta_{difference}$=1.6) between the parent and offspring models results. Furthermore, the subsystem reliability of the hanger region is calculated as 8.25 for the parent model and 6.25 for the offspring models. Based on these observations, it can be argued that a reasonably designed and constructed retrofit for such bridges increases the system reliability of the hanger system practically to the highest level for a limit state that employs the axial strain capacity. The subtle point here is that the impact of uncertainty can play a major role irrespective of the extremely high reliability indices as can be seen here when the parent model and offspring models are considered.

Finally, this chapter again clearly illustrates the importance of uncertainties for the evaluation of structure's critical elements and retrofit. It is recommended that models be developed and calibrated using monitoring data, while still considering the uncertainties from various sources.

CHAPTER 7.
SUMMARY AND CONCLUSIONS

The principle objective of this dissertation is to investigate nonparametric and parametric approaches within the general Structural Identification (St-Id) framework by taking uncertainties into account for improved decision making. These approaches are explored for detecting and locating structural changes with higher efficiency by means of nonparametric analysis, and for improved accuracy by means of parametric analysis with the inclusion of uncertainties for structural assessment and predictions. The dissertation can mainly be summarized in five parts: (1) general explanation of St-Id framework steps with real-life case studies; (2) introduction and demonstration of a nonparametric methodology for damage detection and localization with laboratory experiments and real-life data; (3) introduction of a family-of-models approach for characterizing uncertainties and a demonstration of continuous calibration of the family of models using structural health monitoring data within the St-Id framework; (4) characterization of performance for a real-life bridge under the effects of deterioration, damage, and traffic increase by using the family-of-models approach; and (5) investigation of bridge performance increase for a real-life long-span bridge due to retrofit by means of a family-of-models approach. The general St-Id framework that is followed in this dissertation is developed by the ASCE Structural Identification Committee and is defined in more detail in the ASCE report documenting the six steps of the framework (Catbas et al. 2012d).

The steps of the general St-Id framework are presented and exemplified with laboratory and real-life bridges. A movable bridge, which is studied in detail as a unique structure not commonly found in the literature, is employed for different St-Id steps. In addition, the

performance of a long-span cantilever truss bridge is investigated after the fracture critical hanger members are retrofitted to increase the redundancy and reliability of the bridge.

Nonparametric methods are becoming more attractive because of the ease of use and rapid analysis of large sets of data to determine changes in some representative features. In this dissertation, a practical and effective nonparametric (data-driven) approach is explored for the identification and localization of structural changes due to damage. This method is also employed to determine the effectiveness of structural repair, which was implemented to bring the structure to its previous performance levels. In this approach, cross-correlation analyses between strain data sets are utilized for damage detection, and correlation matrices are employed for damage localization. First, the efficient methodology is demonstrated on a laboratory test structure for undamaged and different damaged conditions. Then, the methodology is validated on a real-life bridge, where the bridge is monitored before the damage, after the damage occurred, and after the damage was repaired.

One of the advantages of this approach is the use of most commonly used sensors (strain gages) without the need for loading information (magnitude and placement) for strain monitoring applications. Strain time histories used for the data analysis are obtained from arbitrary operating traffic conditions. If the correlation analysis is not employed, raw strain data may lead to false negatives and/or false positives since the levels will depend on the operating traffic. For example, the strain levels in a damaged bridge may not be very high depending on the operating traffic. At the same time, an intact bridge may produce high strain measurements under heavy traffic, which are not necessarily indicators of damage. As a result, the structure can be monitored over a long period of time without any special loading considerations. This is one of

the strengths of the method that any loading can be used to detect damage. Moreover, the correlation-based data analysis methodology is computationally efficient and easy to use, especially for handling large amounts of monitoring data. In addition, in the real-life bridge case, it is also shown that the method can be utilized to evaluate the effectiveness of maintenance (including repair) by checking the variations of the correlation coefficients before and after the maintenance application. The separation of correlation coefficients over time is an indicator of a structural change and possibly damage. However, the separation of correlation coefficients may not be clear due to uncertainties. As a result, the cluster of correlation coefficients for a particular condition of the structure and the cluster corresponding to another condition state are to be statistically evaluated. For this, the distributions of different clusters are analyzed for the real life case and it is seen that the probability of separation of two sets was quantified as almost 99% for the worst case. Consequently, this methodology has the potential to be easily applied by engineers to different kinds of civil infrastructure for condition monitoring and maintenance.

Structural Identification using parametric methods provide more insight to the behavior; root causes of the problems can be determined, and better predictive analyses can be carried out with the physical interpretation of the structural responses. For the parametric St-Id, a family-of-models approach is presented using Monte Carlo simulations and finite element analyses with special consideration of the uncertainties coming from different sources, such as measurement, modeling, and data post-processing. In this dissertation, the family of models is developed from a parent model, which is calibrated using monitoring data. While there are a number of methods and approaches for FEM calibration (updating), the calibration is carried out using ANNs to obtain the parent model, then the offspring models are generated from the parent model. The

167

responses from the family of models are employed to predict the performance of a structure in terms of its structural load rating and reliability, with special emphasis on different sources of uncertainties. The family-of-models technique is initially investigated for a laboratory structure and two real-life structures under performance decrease and increase circumstances.

In the laboratory demonstration of the family-of-models technique, the impact of uncertainty is investigated in predicting the system reliability obtained by a single calibrated FEM and then by a family of models that are continuously calibrated with SHM data. After discussing the laboratory structure, instrumentation plan, experimentation during support deterioration, and ANN-based model calibration, the family of models is employed for system reliability calculations. In terms of the probability of unsatisfactory performance, the difference in the predictions (obtained using the initially calibrated FEM and a family of models continuously calibrated with monitoring data) can be as large as an order of magnitude when uncertainties are not reduced by using monitoring data. This illustrates the importance of continuously calibrating the models with monitoring data and incorporating uncertainties for better predicting the reliability of structures. It should be noted that the use of parent-offspring FEMs becomes important especially when critical parameters (i.e., boundary spring constants) that have impact on the models cannot be well-defined.

As a first real-life application, movable bridge performance is evaluated for deterioration of the sections, traffic load increase over a 75-year period, and sudden span lock failure by employing the family-of-models approach. The calibration for the parent model is successfully accomplished using the ANN-based calibration methodology with multiple sensor measurements

and multiple objectives to minimize the error between the model response and monitoring data obtained from the truck load testing, operational traffic, and opening/closing of the bridge.

After the parent and the offspring models are developed, load rating values from each single model (parent model) representing a certain condition and load rating distributions from offspring models are obtained and compared for different deterioration and damage conditions. As expected, the load rating decreases over time, along with an increased coefficient of variation. It is also observed that the effect of the instantaneous damage simulating the span lock failure can be equivalent to a 45-year deterioration in terms of load rating of the bridge. With the family-of-models approach, the probability of not meeting a certain level of load rating for this bridge is explored. In this discussion, this probability is deemed as risk. Based on family-of-models approach, the probability ("risk") for having a load rating less than 1.0 is calculated as 1.6%. The family-of-model approach, therefore, not only provides the bounds and distributions of load ratings in a non-deterministic manner by considering different uncertainty sources but also quantifies the risks for structures. Further improvement to this computation can be made with the inclusion of importance of structures and a more general inclusion of hazards in terms of natural disasters, extreme loadings cases and accidents.

The system reliability of the bridge is also evaluated by using four different system models and three different correlation margins to determine the effect of data post-processing uncertainties. Perfectly correlated safety margins, partial correlation, and independent safety margins are considered, and the reliability of the system is predicted within bounds over a period of time. The most critical case is determined to be the series system model with the system safety being minimum when the safety margins of components are independent. Due to deterioration

169

and anticipated load increase, the reliability index decreases from 4.5 to 1.0 levels over a 75-year period. In addition, reliability results show that the configuration of the bridge and the correlation of variables are important factors for system reliability calculations. Finally, it is also observed that the effect of the span lock damage to the system reliability can be equivalent to a 45-year deterioration, which is also similar to the findings for the load rating analysis.

In the second real-life application, performance of a long-span cantilever truss bridge before and after retrofit applications is investigated with a calibrated model and a family-of-models approach. The fracture critical hanger members are retrofitted by adding additional rods around the hanger members to increase the redundancy and also to decrease the dead-load forces on the hangers by post-tensioning the retrofit rods. The particular uncertainties considered in this analysis are the variation in dead load, lane load, truck load, post-tension load due to application and losses, modulus of elasticity, yield stress, and cross-sectional areas.

First, the family of models is used to evaluate the load rating of the bridge with emphasis on the uncertainties. From the calculations, load rating of the hanger element, which is 2.46 before the retrofit, is increased to 5.86 for the a-priori model with retrofit and 7.66 for the calibrated (parent) model with retrofit. In addition, the mean and the standard deviation of the load rating distribution coming from the offspring models are found to be 6.87 and 1.29, respectively. These results indicate that the design load rating coming from the a-priori model without retrofit is almost tripled when compared to the calibrated (parent) model after the retrofit application. The difference in load rating between the parent model and the mean of the offspring models is about 0.80, which indicates that the uncertainties can lead to a difference of as much as 0.80 times the HL-93 loading. Moreover, the load rating ratio between the parent model with

170

retrofit (LR=7.66) and the offsprings with retrofit (LR=6.87) is calculated as 90%, in other words the reduction in load carrying capacity is found as 10% independent of the loading when the uncertainties defined above are incorporated. Another important load rating difference between the a-priori model with retrofit and the parent (retrofitted and calibrated) model is determined to be 1.80, which clearly illustrates the a-priori model can produce underestimated results in this case, potentially resulting in unnecessarily conservative decision making. From the ratio of the load ratings, the load carrying capacity is found to be 25% less for the a-priori model with retrofit compared to the parent model with retrofit.

Next, component and subsystem reliability results are presented in a comparative fashion for the different models of the long-span bridge: a-priori model without retrofit, calibrated model without retrofit, a parent model with retrofit, and offspring models with retrofit. As expected, the component reliability index of the hanger element increases due to the significant decrease in the dead-load strains. Before the retrofit application, the component reliability index of the hanger bar is calculated as 2.61 from the calibrated model. With the addition of the rods to the hanger region, the subsystem (hanger and four retrofit rods) reliability index is calculated as 6.25 from the offspring models. In this dissertation, the scope is limited to the performance evaluation of the hanger retrofit for a hanger subsystem. However, the implication of the consideration of the uncertainties may be more critical if all the elements of the system are analyzed to evaluate the system reliability of the entire bridge, as described in (Catbas et al. 2008b), where all upper chord elements, vertical, diagonal, and lower chord elements are employed for the structural system reliability computations. It is seen that a reasonably designed and constructed retrofit for such bridges increases the system reliability of the hanger system practically to the highest level

171

when a limit state that employs the axial strain capacity. The subtle point here is that the impact of uncertainty can play a major role irrespective of the high reliability indices, as can be seen here when the parent model and offspring models are considered.

All in all, it is observed that the uncertainties play a considerable role even when compared to calibrated model-based predictions for reliability and load rating, especially when the structure is complex, deteriorated and aged, and subjected to variable environmental and operational conditions. A family-of-models approach can be suitable especially for structures that have less redundancy, high operational importance, are deteriorated, and seem to perform for load level demands approaching the capacity. With such models, it is possible to make more reliable and informed decisions for structures current and future performance.

LIST OF REFERENCES

AASHTO (2002). Transportation Asset Management Guide. Washington, DC, Report Prepared for the National Cooperative Highway Research Program (NCHRP) Project 20-24(11).

AASHTO (2004). LRFD Bridge Design Specifications. Washington, DC.

Abdel-Ghaffar, A. M. and G. W. Housner (1978). "Ambient Vibration Tests of Suspension Bridge." Journal of Engineering Mechanics **104**(5): 983-999.

Abdel-Ghaffar, A. M. and A. S. Nazmy (1991). "3-D Nonlinear Seismic Behavior of Cable-Stayed Bridges." Journal of Structural Engineering **117**(11): 3456-3476.

Aktan, A. E., F. N. Catbas, K. A. Grimmelsman and C. J. Tsikos (2000a). "Issues in Infrastructure Health Monitoring for Management." Journal of Engineering Mechanics **126**(7): 711-724.

Aktan, A. E., F. N. Catbas, A. Turer and Z. Zhang (1998a). "Structural Identification: Analytical Aspects." Journal of Structural Engineering **124**(7): 817-829.

Aktan, A. E., D. N. Farhey, D. L. Brown, V. Dalal, A. J. Helmicki, V. J. Hunt and S. J. Shelley (1996). "Condition Assessment for Bridge Management." Journal of Infrastructure Systems **2**(3): 108-117.

Aktan, A. E., D. N. Farhey, A. J. Helmicki, D. L. Brown, V. J. Hunt, K. L. Lee and A. Levi (1997). "Structural Identification for Condition Assessment: Experimental Arts." Journal of Structural Engineering **123**(12): 1674-1684.

Aktan, A. E., A. J. Helmicki and V. J. Hunt (1998b). "Issues in Health Monitoring for Intelligent Infrastructure." Smart Materials and Structures **7**: 674-692.

Aktan, A. E., M. Pervizpour, F. N. Catbas, R. A. Barrish, K. A. Grimmelsman, X. Qin, E. Kulcu, S. K. Ciloglu, J. Curtis and G. V. Haza-Radlitz (2000b). Integrated Field, Theoretical and Laboratory Research for Solving Large System Identification Problems. Advances in Structural Dynamics, Hong Kong.

Albrecht, P. and A. H. Naeemi (1984). Performance of Weathering Steel in Bridges. NCHRP Report 272. Washington, DC., Transportation Research Board.

Ang, A. H.-S. and W. H. Tang (1984). Probability Concepts in Engineering Planning and Design Vol.II. New York, Wiley.

Ang, A. H. S. and D. De Leon (2005). "Modeling and Analysis of Uncertainties for Risk-Informed Decisions in Infrastructures Engineering." <u>Structure and Infrastructure Engineering</u> **1**(1): 19-31.

Azizinamini, A. (2002). "Full scale testing of old steel truss bridge." <u>Journal of Constructional Steel Research</u> **58**(5–8): 843-858.

Bakhtiari-Nejad, F., A. Rahai and A. Esfandiari (2005). "A structural damage detection method using static noisy data." <u>Engineering Structures</u> **27**(12): 1784-1793.

Beck, J. L. and S. K. Au (2002). "Bayesian Updating of Structural Models and Reliability using Markov Chain Monte Carlo Simulation." <u>Journal of Engineering Mechanics</u> **128**(4): pp.380-391.

Beck, J. L. and L. S. Katafygiotis (1998). "Updating Models and Their Uncertainties I: Bayesian Statistical Framework." <u>Journal of Engineering Mechanics</u> **124**(4): pp. 455-461.

Bell, E. S., M. Sanayei, N. J. Chitra and S. Eugene (2007a). "Multiresponse Parameter Estimation for Finite-Element Model Updating Using Nondestructive Test Data." <u>Journal of Structural Engineering</u> **133**(8): 1067-1079.

Bell, E. S., M. Sanayei, C. N. Javdekar and E. Slavsky (2007b). "Multiresponse Parameter Estimation for Finite-Element Model Updating Using Nondestructive Test Data." <u>Journal of Structural Engineering</u> **133**(8): 1067-1079.

Bernal, D. (2002). "Load Vectors for Damage Localization." <u>Journal of Engineering Mechanics</u> **128**(1): pp. 7-14.

Besterfield, G., S. Nichani, A. K. Kaw and T. Eason (2003). "Full-Scale Testing of Procedures for Assembling Trunnion-Hub-Girder in Bascule Bridges." <u>Journal of Bridge Engineering</u> **8**(4): 204-211.

Bhattacharya, B., D. Li, M. Chajes and J. Hastings (2005). "Reliability-Based Load and Resistance Factor Rating Using In-Service Data." <u>Journal of Bridge Engineering</u> **10**(5): 530-543.

Biezma, M. V. and F. Schanack (2007). "Collapse of Steel Bridges." <u>Journal of Performance of Constructed Facilities</u> **21**(5): 398-405.

Biondini, F. and D. M. Frangopol (2009). "Lifetime reliability-based optimization of reinforced concrete cross-sections under corrosion." <u>Structural Safety</u> **31**(6): 483-489.

Bodeux, J. B. and J. C. Golinval (2001). "Application of ARMAV models to the identification and damage detection of mechanical and civil engineering structures." <u>Smart Materials and Structures</u> **10**(3): 479.

174

Boothby, T. E. and R. J. Craig (1997). "Experimental Load Rating Study of a Historic Truss Bridge." Journal of Bridge Engineering **2**(1): 18-26.

Brownjohn, J. M. (2003). "Ambient Vibration Studies for System Identification of Tall Buildings." Earthquake Engineering and Structural Dynamics **32**(1): pp. 71-95.

Brownjohn, J. M., S.-C. Tjin, G.-H. Tan and B.-L. Tan (2004). A Structural Health Monitoring Paradigm for Civil Infrastructure. 1st FIG International Symposium on Engineering Surveys for Construction Works and Structural Engineering, Nottingham, UK.

Brownjohn, J. M., A. Zasso, G. A. Stephen and R. T. Severn (1995). "Analysis of Experimental Data from Wind-Induced Response of a Long Span Bridge." Journal of Wind Engineering and Industrial Aerodynamics **54/55**: pp. 13-24.

Brownjohn, J. M. W., P. Moyo, P. Omenzetter and Y. Lu (2003). "Assessment of Highway Bridge Upgrading by Dynamic Testing and Finite-Element Model Updating." Journal of Bridge Engineering **8**(3): 162-172.

Brownjohn, J. M. W., T. C. Pan and X. Y. Deng (2000). "Correlating Dynamic Characteristics from Field Measurements and Numerical Analysis of a High-rise Building." Earthquake Engineering and Structural Dynamics **29**: 523-543.

Carden, E. P. and J. M. Brownjohn (2008). "ARMA Modelled Time-Series Classification for Structural Health Monitoring of Civil Infrastructure." Mechanical Systems and Signal Processing **22**(2): pp. 295-314.

Casas, J. R. and P. J. S. Cruz (2003). "Fiber Optic Sensors for Bridge Monitoring." Journal of Bridge Engineering **8**(6): 362-373.

Casciati, F., G. P. Cimellaro and M. Domaneschi (2008). "Seismic reliability of a cable-stayed bridge retrofitted with hysteretic devices." Computers and Structures **86**(17–18): 1769-1781.

Catbas, F. N. and A. E. Aktan (2002). "Condition and Damage Assessment: Issues and Some Promising Indices." Journal of Structural Engineering **128**(8): pp. 1026-1036.

Catbas, F. N., D. L. Brown and A. E. Aktan (2004a). "Parameter Estimation for Multiple-Input Multiple-Output Modal Analysis of Large Structures." Journal of Engineering Mechanics **130**(8): 921-930.

Catbas, F. N., D. L. Brown and A. E. Aktan (2006). "Use of Modal Flexibility for Damage Detection and Condition Assessment: Case Studies and Demonstrations on Large Structures." Journal of Structural Engineering **132**(11): 1699-1712.

Catbas, F. N., S. K. Ciloglu, K. A. Grimmelsman, Q. Pan, M. Pervizpour and A. E. Aktan (2003). <u>Limitations in Structural Identification of Long Span Bridges</u>. International Workshop on Structural Health Monitoring of Bridges, Kitami Institute of Technology, Japan.

Catbas, F. N., S. K. Ciloglu, O. Hasancebi, K. A. Grimmelsman and A. E. Aktan (2007). "Limitations in Structural Identification of Large Constructed Structures." <u>Journal of Structural Engineering</u> **133**(8): pp. 1051-1066.

Catbas, F. N., H. B. Gokce and D. M. Frangopol (2012a). "Predictive Analysis by Incorporating Uncertainty through a Family of Models Calibrated with Structural Health Monitoring Data." <u>Journal of Engineering Mechanics</u> (in press).

Catbas, F. N., H. B. Gokce and M. Gul (2012b). "Non-parametric Analysis of Structural Health Monitoring Data for Identification and Localization of Changes: Concept, Lab and Real Life Studies." <u>Structural Health Monitoring</u> (in press).

Catbas, F. N., H. B. Gokce and M. Gul (2012c). "A Practical Approach for Estimating Distribution Factor and Load Rating: Demonstration on Reinforced Concrete T-Beam Bridges." <u>Journal of Bridge Engineering</u> (in press).

Catbas, F. N., H. B. Gokce, M. Gul and D. M. Frangopol (2011). "Movable Bridges: Condition, Modeling and Damage Simulations." <u>Institution of Civil Engineers - Bridge Engineering</u> **164**(3): 145 –155.

Catbas, F. N., M. Gul and J. L. Burkett (2008a). "Damage Assessment Using Flexibility and Flexibility-Based Curvature for Structural Health Monitoring." <u>Smart Materials and Structures</u> **17**(1): 015024.

Catbas, F. N., M. Gul, R. Zaurin, H. B. Gokce, T. Terrell, T. Dumlupinar and D. Maier (2010). Long Term Bridge Maintenance Monitoring Demonstration on a Movable Bridge. A Framework for Structural Health Monitoring of Movable Bridges, Florida Department of Transportation (FDOT).

Catbas, F. N. and T. Kijewski-Correa (2012). "Structural Identification of Constructed Systems: A collective Effort toward an Integrated Approach that Reduces Barriers to Adoption." <u>Journal of Structural Engineering</u> (accepted).

Catbas, F. N., T. Kijewski-Correa and A. E. Aktan (2012d). Structural Identification (St-Id) of Constructed Facilities (in press).

Catbas, F. N., M. Shah, J. Burkett and A. Basharat (2004b). <u>Challenges in Structural Health Monitoring</u>. Proceedings of the 4th International Workshop on Structural Control, Columbia University, New York.

Catbas, F. N., M. Susoy and D. M. Frangopol (2008b). "Structural health monitoring and reliability estimation: Long span truss bridge application with environmental monitoring data." Engineering Structures **30**(9): 2347-2359.

Catbas, F. N., R. Zaurin, M. Gul and H. B. Gokce (2012e). "Sensor networks, Computer Imaging and Unit Influence Lines for Structural Health Monitoring: A Case Study for Bridge Load Rating." Journal of Bridge Engineering (in press).

Chajes, M. J., D. R. Mertz and B. Commander (1997). "Experimental Load Rating of a Posted Bridge." Journal of Bridge Engineering **2**(1): 1-10.

Chang, C. C., T. Y. P. Chang and Q. W. Zhang (2001). "Ambient Vibration of Long-Span Cable-Stayed Bridge." Journal of Bridge Engineering **6**(1): 46-53.

Chang, P. C., A. Flatau and S. C. Liu (2003). "Review Paper: Health Monitoring of Civil Infrastructure." Structural Health Monitoring **2**(3): pp. 257-267

Ching, J. and Y.-H. Hsieh (2009). "Updating real-time reliability of instrumented systems with stochastic simulation." Probabilistic Engineering Mechanics **24**(2): 242-250.

Der Kiureghian, A. and O. Ditlevsen (2009). "Aleatory or epistemic? Does it matter?" Structural Safety **31**(2): 105-112.

Der Kiureghian, A., T. Haukaas and K. Fujimura (2006). "Structural reliability software at the University of California, Berkeley." Structural Safety **28**(1–2): 44-67.

Ditlevsen, O. (1979). "Narrow Reliability Bounds for Structural Systems." Journal of Structural Mechanics **7**(4): 453 - 472.

Doebling, S. W., C. R. Farrar and M. B. Prime (1998). "A Summary Review of Vibration-Based Damage Identification Methods." The Shock and Vibration Digest **30**(2): pp. 91-105.

Doebling, S. W., C. R. Farrar, M. B. Prime and D. W. Shevitz (1996). Damage Identification in Structures and Mechanical Systems Based on Changes in Their Vibration Characteristics: A Detailed Literature Survey. Los Alamos, NM, Los Alamos National Laboratory Report No. LA-13070-MS.

Dyke, S. J., J. M. Caicedo, G. Turan, L. A. Bergman and S. Hague (2003). "Phase I Benchmark Control Problem for Seismic Response of Cable-Stayed Bridges." Journal of Structural Engineering **129**(7): pp. 857-872.

Ecale, H. and T.-H. Lu (1983). "New Chicago-Type Bascule Bridge." Journal of Structural Engineering **109**(10): 2340-2354.

Ellingwood, B. R. (2005). "Risk-Informed Condition Assessment of Civil Infrastructure: State of Practice and Research Issues." Structure and Infrastructure Engineering **1**(1): 7-18.

Ellingwood, B. R., T. V. Galambos, J. G. MacGregor and C. A. Cornell (1980). Development of a Probability Based Load Criterion for American National Standard A58. Washington, DC: National Bureau of Standards, NBS Special Publication 577.

Enright, M. P. and D. M. Frangopol (1999). "Condition Prediction of Deteriorating Concrete Bridges Using Bayesian Updating." Journal of Structural Engineering **125**(10): 1118-1125.

Ermopoulos, J. and C. C. Spyrakos (2006). "Validated analysis and strengthening of a 19th century railway bridge." Engineering Structures **28**(5): 783-792.

Estes, A. C. and D. M. Frangopol (1998). "RELSYS: A Computer Program for Structural System Reliability Analysis." Journal of Structural Engineering and Mechanics **6**(8): 901-919.

Estes, A. C. and D. M. Frangopol (1999). "Repair Optimization of Highway Bridges Using System Reliability Approach." Journal of Structural Engineering **125**(7): 766-775.

Estes, A. C. and D. M. Frangopol (2005). "Load Rating versus Reliability Analysis." Journal of Structural Engineering **131**(5): 843-847.

Farhey, D. N., R. Naghavi, A. Levi, A. M. Thakur, M. A. Pickett, D. K. Nims and A. E. Aktan (2000). "Deterioration Assessment and Rehabilitation Design of Existing Steel Bridge." Journal of Bridge Engineering **5**(1): 39-48.

Farrar, C. R., W. E. Baker, T. M. Bell, K. M. Cone and T. W. Darling (1994). Dynamic characterization and damage detection in the I-40 bridge over the Rio Grande. Los Alamos National Laboratory, Los Alamos, NM, Report LA-12767-MS.

Farrar, C. R. and D. A. Jaureguiz (1998). "Comparative Study of Damage Identification Algorithms Applied to a Bridge: I. Experiment." Smart Material and Structures **7**: 704-719.

FHWA (1995). Recording and Coding Guide for the Structural Inventory and Appraisal of the Nation's Bridges, Federal Highway Administration

FHWA (2008). Deficient Bridges by State and Highway System, Federal Highway Administration

Fisher, A. D. and A. M. Robitaille (2011). "Replacement of the Movable Span of the Thames River Bridge: How 19th Century Technology Impacted 21st Century Construction." Journal of Construction Engineering and Management **137**(10): 895-900.

Frangopol, D. M. (2011a). "Life-cycle performance, management, and optimisation of structural systems under uncertainty: accomplishments and challenges." Structure and Infrastructure Engineering **7**(6): 389-413.

Frangopol, D. M. (2011b). "Life-cycle performance, management, and optimisation of structural systems under uncertainty: accomplishments and challenges 1." Structure and Infrastructure Engineering **7**(6): 389-413.

Frangopol, D. M. and K. Imai (2004). "Reliability of Long Span Bridges Based on Design Experience with the Honshu-Shikoku Bridges." Journal of Constructional Steel Research **60**(3-5): pp. 373-392.

Frangopol, D. M., A. Strauss and S. Kim (2008). "Bridge Reliability Assessment Based on Monitoring." Journal of Bridge Engineering **13**(3): 258-270.

Fränkel, W. (1882). Der Brückenbau - Bewegliche Brücken. T. Schäffer and E. Sonne eds, Verlag Wilhelm Engelmann. Leipzig, Germany.

Fujino, Y. (2002). "Vibration, Control and Monitoring of Long-Span Bridges – Recent Developments and Practice in Japan." Journal of Construction Steel Research **58**: 71-97.

Garrett, G. P. (2007). "Analytical load rating of an open-spandrel arch bridge: Case study." Journal of Bridge Engineering **12**(1): 13-20.

Ghanem, R. and M. Shinozuka (1995). "Structural-System Identification. I: Theory." Journal of Engineering Mechanics **121**(2): 255-264.

Ghosn, M., F. Moses and D. M. Frangopol (2010). "Redundancy and robustness of highway bridge superstructures and substructures." Structure and Infrastructure Engineering **6**(1): 257 - 278.

Giraldo, D. and S. J. Dyke (2004). Damage Localization in Benchmark Structure Considering Temperature Effects. 7th International Conference on Motion and Vibration Control, St. Louis, MO.

Gokce, H. B., F. N. Catbas and D. M. Frangopol (2011). "Evaluation of Load Rating and System Reliability of Movable Bridge." Transportation Research Record: Journal of the Transportation Research Board **2251**(1): 114-122.

Gokce, H. B., F. N. Catbas, M. Gul and D. M. Frangopol (2012a). "Structural Identification for Performance Prediction Considering Uncertainties: A Case Study of a Movable Bridge." Journal of Structural Engineering (in press).

Gokce, H. B., M. Gul and F. N. Catbas (2012b). "Implementation of Structural Health Monitoring for Movable Bridges." Transportation Research Record: Journal of the Transportation Research Board (in press).

Goulet, J., P. Kripakaran and I. F. Smith (2010). "Multimodel Structural Performance Monitoring." Journal of Structural Engineering **136**(10): 1309.

Greene, W. K. and E. E. McKeen (1938). "Erecting the Marine Parkway Bridge." Engineering News-Record: 371-374.

Griggs, J. F. E. (2006). "Development of the Vertical Lift Bridge: Squire Whipple to J. A. L. Waddell, 1872--1917." Journal of Bridge Engineering **11**(5): 642-654.

Gul, M. and F. N. Catbas (2009). "Statistical pattern recognition for Structural Health Monitoring using time series modeling: Theory and experimental verifications." Mechanical Systems and Signal Processing **23**(7): 2192-2204.

Gul, M. and F. N. Catbas (2011). "Structural health monitoring and damage assessment using a novel time series analysis methodology with sensor clustering." Journal of Sound and Vibration **330**(6): 1196-1210.

Gul, M. and F. N. Catbas (2012). "Damage Assessment with Ambient Vibration Data using a Novel Time Series Analysis Methodology." Journal of Structural Engineering (in press).

Gul, M., H. B. Gokce and F. N. Catbas (2011). Long-term Maintenance Monitoring Demonstration on a Movable Bridge, Florida Department of Transportation (FDOT).

Gurley, K. and A. Kareem (1999). "Applications of wavelet transform in earthquake, wind and ocean engineering." Engineering Structures **21**(2): 149-167.

Hardesty, E. R., R. W. Christie and H. W. Fischer (1975a). "Fifty-Year History of Movable Bridge Construction- Part I." Journal of the Construction Division **101**(3): 511-527.

Hardesty, E. R., R. W. Christie and H. W. Fischer (1975b). "Fifty-Year History of Movable Bridge Construction- Part II." Journal of the Construction Division **101**(3): 529-543.

Hart, G. C. and J. T. P. Yao (1977). "System Identification in Structural Dynamics." Journal of Engineering Mechanics **103**(6): pp. 1089-1104.

Haukaas, T. and A. Der Kiureghian (2007). "Methods and Object-Oriented Software for FE Reliability and Sensitivity Analysis with Application to a Bridge Structure." Journal of Computing in Civil Engineering **21**(3): 151-163.

Hoang, N., Y. Fujino and P. Warnitchai (2008). "Optimal tuned mass damper for seismic applications and practical design formulas." Engineering Structures **30**(3): 707-715.

Hogue, T. D., A. E. Aktan and A. Hoyos (1991). "Localized Identification of Constructed Facilities." Journal of Structural Engineering **117**(1): 128-148.

Hou, Z., M. Noori and R. St. Amand (2000). "Wavelet-Based Approach for Structural Damage Detection." Journal of Engineering Mechanics **126**(7): 677-683.

Huang, C. S., Y. B. Yang, L. Y. Lu and C. H. Chen (1999). "Dynamic testing and system identification of a multi-span highway bridge." Earthquake Engineering and Structural Dynamics **28**(8): 857-878.

Imai, K. and D. M. Frangopol (2001). "Reliability-based Assessment of Suspension Bridges: Application to the Innoshima Bridge." Journal of Bridge Engineering **6**(6): 398-411.

Imai, K. and D. M. Frangopol (2002). "System Reliability of Suspension Bridges." Structural Safety, Elsevier **24**(2-4): pp. 219-259.

Ingham, T. J., S. Rodriguez and M. Nader (1997). "Nonlinear analysis of the Vincent Thomas Bridge for seismic retrofit." Computers and Structures **64**(5–6): 1221-1238.

Jaishi, B. and W.-X. Ren (2005). "Structural Finite Element Model Updating Using Ambient Vibration Test Results." Journal of Structural Engineering **131**(4): 617-628.

Kao, C. Y. and S.-L. Hung (2003). "Detection of Structural Damage via Free Vibration Responses Generated by Approximating Artificial Neural Networks." Computers and Structures **81**: pp. 2631-2644.

Katafygiotis, L. S. and J. L. Beck (1998). "Updating Models and Their Uncertainties. II: Model Identifiability." Journal of Engineering Mechanics **124**: 463-467.

Kijewski, T. and A. Kareem (2003). "Wavelet Transforms for System Identification in Civil Engineering." Computer-Aided Civil and Infrastructure Engineering **18**(5): 339-355.

Kim, S. and D. M. Frangopol (2011a). "Cost-Based Optimum Scheduling of Inspection and Monitoring for Fatigue-Sensitive Structures under Uncertainty." Journal of Structural Engineering **137**(11): 1319-1331.

Kim, S. and D. M. Frangopol (2011b). "Cost-Effective Lifetime Structural Health Monitoring Based on Availability." Journal of Structural Engineering **137**(1): 22-33.

Kim, S. and D. M. Frangopol (2011c). "Optimal planning of structural performance monitoring based on reliability importance assessment." Probabilistic Engineering Mechanics **25**(1): 86-98.

Ko, J. M. and Y. Q. Ni (2005). "Technology Developments in Structural Health Monitoring of Large-scale Bridges " Engineering Structures **27**: pp. 1715-1725.

181

Koglin, T. L. (2003). <u>Movable Bridge Engineering</u>, John Wiley and Sons.

Kondoh, M., M. Okuda, K. Kawaguchi and T. Yamazaki (2001). "Design Method of a Hanger System for Long-Span Suspension Bridge." <u>Journal of Bridge Engineering</u> **6**(3): 176-182.

Kripakaran, P. and I. F. C. Smith (2009). "Configuring and enhancing measurement systems for damage identification." <u>Advanced Engineering Informatics</u> **23**(4): 424-432.

Kwon, K. and D. M. Frangopol (2010). "Bridge fatigue reliability assessment using probability density functions of equivalent stress range based on field monitoring data." <u>International Journal of Fatigue</u> **32**(8): 1221-1232.

Laory, I., T. N. Trinh and I. F. C. Smith (2011). "Evaluating two model-free data interpretation methods for measurements that are influenced by temperature." <u>Advanced Engineering Informatics</u> **25**(3): 495-506.

LeBeau, K. and S. Wadia-Fascetti (2007). "Comparative probabilistic initial bridge load rating model." <u>Journal of Bridge Engineering</u> **12**(6): 785-793.

Levenberg, K. (1944). "A method for the solution of certain problems in least squares." <u>Quarterly of Applied Mathematics</u> **2**: 164-168.

Levi, A. (1997). <u>Instrumented Monitoring & Diagnostic Load Testing for Condition Assessment and Evaluation of Bridges</u> PhD Thesis, University of Cincinnati.

Li, S., Z. Wu and L. Zhou (2010). "Health monitoring of flexural steel structures based on distributed fibre optic sensors." <u>Structure and Infrastructure Engineering: Maintenance, Management, Life-Cycle Design and Performance</u> **6**(3): 303 - 315.

Lichtenstein, A. G. (1993). "The Silver Bridge Collapse Recounted." <u>Journal of Performance of Constructed Facilities</u> **7**(4): 249-261.

Little, R. G. (2002). "Controlling Cascading Failure: Understanding the Vulnerabilities of Interconnected Infrastructures." <u>Journal of Urban Technology</u> **9**(1): 109-123.

Liu, M., D. M. Frangopol and S. Kim (2009). "Bridge System Performance Assessment from Structural Health Monitoring: A Case Study." <u>Journal of Structural Engineering</u> **135**(6): 733-742.

Liu, M., D. M. Frangopol and K. Kwon (2010). "Fatigue reliability assessment of retrofitted steel bridges integrating monitored data." <u>Structural Safety</u> **32**(1): 77-89.

Liu, S. C. and J. T. P. Yao (1978). "Structural Identification Concept." <u>Journal of Structural Division, ASCE</u> **104**(12): 1845-1858.

Ljung, L. (1999). <u>System Identification: Theory for the User</u>. Upper Saddle River, NJ, Prentice-Hall.

Lus, H., R. Betti and R. W. Longman (1999). "Identification of Linear Structural Systems Using Earthquake-Induced Vibration Data." <u>Earthquake Engineering and Structural Dynamics</u> **28**: pp. 1449-1467.

Lynch, J. P., K. H. Law, A. S. Kiremidjian, E. Carryer, C. R. Farrar, H. Sohn, D. W. Allen, B. Nadler and J. R. Wait (2004). "Design and Performance Validation of a Wireless Sensing Unit for Structural Monitoring Applications." <u>Structural Engineering and Mechanics</u> **17**(3-4): pp. 393-408.

Lynch, J. P. and K. Loh (2005). "A Summary Review of Wireless Sensors and Sensor Networks for Structural Health Monitoring." <u>The Shock and Vibration Digest</u> **38**(2): 91-128.

Maeck, J. and G. De Roeck (2003). "Damage Assessment Using Vibration Analysis on the Z24-Bridge." <u>Mechanical Systems and Signal Processing</u> **17**(1): pp. 133-142.

Marquardt, D. W. (1963). "An Algorithm for Least-Squares Estimation of Nonlinear Parameters." <u>Journal of the Society for Industrial and Applied Mathematics</u> **11**(2): 431-441.

Masri, S. F., M. Nakamura, A. G. Chassiakos and T. K. Caughey (1996). "Neural Network Approach to Detection of Changes in Structural Parameters." <u>Journal of Engineering Mechanics</u> **122**(4): 350-360.

Masri, S. F., L.-H. Sheng, J. P. Caffrey, R. L. Nigbor, M. Wahbeh and A. M. Abdel-Ghaffar (2004). "Application of a Web-enabled Real-time Structural Health Monitoring System for Civil Infrastructure Systems." <u>Smart Materials and Structures</u> **13**: 1269-1283.

Masri, S. F., A. W. Smyth, A. G. Chassiakos, T. K. Caughey and N. F. Hunter (2000). "Application of Neural Networks for Detection of Changes in Nonlinear Systems." <u>Journal of Engineering Mechanics</u> **126**(7): pp. 666-676.

Mehta, S. (2001). "Stress Spikes in Pin and Hanger System of Truss Bridge." <u>Journal of Bridge Engineering</u> **6**(2): 103-109.

Moon, F. L. and A. E. Aktan (2006a). "Impacts of Epistemic Uncertainty on Structural Identification of Constructed Systems." <u>The Shock and Vibration Digest</u> **38**(5).

Moon, F. L. and A. E. Aktan (2006b). <u>Structural Identification of Constructed Systems and the Impact of Epistemic Uncertainty</u>. Proceedings of the 3rd International Conference on Bridge Maintenance, Safety, and Management (IABMAS), Porto, Portugal.

Murphy, T. P. and K. R. Collins (2004). "Retrofitting Suspension Bridges Using Distributed Dampers." Journal of Structural Engineering **130**(10): 1466-1474.

Nagavi, R. S. and A. E. Aktan (2003). "Nonlinear Behavior of Heavy Class Steel Truss Bridges." Journal of Structural Engineering **129**(8): 1113-1121.

Nakamura, M., S. F. Masri, A. G. Chassiakos and T. K. Caughey (1998). "A method for non-parametric damage detection through the use of neural networks." Earthquake Engineering and Structural Dynamics **27**(9): 997-1010.

National Bridge Inventory (2009). "Public Disclosure of National Bridge Inventory (NBI) Data."

Natke, H. G. and J. T. P. Yao (1987). System Identification Approaches in Structural Safety Evaluation. Proceeedings of the Workshop on Structural Safety Evaluation Based on System Identification Approaches, Lambrecht/Pfalz, Germany.

Nowak, A. S. (1999). Calibration of LRFD Bridge Design Code. Washington, DC, NCHRP Report 368.

Nowak, A. S. and K. R. Collins (2000). Reliability of Structures, McGraw-Hill.

Okasha, N. M. and D. M. Frangopol (2010). "Time-variant redundancy of structural systems." Structure and Infrastructure Engineering **6**(1): 279 - 301.

Okasha, N. M., D. M. Frangopol, D. Saydam and L. W. Salvino (2011). "Reliability analysis and damage detection in high-speed naval craft based on structural health monitoring data." Structural Health Monitoring **10**(4): 361-379.

Omenzetter, P. and J. M. Brownjohn (2006). "Application of Time Series Analysis for Bridge Monitoring." Smart Material and Structures **15**: pp. 129-138.

OpenSees. (2009). "Open system for earthquake engineering simulation, Pacific Earthquake Engineering Research Center, University of California, Berkeley, CA." from http://opensees.berkeley.edu/index.php.

Padgett, J. E., K. Dennemann and J. Ghosh (2010). "Risk-based seismic life-cycle cost–benefit (LCC-B) analysis for bridge retrofit assessment." Structural Safety **32**(3): 165-173.

Padgett, J. E. and R. DesRoches (2007). "Sensitivity of Seismic Response and Fragility to Parameter Uncertainty." Journal of Structural Engineering **133**(12): 1710-1718.

Papadimitriou, C., J. L. Beck and S.-K. Au (2000). "Entropy-Based Optimal Sensor Location for Structural Model Updating." Journal of Vibration and Control **6**(5): 781-800.

Papadimitriou, C., J. L. Beck and L. S. Katafygiotis (2001). "Updating Robust Reliability using Structural Test Data." Probabilistic Engineering Mechanics **16**: pp. 103-113.

Philips Adewuyi, A., Z. Wu and N. H. M. Kammrujaman Serker (2009). "Assessment of Vibration-based Damage Identification Methods Using Displacement and Distributed Strain Measurements." Structural Health Monitoring **8**(6): 443-461.

Pollino, M. and M. Bruneau (2007). "Seismic Retrofit of Bridge Steel Truss Piers Using a Controlled Rocking Approach." Journal of Bridge Engineering **12**(5): 600-610.

Posenato, D., P. Kripakaran, D. Inaudi and I. F. C. Smith (2010). "Methodologies for model-free data interpretation of civil engineering structures." Computers and Structures **88**(7-8): 467-482.

Quade, M. N. (1954). "Special design features of the Yorktown Bridge." Transactions of the American Society of Civil Engineers **119**(1): 109–123.

Ramey, G. E. (1983). "Lift System for Raising Continuous Concrete Bridges." Journal of Transportation Engineering **109**(5): 733-746.

Robert-Nicoud, Y., B. Raphael, O. Burdet and I. F. C. Smith (2005a). "Model Identification of Bridges Using Measurement Data." Computer-Aided Civil and Infrastructure Engineering **20**(2): pp. 118-131.

Robert-Nicoud, Y., B. Raphael, O. Burdet and I. F. C. Smith (2005b). "System Identification through Model Composition and Stochastic Search." Journal of Computing in Civil Engineering **19**(3): pp. 239-247.

Saitta, S., P. Kripakaran, B. Raphael and I. F. C. Smith (2008). "Improving System Identification Using Clustering." Journal of Computing in Civil Engineering **22**(5): 292-302.

Sanayei, M. (1997). PARIS-PARameter identification system. T. University. Medford, Mass.

Sanayei, M., E. S. Bell, C. N. Javdekar, J. Edelmann and E. Slavsky (2006). "Damage Localization and Finite-Element Model Updating Using Multiresponse NDT Data." Journal of Bridge Engineering **11**(6): pp, 688-698.

Sanayei, M., G. R. Imbaro, J. A. S. McClain and L. C. Brown (1997). "Structural Model Updating Using Experimental Static Measurements." Journal of Structural Engineering **123**(6): 792-798.

Sarraf, M. and M. Bruneau (1998). "Ductile Seismic Retrofit of Steel Deck-Truss Bridges. II: Design Applications." Journal of Structural Engineering **124**(11): 1263-1271.

Shinozuka, M. and R. Ghanem (1995). "Structural System Identification. II: Experimental Verification." Journal of Engineering Mechanics **121**(2): 265-273.

Skolnik, D., Y. Lei, E. Yu and J. W. Wallace (2006). "Identification, Model Updating, and Response Prediction of an Instrumented 15-Story Steel-Frame Building." Earthquake Spectra **22**(3): 781-802.

Smith, I. F. C. (2011). Anomaly Detection without Structural Behavior Models. ASCE Structures Congress, Las Vegas, NV.

Smith, I. F. C. and S. Saitta (2008). "Improving Knowledge of Structural System Behavior through Multiple Models." Journal of Structural Engineering **134**(4): 553-561.

Sohn, H. and C. R. Farrar (2001). "Damage Diagnosis Using Time Series Analysis of Vibration Signals." Smart Materials and Structures **10**: 1-6.

Sohn, H., C. R. Farrar, F. M. Hemez, D. D. Shunk, D. W. Stinemates and B. R. Nadler (2004). A Review of Structural Health Monitoring Literature: 1996-2001, Los Alamos National Laboratory Report.

Sohn, H., C. R. Farrar, N. F. Hunter and K. Worden (2001). "Structural Health Monitoring Using Statistical Pattern Recognition Techniques." Journal of Dynamic Systems, Measurement, and Control **123**: 706-711.

Sohn, H. and K. H. Law (1997). "A Bayesian probabilistic approach for structure damage detection." Earthquake Engineering and Structural Dynamics **26**(12): 1259-1281.

Song, J. and W.-H. Kang (2009). "System reliability and sensitivity under statistical dependence by matrix-based system reliability method." Structural Safety **31**(2): 148-156.

Soyoz, S. and M. Q. Feng (2009). "Long-Term Monitoring and Identification of Bridge Structural Parameters." Computer-Aided Civil and Infrastructure Engineering **24**: pp 82-92.

Teughels, A., J. Maeck and G. De Roeck (2002). "Damage assessment by FE model updating using damage functions." Computers and Structures **80**(25): 1869-1879.

Toksoy, T. and A. E. Aktan (1994). "Bridge Condition Assessment by Modal Flexibility." Experimental Mechanics **34**(3): 271-278.

Turner-Fairbank Highway Research Center (2005). Bridge Study Analyzes Accuracy of Visual Inspections, http://www.tfhrc.gov/focus/jan01/bridge_study.htm.

Waddell, J. A. L. (1895). "The Halstead Street lift bridge." Transactions of the American Society of Civil Engineers **33(1)**: 1-60.

Wallner, M. and M. Pircher (2007). "Kinematics of Movable Bridges." Journal of Bridge Engineering **12**(2): pp. 147-153.

Wengenroth, R. H., E. R. Hardesty and H. A. Mix (1975). "Fifty-Year History of Movable Bridge Construction- Part III." <u>Journal of the Construction Division</u> **101**(3): 545-557.

Worden, K. (1997). "Structural Fault Detection Using a Novelty Measure." <u>Journal of Sound and Vibration</u> **201**(1): 85-101.

Worden, K. and J. M. Dulieu-Barton (2004). "An Overview of Intelligent Fault Detection in Systems and Structures." <u>Structural Health Monitoring</u> **3**(1): pp 85-98.

Worden, K., G. Manson and N. R. J. Fieller (2000). "Damage Detection Using Outlier Analysis." <u>Journal of Sound and Vibration</u> **229**(3): pp. 647-667.

Yang, J. N., Y. Lei, S. Lin and N. Huang (2004). "Identification of Natural Frequencies and Dampings of In Situ Tall Buildings Using Ambient Wind Vibration Data." <u>Journal of Engineering Mechanics</u> **130**(5): pp. 570-577.

Yonaba, H., F. Anctil and V. Fortin (2010). "Comparing Sigmoid Transfer Functions for Neural Network Multistep Ahead Streamflow Forecasting." <u>Journal of Hydrologic Engineering</u> **15**(4): 275-283.

Yun, H.-B. and S. F. Masri (2009). "Stochastic change detection in uncertain nonlinear systems using reduced-order models: classification." <u>Smart Materials and Structures</u> **18**(1): 015004.

Yun, H.-B., S. F. Masri, R. W. Wolfe and G. Benzoni (2009). "Data-driven methodologies for change detection in large-scale nonlinear dampers with noisy measurements." <u>Journal of Sound and Vibration</u> **322**(1-2): 336-357.

Zapico, J. L., M. P. GonzÁLez and K. Worden (2003). "Damage Assessment Using Neural Networks." <u>Mechanical Systems and Signal Processing</u> **17**(1): 119-125.

Zaurin, R. (2009). <u>Structural Health Monitoring with Emphasis on Computer Vision, Damage Indices and Statistical Analysis</u> PhD Thesis, University of Central Florida.

Zaurin, R. and F. N. Catbas (2011). "Structural health monitoring using video stream, influence lines, and statistical analysis." <u>Structural Health Monitoring</u> **10**(3): 309-332.

Zhang, Q. W., T. Y. P. Chang and C. C. Chang (2001). "Finite-Element Model Updating for the Kap Shui Mun Cable-Stayed Bridge." <u>Journal of Bridge Engineering</u> **6**(4): pp. 285-293.

Zhao, Y., J. F. Wang and M. Pang (2012). "The Integral Lifting Project of the Qifeng Bridge : Case Study " <u>Journal of Performance of Constructed Facilities </u>(in press).